GEOLOGY OF THE THREE LADIES MOUNTAIN/MOUNT STEVENSON AREA, QUESNEL HIGHLAND, BRITISH COLUMBIA

by

JENNIFER SUZANNE GETSINGER

A.B., HARVARD UNIVERSITY, 1974

M.S., UNIVERSITY OF WASHINGTON, 1978

A THESIS SUBMITTED IN PARTIAL FULFILMENT OF

THE REQUIREMENTS FOR THE DEGREE OF

DOCTOR OF PHILOSOPHY

in

THE FACULTY OF GRADUATE STUDIES

DEPARTMENT OF GEOLOGICAL SCIENCES

We accept this thesis as conforming

to the required standard

THE UNIVERSITY OF BRITISH COLUMBIA

APRIL 1985

In presenting this thesis in partial fulfilment of the requirements for an advanced degree at the University of British Columbia, I agree that the Library shall make it freely available for reference and study. I further agree that permission for extensive copying of this thesis for scholarly purposes may be granted by the head of my department or by his or her representatives. It is understood that copying or publication of this thesis for financial gain shall not be allowed without my written permission.

Department of _GEOLOGICAL SCIENCES_

The University of British Columbia
1956 Main Mall
Vancouver, Canada
V6T 1Y3

Date _____APRIL 1985_____

DE-6 (3/81)

ABSTRACT

In late Proterozoic to early Paleozoic time, continent-derived clastic sediment and minor carbonate of the Snowshoe Group were deposited in a continental slope to shelf environment, and shallow marine clastics and carbonates of the Cariboo Group were deposited nearer to the shore of North America. The Snowshoe Group is divided into a lower sequence of micaceous quartzite, pelite, and minor amphibolite, all interlayered with quartz diorite sheets; and an upper sequence of micaceous quartzite, pelite, and carbonate with minor calc-silicate and amphibolitic rocks.

Early isoclinal (F1A) and NE-verging tight folds (F1B) formed together with a metamorphic foliation. Tight to normal, cylindroidal second phase (F2) folds, characterized by SW-vergence and NW plunge, formed during the mid-Jurassic Columbian orogeny at about the same time as accretion of suspect terranes southwest of the map area. Prograde metamorphism in the Barrovian series of amphibolite facies was synkinematic to postkinematic to F2 folding, with maximum metamorphic recrystallization outlasting deformation. Garnet-biotite geothermometry indicates temperatures of 525 ± 20°C for pelites near the kyanite to sillimanite zone isograd. Garnet-aluminosilicate-ilmenite geobarometry limits P to less than 7 kb. Grossular-anorthite-aluminosilicate geobarometry gives P = 5.5 ± 0.7 kb.

Retrograde metamorphism and F3 kink-folding occurred
during uplift, followed by broad warping (F4) with NE trend.
The low-angle, postmetamorphic Little River Fault emplaced
chlorite to biotite zone phyllite and carbonate of the
Cariboo Group, in the hanging wall, against
staurolite-kyanite to sillimanite schists and gneisses of
the Snowshoe Group, in the footwall, with latest movement of
the hanging wall in an ESE direction.

A Rb-Sr model depositional age of approximately 750 Ma,
assuming an initial $^{87}Sr/^{86}Sr$ ratio of 0.708, was obtained
for Snowshoe Group metasedimentary rocks. Paleozoic
plutonism is indicated by a Rb-Sr whole-rock isochron date
of 530 ± 94 Ma with initial $^{87}Sr/^{86}Sr$ ratio of 0.706, and
U-Pb dates on zircon, indicating a minimum age of 335 Ma and
maximum age of about 450 Ma, for quartz dioritic gneiss
intrusive into the Snowshoe Group early in its deformational
history, pre-F1B folding. Late- to post-metamorphic
pegmatite cooled through 400-500°C at 86 ± 3 Ma. The age of
the Little River Fault is bracketed between intrusion of
pegmatite and a Miocene(?) erosion surface.

Table of Contents

40 DR=621 $5.47, $5.57T

LIST OF TABLES

LIST OF FIGURES

LIST OF PLATES

ALL PLATES ARE SEPARATE MAP SHEETS.

ACKNOWLEDGEMENT

1. <u>INTRODUCTION</u>

1.1 <u>LOCATION AND OBJECTIVES</u>

The Three Ladies Mountain/Mount Stevenson area is located along the west side of the north arm of Quesnel Lake, within the Quesnel Highland part of the Cariboo Mountains. It is entirely within the Omineca Belt, although the suture with the Intermontane Belt lies only about 10 km south of Mount Stevenson (see Figure 1).

The present study involved detailed mapping at a scale of 1:25,000 in the Three Ladies Mountain/Mount Stevenson area during the 1979-1982 field seasons, covering an area of approximately 200 km² (see Geologic Map, PLATE I). This rugged terrain is covered with rainforest at Quesnel Lake (725 m) to alpine meadows on Three Ladies Mountain (2187 m) and Mount Stevenson (2243 m), a relief of over 1500 m.

Objectives of this study were to sort out the internal stratigraphic sequence, and structural and metamorphic history of the Snowshoe Group, which was previously poorly defined in this area.

The Snowshoe Group lies within an area of metasedimentary rocks between sediments derived from North America which lie to the east and volcanic and sedimentary rocks belonging to suspect terranes to the west. This area has recently been referred to as the "suspect" Barkerville terrane (Struik 1984, Monger and Berg 1984). The details of

1
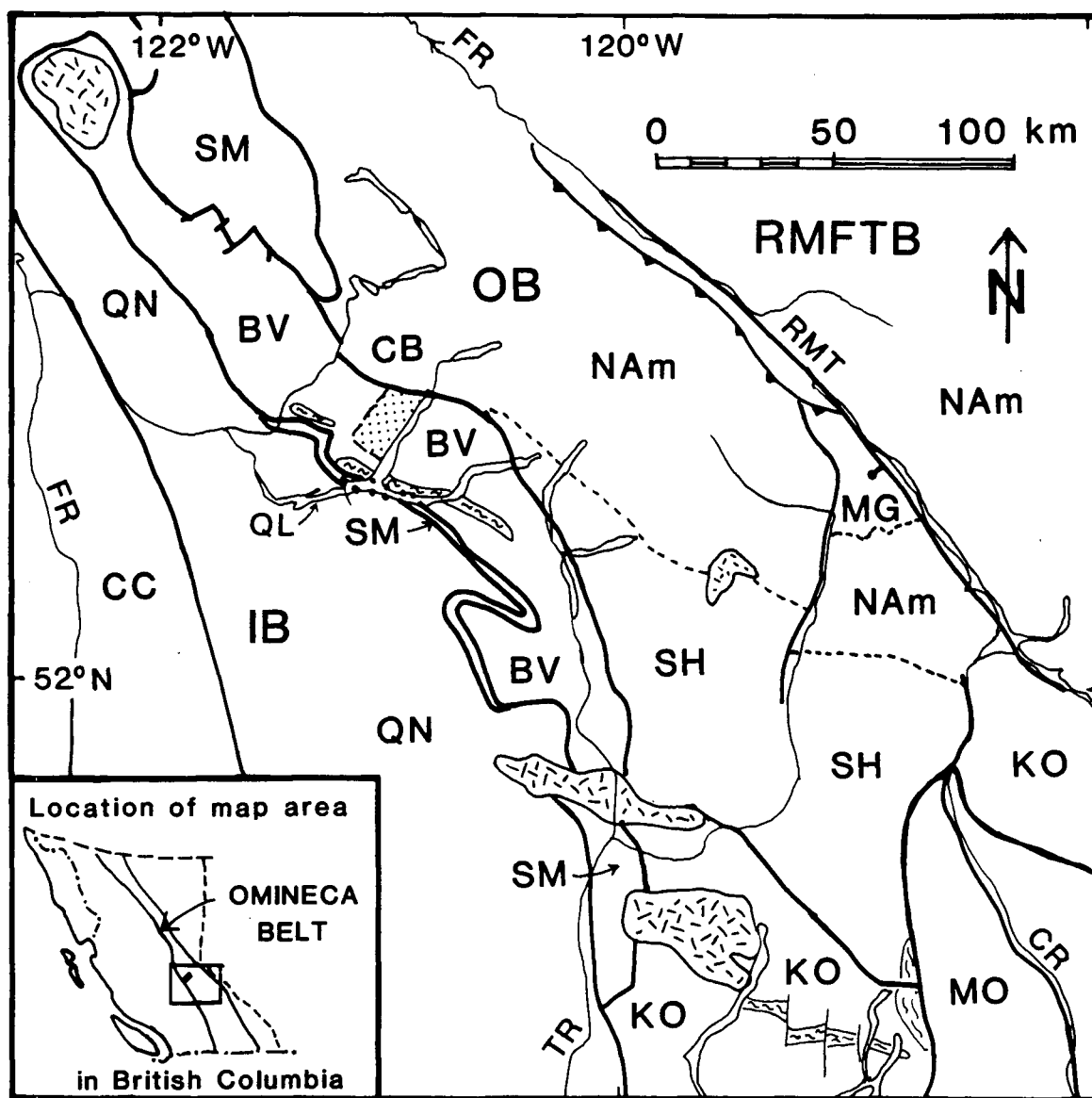
Figure 1. Location map showing relationship of study area (stippled pattern) to terranes of the Canadian Cordillera. Cretaceous and/or Tertiary granitoic bodies are in flecked pattern; Paleozoic orthogneisses are in squiggle pattern. Abbreviations: IB = Intermontane Belt, OB = Omineca Belt, RMFTB = Rocky Mountain Fold and Thrust Belt, NAm = North America, CC = Cache Creek Terrane, QN = Quesnellia, SM = Slide Mountain Terrane, BV = Barkerville Terrane, KO = Kootenay Terrane, CB = Cariboo Terrane, SH = Shuswap Complex, MO = Monashee Complex, MG = Malton Gneiss; FR = Fraser River, QL = Quesnel Lake, TR = Thompson River, RMT = Rocky Mountain Trench, CR = Columbia River. References: Monger and Berg (1984); Tipper et. al (1981).

the structural and metamorphic history of this area are
therefore important in restraining large-scale tectonic
hypotheses and speculations.

1.2 PREVIOUS WORK

Reconnaissance geologic work in the area northwest of
Quesnel Lake was done in the 1950's and early 60's by the
B.C. Department of Mines (Holland 1954; Sutherland Brown
1957, 1963) and the Geological Survey of Canada (Campbell
1961, 1963), partly in response to interest in gold mines
around Wells and Barkerville, B.C. Holland (1954) first
described and named the Snowshoe Formation and assigned it
to the upper part of the Cariboo Group, as did Sutherland
Brown (1957, 1963) and Campbell (1961, 1963). More recent
work has placed the Snowshoe Group either below the Cariboo
Group along with the Kaza Group (Campbell et al. 1973;
Campbell 1978; Struik 1979, 1981a, 1981b); or as part of the
Cariboo Group west of the Pleasant Valley Fault but not east
of it, and possibly partly late Paleozoic in age
(Struik 1982); or as a separate group of rocks of late
Proterozoic and/or Paleozoic age (in "Barkerville terrane")
juxtaposed with the Cariboo Group (in "Cariboo terrane")
along faults (Struik 1983, 1984b).

Many detailed studies by graduate students and their
supervisors have concentrated on various aspects of regional
geologic problems such as stratigraphic correlations,
structural history, apparently steep metamorphic gradients,
and the nature of the boundaries of the Shuswap Metamorphic

Complex (K.V. Campbell 1971; Fletcher 1972; Pigage 1977, 1978; Fletcher and Greenwood 1979; Poulton and Simony 1980; Klepacki 1980, 1981; Rees 1981; Pell and Simony 1981, 1982; Pell 1982; Murphy and Journeay 1982; Getsinger 1982, 1983a, 1983b; Murphy and Rees 1983; Raeside and Simony 1983; Rees and Ferri 1983; Dechesne et al. 1984; Murphy 1984).

1.3 REGIONAL GEOLOGIC SETTING

The Three Ladies Mountain/Mount Stevenson area lies completely within the Omineca Crystalline Belt, which is the eastern of two major exposures of metamorphic and plutonic infrastructural rocks in the Canadian Cordillera. This belt of primarily metamorphic rocks lies between the less metamorphosed and unmetamorphosed suprastructural rocks of the Rocky Mountain Fold and Thrust Belt to the east and the Intermontane Belt to the west (Monger et al. 1982). Regional metamorphism and intense deformation in the Omineca Crystalline Belt took place in mid-Jurassic time during collision of North America with a western composite terrane composed of four variously displaced terranes which were amalgamated by the end of the Triassic (Eastern Assemblage or Terrane, Quesnellia, Cache Creek Terrane, and Stikinia or Stikine Block) (Monger et al. 1982). The Stikine Block subsequently underthrust part of the rest of the composite terrane to the north and east during the mid-Jurassic, thus contributing to increased deformation (Monger et al. 1982).

The Barkerville Terrane, which includes mainly rocks of the Snowshoe Group, lies east of all known accreted terranes, and may be considered to be parautochthonous in relation to North America.

In the Three Ladies Mountain/Mount Stevenson area, the Snowshoe Group consists of a thick section of continental slope and shelf clastics and minor carbonates of probable late Proterozoic age which have been metamorphosed under

amphibolite facies conditions. It is overlain by more
shallow marine rocks of the late Proterozoic to Paleozoic
Cariboo Group, which are metamorphosed to greenschist
facies. Both groups of rocks were folded and metamorphosed
during the mid-Jurassic Columbian orogeny. The present
contact between the Snowshoe Group and the Cariboo Group in
the study area is a low-angle postmetamorphic fault known as
the Little River Fault.

2. LITHOSTRATIGRAPHY

2.1 LITHOSTRATIGRAPHY OF SNOWSHOE GROUP

The rocks in the map area have not been positively correlated with those in any other area of the Cordillera. The high grade metamorphic rocks west of the North Arm of Quesnel Lake, consisting of folded metasediments and various intrusive phases, have been called Snowshoe Group and assigned a late Proterozoic to Paleozoic age by Campbell (1978) and other workers. Fletcher (1972) divided the same rocks into Isaac and Kaza Formations on the basis of a similarity to his own field area at Penfold Creek, east of the North Arm of Quesnel Lake. Snowshoe Group rocks at Three Ladies Mountain may share some similarities with the Snowshoe Group near Wells as mapped by Struik (1981), and resemble parts of the Horsethief Creek Group as mapped by Pell (Pell and Simony, 1981) near Blue River. Fossils and sedimentary structures showing definite facing directions have not been found. Original bedding is obliterated by cleavage and metamorphism, but lithologic units that can be distinguished are shown on the map (Plate I).

The Snowshoe Group in the Three Ladies Mountain map area may be divided into a lower structural sequence, up to 6 km thick, underlying most of the area from Mount Stevenson to the North Arm of Quesnel Lake, and an upper structural sequence best defined in the Three Ladies Mountain area, where it is approximately 3 km thick. Much of the thickness

8

may be due to structural repetition. Thicknesses may have been different before deformation (see Figure 2).

The lower sequence consists of interlayered, foliated grey micaceous quartzite, brownish-weathering quartz-rich biotite-muscovite schist, and minor impure carbonate, calc-silicate, and amphibolitic gneiss. Grain size of the psammitic layers is relatively constant and does not exceed granule size; the coarse granule grit and conglomerate characteristic of the Kaza Group elsewhere are conspicuously lacking. Sedimentary structures other than lithologic layering and possible graded bedding were not observed. Pelitic schist containing aluminosilicate index minerals is rare in the lower sequence. Much of the schist is semi-pelitic, containing quartz, biotite, muscovite, plagioclase, and garnet, with no indicator for distinguishing kyanite zone from sillimanite zone. Amphibolite and carbonate occur as small lenses and are not associated with each other; amphibolite pods tend to occur near quartz dioritic sills, whereas small carbonate units may be found dispersed within the schist. Greenish-grey, hornblende-biotite gneiss intercalated with the paragneiss is interpreted as quartz dioritic sills, and may constitute up to 25% of the foliated rocks. All are irregularly intruded by quartz-plagioclase-muscovite pegmatite, which locally constitute 50% of the total rock mass.

Mixed metasedimentary gneisses and quartz dioritic sills crop out from the western shore of the North Arm of Quesnel

UNIT
Rock Type

BRALCO MARBLE
Coarse white calcite marble

SNOWSHOE FORMATION
UPPER SEQUENCE

Grey, micaceous quartzite
with interlayered pelite

Pelite

Carbonate/Amphibolite

Pelite with impure carbonate

Thinly-layered micaceous
quartzite and pelite

LOWER SEQUENCE

Amphibolite lenses

Quartz dioritic gneiss

Thinly-layered micaceous
quartzite and pelite
(Covered)

Micaceous quartzite, pelite,
rare carbonate, and
migmatitic gneiss

500 m

2 km

100 m
150 m

500 m

6 km

Figure 2. Lithostratigraphy of Snowshoe Group in the Three
Ladies Mountain/Mount Stevenson area.

Lake south of Grain Creek to Mount Stevenson, and are
practically indivisible stratigraphically at the map scale,
although some sills have been mapped over several
kilometres. Alternating lighter and darker gneisses
resembling "lit-par-lit" migmatite, in which distinction
between orthogneisses and paragneisses is uncertain, are
characteristic of the lower part of the section, especially
near Quesnel Lake. The uppermost part of the lower sequence
consists mostly of thinly-layered, biotite-rich micaceous
quartzite and semi-pelite; layers are 5 to 10 cm thick and
flaggy where exposed. This flaggy micaceous quartzite and
pelite is transitional to the upper sequence. The upper
boundary of the lower sequence is arbitrarily chosen at the
top of the first continuously mappable hornblende-bearing
quartz dioritic sill, which is subparallel to the intruded
metasedimentary rocks.

The upper sequence, in contrast, contains major
carbonate and calc-silicate, amphibolite, and common pelitic
schist. It lacks quartz dioritic sills, and is not as
extensively intruded by pegmatite. Internal stratigraphy is
variable due to discontinuous layering and possible
repetition caused by complex folding. The lowermost
subdivision of the upper sequence consists of
rusty-weathering pelitic schist, micaceous quartzite, minor
marble, and some magnetite-bearing schist. Between Welcome
Mountain and Three Ladies Mountain the pelitic schist
contains large porphyroblasts of garnet, staurolite, and

kyanite. Whitish quartzite in distinctive, massive layers about 1 m thick is interlayered with pelite. Some flaggy, micaceous quartzite occurs in the lowermost part of this section, transitional to similar rocks in the lower sequence. This mainly pelitic unit averages about 500 m thick, but is thickened by leucocratic granodioritic gneiss sills north of Welcome Mountain.

Overlying the lower pelite is the most distinctive subdivision of the upper sequence, containing a variety of rock types including hornblende amphibolite, carbonate, and clastic metasedimentary rocks. Most of the unit, which varies in thickness from 10 to over 150 m, weathers recessively to reddish-brown soil, distinctive both on aerial photographs and in the field. Thick, massive amphibolite layers are more resistant, as on the north face of Three Ladies Mountain, where a sheer 60 degree dip-slope of amphibolite drops 500 m from the summit to the valley. The amphibolite unit itself appears to be a combination of amphibolitic metasedimentary rocks formed in reaction between pelitic and carbonate units during regional metamorphism, and metamorphosed dioritic sills. Reaction amphibolite includes nearly monomineralic layers of metamorphic hornblende grains up to several centimetres long, as well as more common calc-silicate gneiss which may contain hornblende, diopside, garnet, epidote, plagioclase, and calcite. Hornblende in layered amphibolite and calc-silicate rocks tends to be aligned along metamorphic

lineations (usually F2 fold axial trends), or else in
radiating habit on foliation planes (garbenschiefer); it may
be either synkinematic or postkinematic to F2 structures.

Other amphibolite, occurring in discontinuous pods, is
unfoliated, with coarse-grained, blocky hornblende and
plagioclase, resembling diorite in hand specimen.
Examination of thin sections shows that the amphibole is
pseudomorphic after former blockier-shaped pyroxene,
although no relict pyroxene was identified.

Other rock types within the carbonate-amphibolite unit
include impure calcite marble up to 20 m thick, minor
calc-silicate zones between pelite and carbonate layers,
flaky quartz-biotite schist, black siltite, and green,
pyritic quartzite (with up to 20 % pyrite locally). The
black siltite is a distinctive rock type, occurring as
discontinuous layers up to 5 m thick of fine-grained, hard,
black, graphitic quartz siltite with a slight phyllitic
sheen, and local "pencil cleavage", interfolded with
porphyroblastic pelitic schist (staurolite-kyanite grade),
limy schist, and amphibolite. The black siltite is not a
graphite schist, as it is not schistose.

The carbonate-amphibolite unit is more highly fractured
than the surrounding pelite and quartzite, and has
apparently suffered more hydrothermal alteration.
Crosscutting rusty zones with sparse sulfide mineralization
are associated with minor, late, near-vertical faults, and
the nearby pelitic schist is more severely retrograded to

chlorite than that farther from the carbonate-amphibolite.

The carbonate-amphibolite unit is generally overlain by another staurolite-kyanite schist with minor magnetite-bearing layers, and a thick section (up to 2 km) of grey, micaceous quartzite interlayered with quartzose, garnetiferous mica schist, which continues up to the base of a coarsely crystalline white marble.

The marble overlying the Snowshoe Group near Maeford Lake was previously mapped as Cunningham Formation (?) (Campbell 1978; Klepacki 1981), and has recently been assigned to the Snowshoe Group as the Bralco Succession marble by Struik (1983).

The marble is up to 500 m thick near Maeford Lake, forms light-grey to buff-weathering cliffs, and can be traced for several kilometres to the northwest. It is a coarsely crystalline, massive, relatively pure white calcite marble, with local siliceous dolomite containing radiating needles of white tremolite. Layering is discontinuous, lensoidal in places, and is marked by faint grey streaks and rare rootless isoclines implying folding and possible transposition of bedding. Typical specimens display criss-crossing foliations which may be interpreted as cleavages from various fold phases or, in some places, as a cataclastic fabric, or as merely fractures.

The base of the marble is apparently conformable on Snowshoe Formation pelite and quartzite. Although there are some thin, garnet and hornblende-bearing calc-silicate

layers in the schist below the contact, the Snowshoe Group
is not gradational across the contact with the marble.
There are no marble units within the Snowshoe near the
contact. The gentler dip of the marble, in contrast to a
steeper dip in the underlying pelite, may be a result of
measuring different foliations in the two units, or evidence
for a ductility contrast or tectonic contact. The contact
is folded along with the rocks on both sides, but there is
no convincing evidence that it is a fault contact.

The environment of deposition of the Snowshoe Group was
offshore from the margin of a continent which contributed
fine pelitic and coarser quartz-rich clastic detritus to a
relatively stable but subsiding slope or basin. The thick
section of quartzitic and pelitic rocks exposed particularly
in the Mount Stevenson area (Snowshoe Group "lower
sequence") could have been deposited off the continental
slope in a rise environment, whereas the carbonate and limy
pelite higher in the section must have been deposited in
water shallower than about 200 m. The Snowshoe Group is
typical of sediments included in the late Proterozoic
package of the Cordilleran miogeosyncline; it is
characterized by voluminous grits and shale deposited in a
thick clastic wedge, with some bank and offbank carbonate,
and minor mafic volcanics (Poulton and Simony 1980).

The stratigraphic position of the Snowshoe Group has
long been unclear; no fossils have been reported. The
Snowshoe Group was believed by early workers to overlie the

Cariboo Group, and is shown as "Lower Cambrian or later" on maps by R.B. Campbell (1961, 1963). Later work by Campbell et al. (1973) suggested that the Snowshoe Group was "a western facies of the Kaza Group" (p. 32), and thus of late Proterozoic Windermere age. Getsinger (1982) suggested that the Snowshoe Group resembles parts of the late Proterozoic Horsethief Creek Group, rather than the Kaza Group. The sedimentology of the Snowshoe Group in the Three Ladies Mountain area is similar to that described by Poulton and Simony (1980) for the Horsethief Creek Group of late Proterozoic age. Struik proposed that one of the uppermost units of the Snowshoe Group (northwest of Wells, B.C.), is late Paleozoic in age, based on uncertain lithologic correlation with a nearby unit consisting of marble, slate, and crinoidal limestone which yielded Mississippian conodonts (Struik 1982). However, it would be pure speculation to try to correlate this unit with any unit in the Three Ladies Mountain area, as further uncertainty would be involved in making lithologic correlation across 100 km (even along strike) of unfossiliferous rocks which themselves cannot be traced with complete confidence directly into the Three Ladies Mountain--Mount Stevenson area.

This study suggests that the age of at least most of the Snowshoe Group in this area is late Proterozoic, by comparison with descriptions from other areas, as well as according to a preliminary Rb-Sr whole rock date of

approximately 750 Ma for the time of sedimentation (see section on geochronology).

2.2 LITHOSTRATIGRAPHY ABOVE THE LITTLE RIVER FAULT

The stratigraphy of the low-grade marble and phyllite above the Little River Fault is not yet uniquely defined. However, the rocks in this area have been assigned to some part of the late Proterozoic to lower Cambrian Cariboo Group (Campbell 1978; Klepacki 1981; Struik 1983) (see Figure 3).

The lowermost units in the upper plate of the Little River Fault are exposed at Limestone Point, just east of where the fault disappears into Quesnel Lake. Below the bluff is a sequence of interlayered grey phyllite and thinly-bedded quartzite, most of which is pinkish-colored from iron-staining, and which is kinked with chevron folds. Bedding is still distinguishable from cleavage in some places. Biotite porphyroblasts are common in muscovite-chlorite phyllite below the limestone, but do not occur north of Service Creek. This unit resembles a description of the uppermost part of the Isaac Formation, "grey phyllite with sparsely interbedded siltstone and limonitic fine-grained sandstone" in Campbell et al. (1973, p. 34).

Limestone Point is named for the massive, white crystalline marble which forms a prominent cliff about 50 m high visible from the whole length of the North Arm of Quesnel Lake. It resembles the Bralco marble in appearance, but occupies a different structural and stratigraphic position. Bedding is difficult to distinguish, but may be indicated by small, thin, sandy layers in the midst of more

Rock Type

50 m	**Grey marble** **(Service Ridge)**
20 m	**Greenish phyllite** **and minor quartzite**
500 m	**Intercalated grey marble** **and calcareous phyllite**
	(Covered)
100 m	**Green and grey phyllite**
	(Covered)
50 m	**White marble** **(Limestone Point)**
100 m	**Pink and grey quartzite** **and phyllite, with biotite**
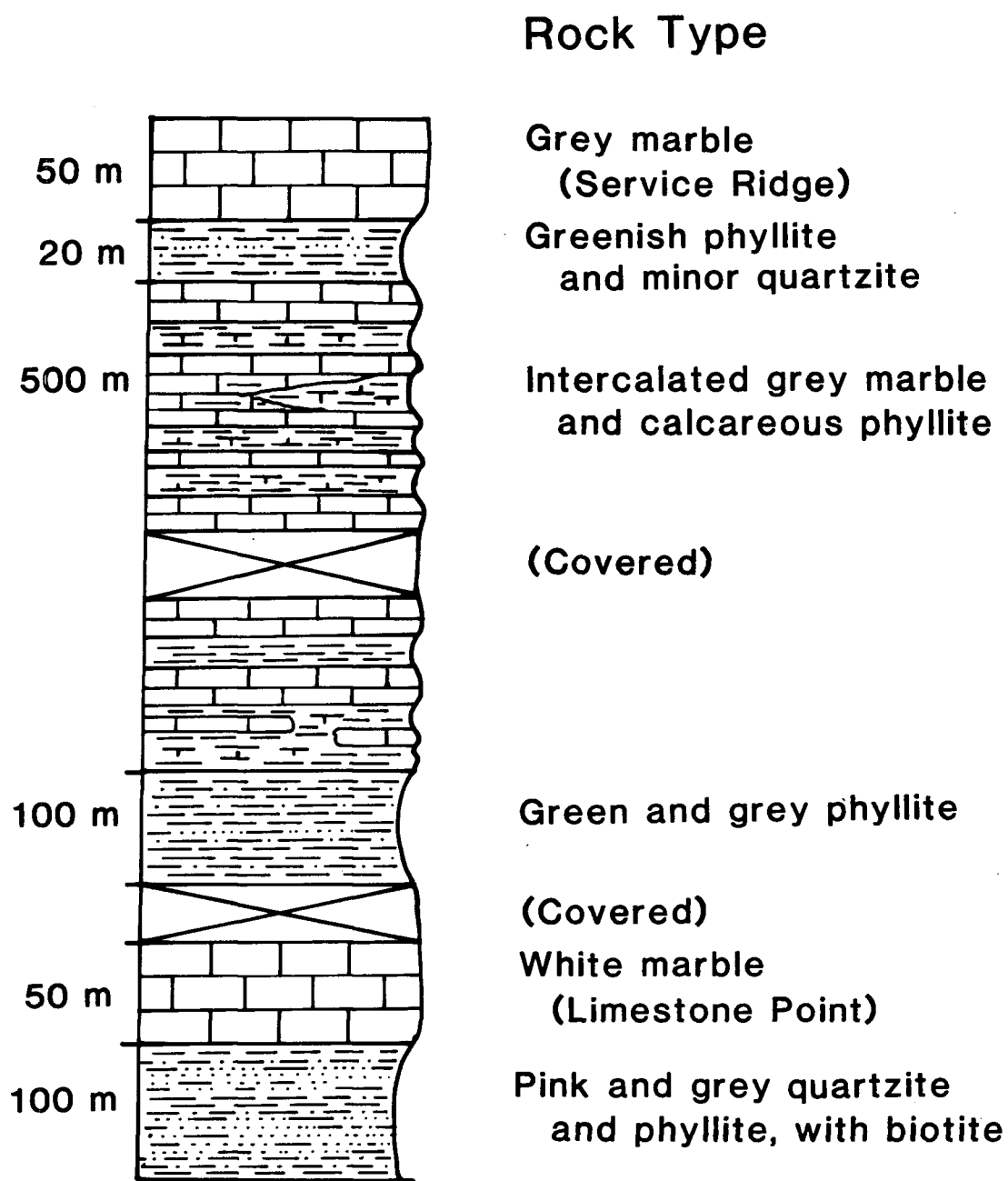
Figure 3. Lithostratigraphy above Little River Fault.

massive layers. Most of the marble is pure calcite, but
some dolomite and more siliceous layers are also present.
Carbonate breccia with brownish-weathering lenses (2-10 cm)
in a whiter matrix is foliated parallel to the base of the
marble unit. It is unclear whether the contact between the
marble and the underlying pelite and quartzite is
sedimentary or tectonic. The marble is directly overlain by
thick glacial drift; its upper contact is not exposed. The
marble at Limestone Point may be correlated with the
Cunningham Formation, as shown on Quesnel Lake map sheet
(Campbell 1978).

The next section of metasedimentary rocks to the north,
and structurally higher than the marble of Limestone Point,
is a sequence of interlayered marbles and limy, siliceous
phyllite, which is exposed up to the top of the ridge above
Service Creek. From Quesnel Lake north of Service Creek, at
least 100 m of grey-green, silvery phyllite is overlain by
alternating cliffs of grey, crystalline calcite marble and
poorly-exposed, recessively-weathered layers of limy
phyllite. There are at least six layers of marble of nearly
uniform thickness (10-15 m) and similar lithology, varying
slightly in color from grey to pinkish with black streaks.

Similar alternating marble and phyllite near the saddle
where the Little River Fault crosses the ridge are probably
correlative with those on the slope above Quesnel Lake.
Poor exposure prevents certain determination of whether the
apparent repetition of rock types is stratigraphic or

structural, or both. This sequence (which is at least 500 m thick) has been mapped by Klepacki (1981) as Yankee Belle Formation, and by Struik (1983) as Cunningham Formation. It resembles the description of the "rhythmic limestone-siltstone-shale facies" of the Yankee Belle Formation in Campbell et al. (1973).

Exposure is better near the top of the ridge, where another greenish-grey phyllite with thin intercalated quartzite layers underlies a thick, grey marble, which forms the peak labelled "6287'" (geodetic survey point), informally referred to as Service Mountain or Service Ridge. It is possible to correlate this phyllite unit with the Midas Formation, which is also recessive and incompetent where folded, and underlies a resistant grey marble (Campbell et al. 1973). The Cariboo Group succession may have been thinner in this area than in the type sections. No unit resembling Yanks Peak Formation quartzite was identified.

The grey marble at "6287'" is about 50 m thick and dips gently to the northeast except where thickened and distorted by major folds, as at the top of the ridge. The grey marble is the most resistant unit in the area and forms the tops of ridges; its upper contact was not observed in this area, so it may be thicker than 50 m. It is a fine-grained, stylolitic, siliceous, grey calcite marble with white and grey streaky layering, and local pyrite, and is inhomogeneous in texture. It is less coarsely crystalline

than the Bralco marble, and could be called a limestone, although it has been recrystallized in greenschist facies conditions. Clots of more resistant white carbonate blebs and oval rings about 1 cm across in one sample suggest recrystallized organically-produced textures, but no recognizable fossils were found. Thin, slabby layers of grey marble about 5 cm thick, which look like bedding on outcrop scale, dip 30-50° to the northeast. These layers intersect the more shallowly east-dipping bedding and contacts of the mappable unit at a high angle. These layers are interpreted as bedding transposed into F2 axial plane orientation.

Locally near Service Mountain the grey marble is crosscut by nearly vertical zones of buff to pink calcite/dolomite breccia trending north to northeast. Calcite crystals up to 5 cm and pink calcite marble form angular clasts in a breccia with boxwork-like, pitted weathering. These areas are interpreted as hydrothermally altered zones along faults or fractures within the grey marble, rather than as separate units.

Struik (1983) divided the grey marble into an upper unit on Service Mountain, which he correlated with the Mural Formation, and the rest, which he correlated with the Cunningham Formation. This study interprets the grey marble as a single, continuous, but complexly folded marble unit probably correlative with the Lower Cambrian Mural Formation.

The entire section of rocks above the Little River Fault is assigned here, with some uncertainty, to undivided Cariboo Group.

The environment of deposition of the Cariboo Group was mainly nearshore, shallow-water marine. According to Campbell et al. (1973), the conditions varied from a fluvial deltaic environment to littoral, shallow shelf, or restricted marine environments to deeper marine depths, but all less than 200 m. These conditions are reasonable for the types of sediments observed, although there is little evidence to support an alluvial environment in this area because of lack of coarse clastics or recognizable sedimentary structures.

The late Proterozoic to Cambrian Cariboo Group was deposited closer to shore and in shallower water than the Snowshoe Group. Either the Cariboo Group was laterally approximately time-equivalent to the Snowshoe Group, and their present juxtaposition is due to telescoping of the continental margin during deformation; or the Cariboo Group was deposited conformably upon and overlying the Snowshoe Group, and their present juxtaposition is due to greater uplift of the deeper rocks with a normal displacement along the Little River Fault. A combination of these interpretations is preferred.

If the correlation of this section of rocks in the hanging wall of the Little River Fault with apparently uninterrupted Cariboo Group is correct, then the Pleasant

Valley Thrust, as mapped by Struik (1983) in the upper plate of the Little River Fault, cannot be a major terrane boundary. Other structural implications of this correlation are discussed in the following section on structure.

3. STRUCTURE

3.1 DEFORMATION: FOLD PHASES

3.1.1 FOLD NOTATION

Four distinct phases of folding have been
distinguished on the basis of orientation of axial
surfaces, associated metamorphic fabrics, and field
relations of refolded folds and intrusive rocks. These
fold phases are designated as F1, F2, F3, and F4 (see
Figure 4). Metamorphic recrystallization was
synkinematic to postkinematic to F2 folding, with
crystallization outlasting deformation. Time
relationships in the field are determined by
observations of refolded folds, crosscutting
relationships, intrusive contacts, and overprinting of
metamorphic fabrics. Figures 5 to 11 are sketches of
folds; Figures 12 to 22 show domains and stereographic
projections.

Pre-F2 folds have been divided into two subphases
(F1A and F1B) of isoclinal and tight folds which may be
related and are commonly indistinguishable in the field
except in a few places. Two lines of evidence led to
their separation. Some intrafolial isoclines were
refolded prior to F2 folding (see Figure S4 A). Near
Mt. Stevenson, quartz dioritic gneiss sills locally
crosscut isoclinal fold limbs and are isoclinally and
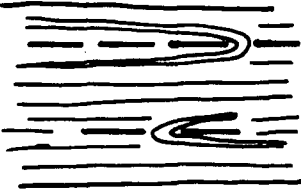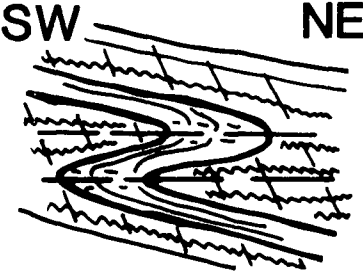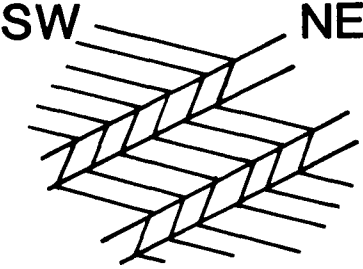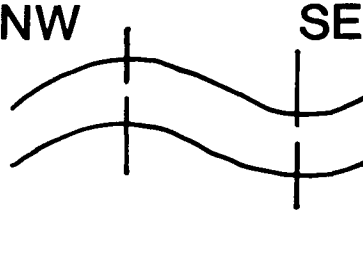
	F1 A	**ISOCLINAL AXIAL PLANES PARALLEL TO FOLIATION**
	F1 B	**NORTH- & EAST-VERGING AXIAL PLANES 084/48N or VARIABLE AXES WNW**
	F2	**WEST-VERGING AXIAL PLANES 118/60NE AXES NW 315-340/30-45**
	F3	**VARIABLE AXIAL PLANES SW- or E-DIPPING AXES NW or SE**
	F4	**UPRIGHT WARPS AXIAL PLANES 040/90 AXES NE 020-050/10-20**

Figure 4. Diagrammatic summary of fold phases.

tightly folded themselves; these structures are overprinted by F2 fabrics.

3.1.2 OUTLINE OF FOLD PHASES

3.1.2.1 F1A

True isoclines, particularly intrafolial isoclines and those refolded by later fold phases, are designated F1A (see Figures 5 and 6). Limbs are attenuated such that some have rootless hinges. Fold geometry tends to approximate that of similar folds (Type II, Ramsay 1967). Axial planes are all parallel to the dominant foliation (S_1), parallel to compositional layering (S_0), except locally in the carbonate layers, where they are variable. Fold axes were not easy to measure in most intrafolial isoclines; they show no particular pattern but tend to lie in the northwest quadrant; some also plunge northeast. The inconsistent trends are interpreted as consistent with an earlier fold episode.

3.1.2.2 F1B

Tight to isoclinal, asymmetrical folds which fold foliation (S_1) and are also overprinted by crosscutting F2 axial plane crenulation cleavage (S_2) are assigned to phase F1B. They tend to verge to the north and east, with SW-NW dipping axial planes, unlike the more obvious F2 folds which verge west with NE-dipping axial planes. Phase F1B folds are rarely preserved, most commonly in competent quartzite layers in the lower sequence, as near Welcome Mountain and Mount Stevenson; the quartz dioritic sills also show this style of folding. These
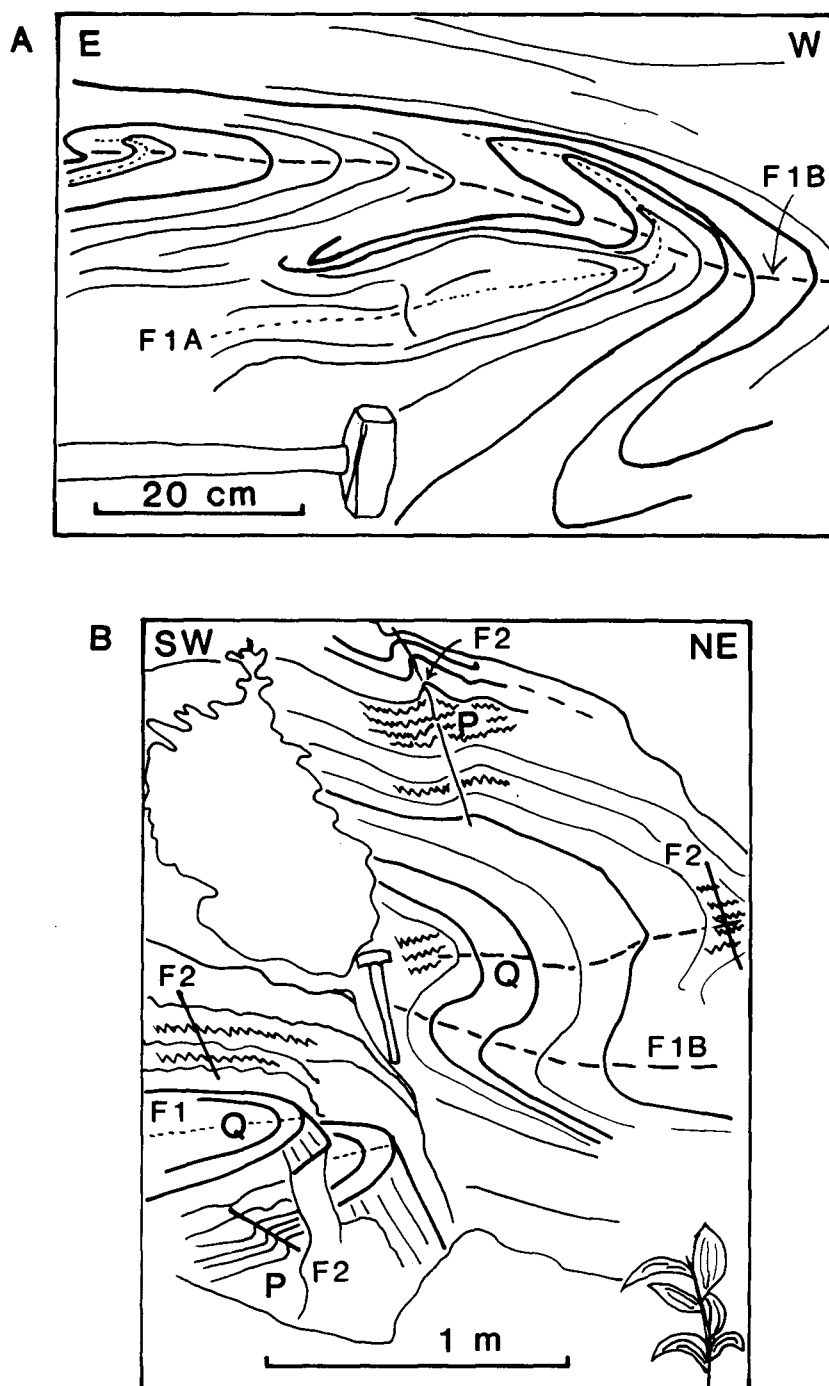
Figure 5. A. Refolded isocline (F1A, F1B) in quartzite; hammer is parallel to dominant regional foliation. 2 km east of Three Ladies Mountain.

B. Quartzite layers (Q) preserve F1 isoclinal and NE-verging (F1B) folds whereas pelitic layers (P) are refolded into SW-verging F2 folds. 3 km east of Mount Stevenson.
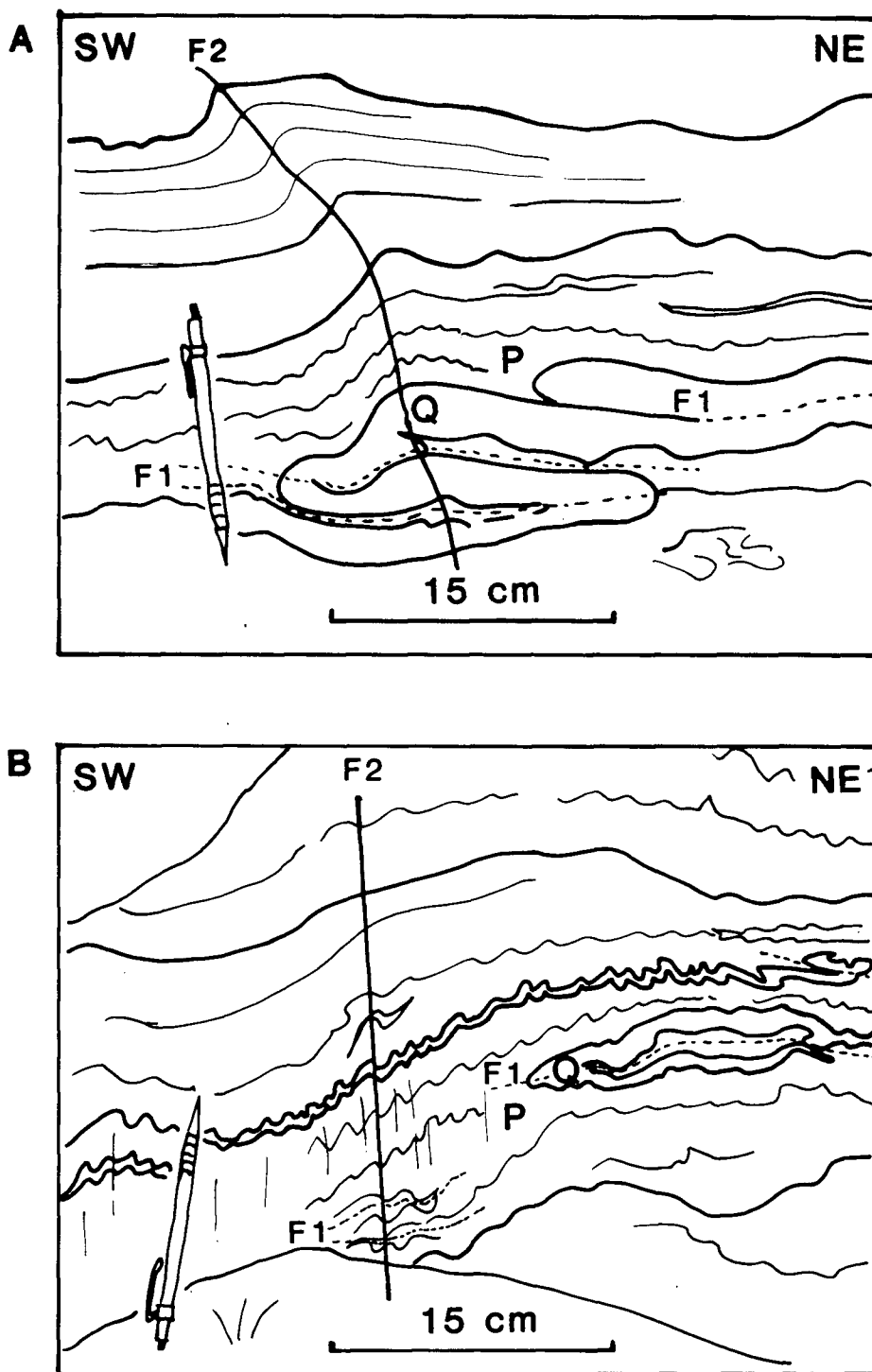
Figure 6 A and B. Quartzitic layers (Q) preserve F1 isoclines whereas surrounding pelite (P) is crenulated and incipiently transposed along NE-dipping F2 axial planes. 3 km south of Mount Stevenson.

more competent layers folded by buckling, whereas the
less competent pelitic layers show thickening in hinge
zones, as well as a tendency to become transposed by
later folding. F1B folds were recognized locally by
clear crosscutting relationships in which the F1B
Z-folds had retained their geometry in the more
competent layers whereas the pelitic layers had
developed crenulation cleavage axial planar to
superimposed F2 S-folds on the same outcrop (see Figure
5 B).

On most outcrops, F1B fold axes are nearly coaxial
with F2 fold axes. On outcrops where a quartz rod
lineation lies at an angle to the dominant lineation,
the quartz rod lineation is parallel to F1B fold axes,
whereas the dominant lineation (a combination of
intersection and mineral orientation lineations) lies
parallel to F2 fold axes.
This implies that most quartz rod lineations observed
were formed during early folding.

3.1.2.3 F1A and F1B

Both F1A and F1B appear to fold previous foliations
and compositional layering. The dominant foliation (S_1)
seen in outcrop in the Three Ladies Mountain/ Mount
Stevenson area is axial planar to F1A and F1B folds;
variation in limb attitudes lies within the spread of
values for each limb and the axial planes, showing that
they are essentially parallel.

No pre-F2 folds larger than outcrop scale have been positively identified in the field but it is suspected that they may be there in the form of repetition of compositional layering. A possible closure near Three Ladies Mountain (between middle and south peaks) defined by narrowing and pinching out of an amphibolite unit, with porphyroblastic, aluminous pelite on either side, is folded around an F2 synform (about 3 km across), ending in the hinge zone of the corresponding antiform. It is possible that this structure is not an F1 closure but the regular succession truncated by a tectonic slide near-parallel to the F2 axial plane (see Figure 7 and Plate I). The more monotonous quartzites and pelites of the lower sequence east of Mount Stevenson to Quesnel Lake may contain several repetitions of original stratigraphy, but even more extensive fieldwork would not be expected to show this as there are no clear marker units and the sequence is thickened by various granitoid intrusions. If pre-F2 folds do exist on a regional scale, they could be very large and essentially isoclinal, with limbs possibly exceeding 10 km in length.

The reasons for separating F1 folds into F1A and F1B are that (1) in some places, mid-Paleozoic quartz dioritic gneiss, which appears to crosscut earlier isoclines and foliation, is folded by tight folds which are overprinted by F2 axial planar fabric, and (2) some

Figure 7. Tectonic profile through Three Ladies Mountain projected to a surface with orientation 060/45 SE, approximately perpendicular to F2 fold axis (330/45), with datum (X-X') at 1970 m (6000').

isoclines are refolded by nearly isoclinal folds which
are in turn folded by F2 folds. Such relationships are
not conclusive, but rather suggestive evidence hinting
at a possible Paleozoic deformation. Because the
evidence for separating F1A from F1B is sparse, and
because it is possible to explain these structures in
more than one way, they are designated as subphases to
one episode of F1 or "pre-F2" folding.

3.1.2.4 F2

Folds assigned to phase F2 are the most prominent
penetrative structures seen in the Three Ladies
Mountain/Mount Stevenson area (see Figures 5 B, 6, 8,
9 A, 11, 13-15, and 19). They vary in scale from
microscopic to macroscopic. A large F2-fold with
wavelength about 5 km has been mapped on Three Ladies
Mountain (see map Plate I and Figure 7). Hinge zones
lie in large cirques, in which steep north faces are
limb dipslopes.

F2 folds are tight to normal, inclined plunging,
asymmetrical S-folds that fold the dominant foliation
(S_1). Some thickening of layers in fold hinges occurs,
especially in the more pelitic layers. They are mainly
flattened flexural slip folds (Type IC and II, Ramsay
1967). Peak metamorphic conditions accompanied F2
folding, implying a warm, ductile environment of
formation.
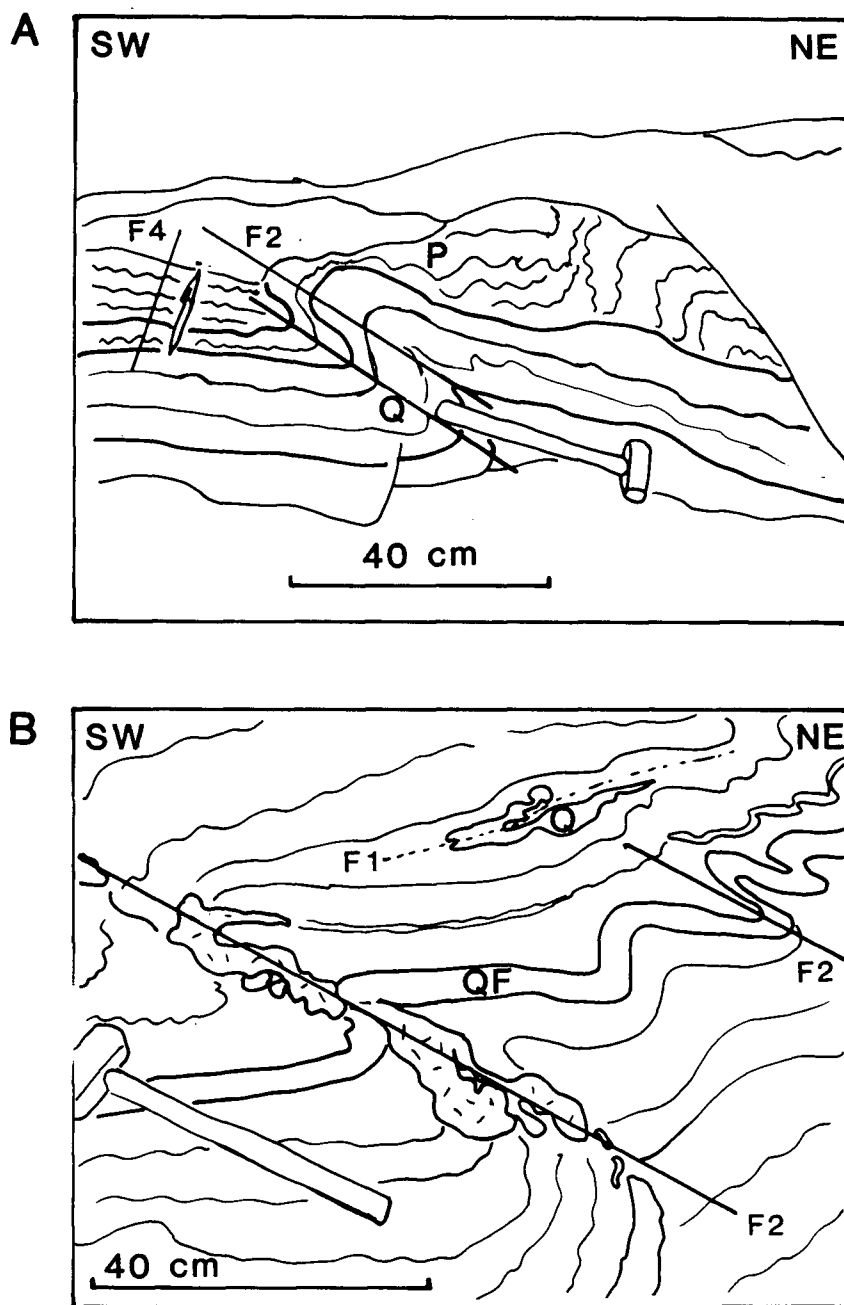
Figure 8. A. SW-verging F2 fold in quartzite (Q) is flanked by pelite (P) showing NE-trending F4 crenulations (left) and interference patterns (right). 2 km east of Three Ladies Mountain.

B. Isoclinally folded quartz segregation (Q) and quartzo-feldspathic layer (QF) in kyanite-grade gneiss are refolded by SW-verging F2 fold. Large feldspar porphyroblasts form pegmatitic segregation (pattern) along F2 axial plane, suggesting partial melt origin for pegmatite dikes. 3 km southeast of Three Ladies Mountain.

Probably over 75% of folds definitely identified as F2 folds verge southwest. They have consistently NE-dipping axial planes with average attitude 118/60 NE. Fold axes plunge 20 to 60 degrees to the NNW and NW, varying from more steep at Three Ladies Mountain to less steep at Mount Stevenson (see stereographic projections).

Well-defined mineral lineations (L_2) are parallel or subparallel to F2 fold axes. Fold axes and lineations are perpendicular to the plane containing poles to folded foliation, demonstrating the generally cylindrical nature of the folding. F2 folds are most obvious in contrasting and competent compositional layers such as quartzites and carbonates. Crenulation cleavage (S_2) is developed parallel to F2 axial planes in pelites, and is completely transposed parallel to the F2 axial plane in some places, particularly in large hinge zones.

Parasitic folds on the large S-shaped fold at Three Ladies Mountain are also dominantly west-verging, although some reversals in vergence were noted. Where both S-shaped and Z-shaped folds are seen in the same outcrop, the Z-folds are overprinted by crenulation cleavage axial planar to the S-folds (see Figure 5 B).

3.1.2.5 F3

Local kinking and crenulation folds which are clearly post-F2 have been assigned to F3 (see Figure 9).
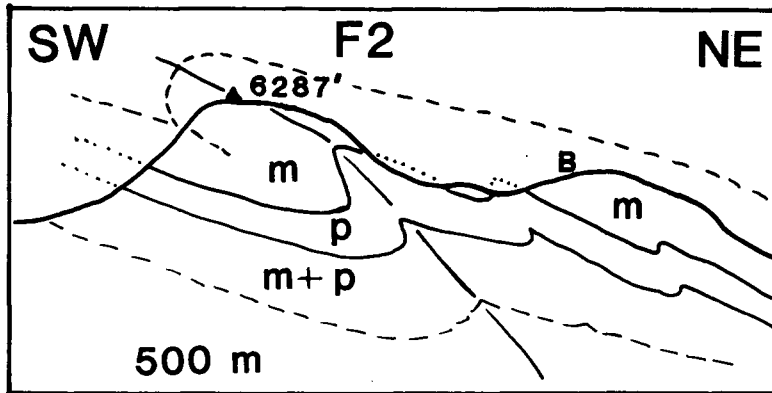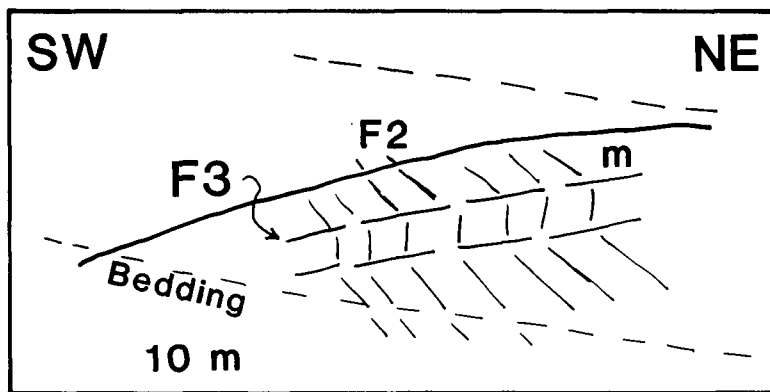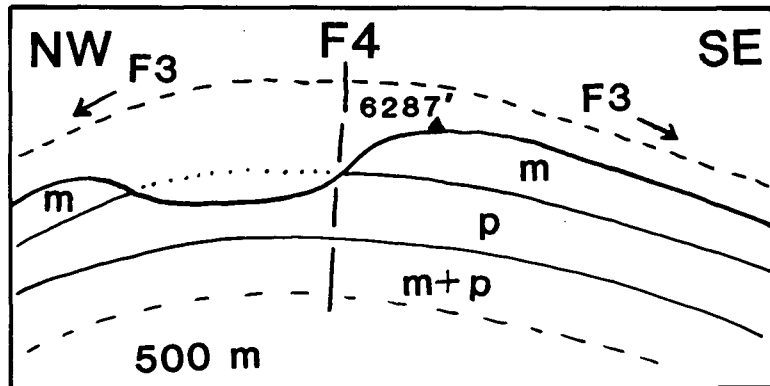
Figure 9. A, B, C. Generalized cross sections through Service Mountain ("6287'") showing geology and relationships among F2, F3, and F4 folds. m = marble; p = phyllite and micaceous quartzite.
The small "B" in A locates the outcrop shown in B.

Many F3 folds are coaxial or nearly so with F1 and F2 folds plunging NW, and some are east-verging with southwest-dipping axial planes. Axial planes of F3 folds tend to be relatively upright except for one group, which appears to be parallel to joint planes perpendicular to F2 fold axes (see Figure 18 C). These lower angle features may be due to slightly later fault-related deformation. F3 deformation had the effect of tightening and steepening F2 structures in the Three Ladies Mountain area, and may have initiated sliding along steepened F2 axial planes. Kinks and chevron folds are particularly well-developed in phyllites in the hanging wall of the Little River Fault, but less visible in the more highly metamorphosed Snowshoe Group schist, where F3 folds are observed mainly in pelitic units. Rare sets of conjugate kinks were observed. Variable fold attitudes and sparse occurrence account for the irregular and spread-out pattern on the stereographic projections (see Figure 18 C and D).

In one case, east-verging, NW-plunging F3 crenulation folds folding F2 axial plane cleavage in pelite are clearly superimposed on an east-verging WNW-plunging F1B fold preserved in a felsic layer (see Figure 10). In this sample, quartz-rod lineations are parallel to the F1B fold axis and mica crenulations are parallel to the F3 fold axis, they diverge by about 25°.
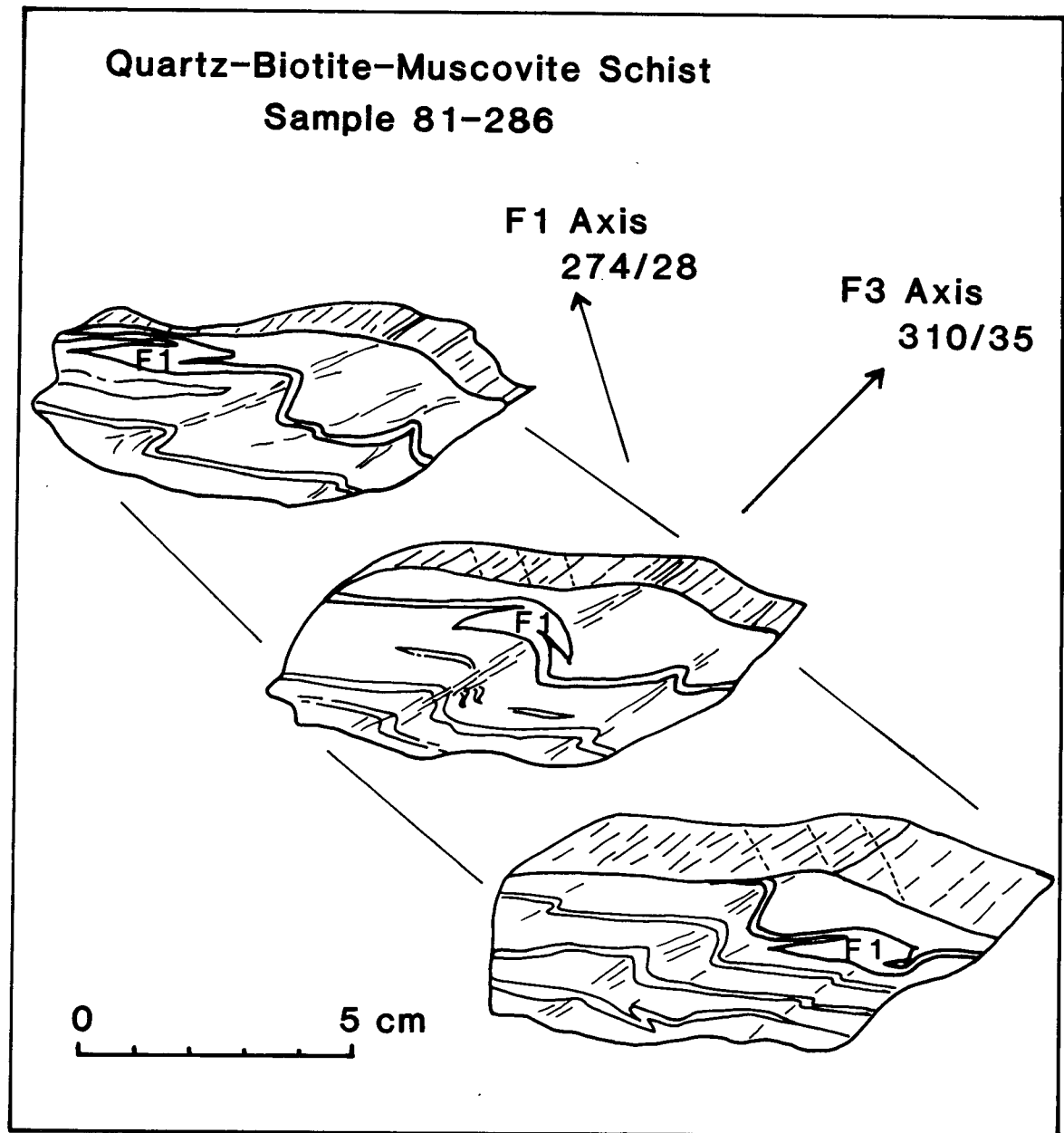
Figure 10. Sketch of sample 81-286, a quartz-biotite muscovite schist from Station 104, showing F3 crenulation cleavage in pelite crosscutting an F1 fold in a felsic layer.

Specific examples of crosscutting and superposition of fold styles such as these have allowed for distinction of fold elements that plot as overlapping distributions because of the variability in each data set. Pegmatite intruded along F2 axial planes shows poorly-defined foliation parallel to F3 trends in some outcrops. In thin section, green chlorite is aligned along F3 axial planes, and appears to be retrograde. Retrograde metamorphism is believed to be contemporaneous with or later than F3 deformation.

3.1.2.6 F4

Large to small, upright open folds with vertical axial planes and shallow NNE to NE plunge, accompanied by minor crenulations in pelitic layers, are assigned to fold episode F4 (see Figure 8 A, 9 C). Large F4 folds are concentric buckle folds of moderate amplitude with wavelength on the order of a few kilometers. These folds may account for the wide variation in plunge of F2 axes and lineations, including the southeast dip in parts of the map area. Quartz veins near Mount Stevenson are commonly nearly vertical with NE strike, parallel to F4 axial plane fractures. Some of the curvature in the Little River Fault surface may be due to warping by F4 deformation, or perhaps both faulting and F4 folding occurred during the same extensional event.

3.1.3 FOLDS ABOVE LITTLE RIVER FAULT

Fold history in Cariboo Group rocks above the Little River Fault is similar to that in the Snowshoe Group below it, but only one possible first-phase, isoclinal fold was observed. In the hanging wall of the Little River Fault, the grey marble has near-horizontal to gently east-dipping bedding (S_0), but is broken into slabs (average 5 cm thick) parallel to F2 axial planes (S_2) except where refolded into F3 kinks and chevron folds (see Figure 11 B). The pelite, which is a chlorite grade phyllite, exhibits either F2 axial plane cleavage (S_2) or is transposed locally to F3 axial plane cleavage (S_3); both cleavages may be developed in the same outcrop. Quartzite layers in the pelitic units tend to retain pre-F2 layering (S_0?), although micas in fold hinges are reoriented on F2 axial planes (S_2) (see Figure 11 A). F3 kinks and chevron folds plunge 080 to 100 (approximately E-W) and plunge up to 30° to the west or up to 15° to the east, depending on the limb of the F4 warp. Axial planes of kink folds trend around 010/30E locally, parallel to minor fault surfaces related to the Little River Fault. This suggests that movement related to the Little River Fault took advantage of F3 axial plane surfaces, or that there is some genetic relationship between faulting and kink folding.
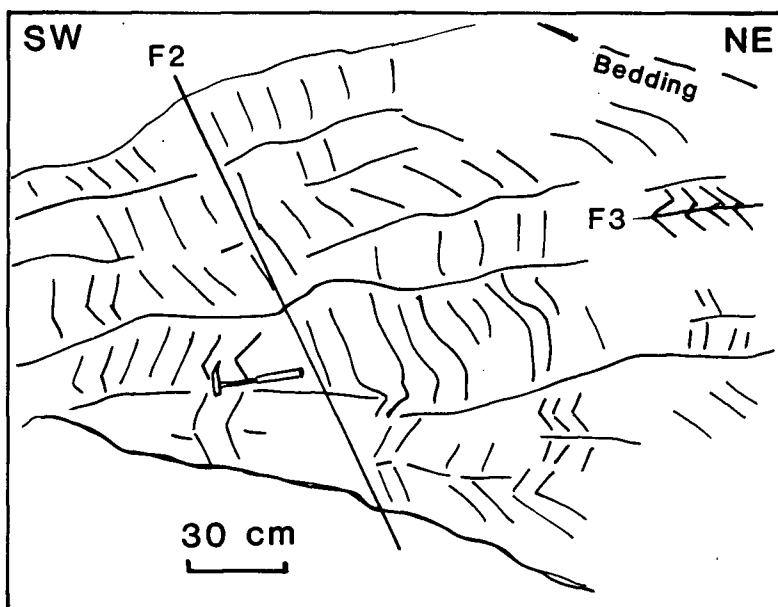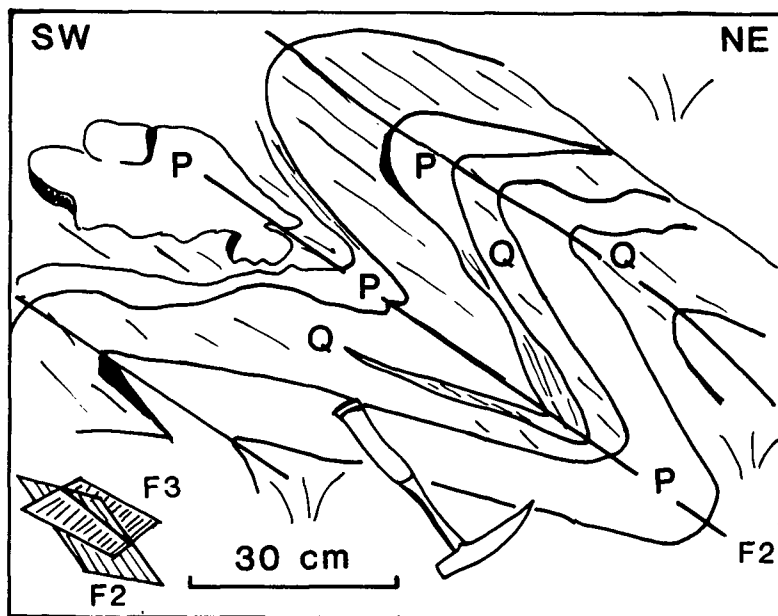
Figure 11. A. Weak foliation in micaceous quartzite (Q) is parallel to NE-dipping axial plane of SW-verging fold (F2), whereas cleavage of interlayered phyllite (P) dips southeast (F3 axial plane), parallel to the face of the outcrop. Near Service Mountain ("6287'").

B. Thin layers in grey marble at "6287'" are subparallel to regional NE-dipping F2 axial plane, but locally kinked by F3 folds with SE-dipping axial planes.

3.2 STEREOGRAPHIC PROJECTIONS OF STRUCTURAL ELEMENTS

Domains are shown on Figure 12 and stereographic projections for various structural elements in eleven domains are shown in Figures 13 to 22.

3.2.1 DOMAINS

Domains for plotting structural elements were chosen on the basis of large structures and lithostratigraphic boundaries in the field. Domains I through VII are in Snowshoe Group "upper sequence"; Domains VIII, IX, and X are in Snowshoe Group "lower sequence"; and Domain XI is in Cariboo Group rocks above the Little River Fault. Domains I, V, VII, and IX include areas of generally homoclinally dipping foliation (on a large scale); Domains II, III, IV, and X include known hinge zones of large F2 folds; Domain VI contains a fault which locally tilts foliation; and Domain VIII spans an area believed to be affected by movement on the Little River Fault.

Collected data are more numerous in some domains than in others, and for some structural elements (such as foliation). Where data are sparse, or where stereograms plotted separately were essentially the same, data from two or more domains have been combined in one stereogram.

Centers of concentrations of points were calculated by computer plotting program or by eye; where both methods were used there was good agreement between them.
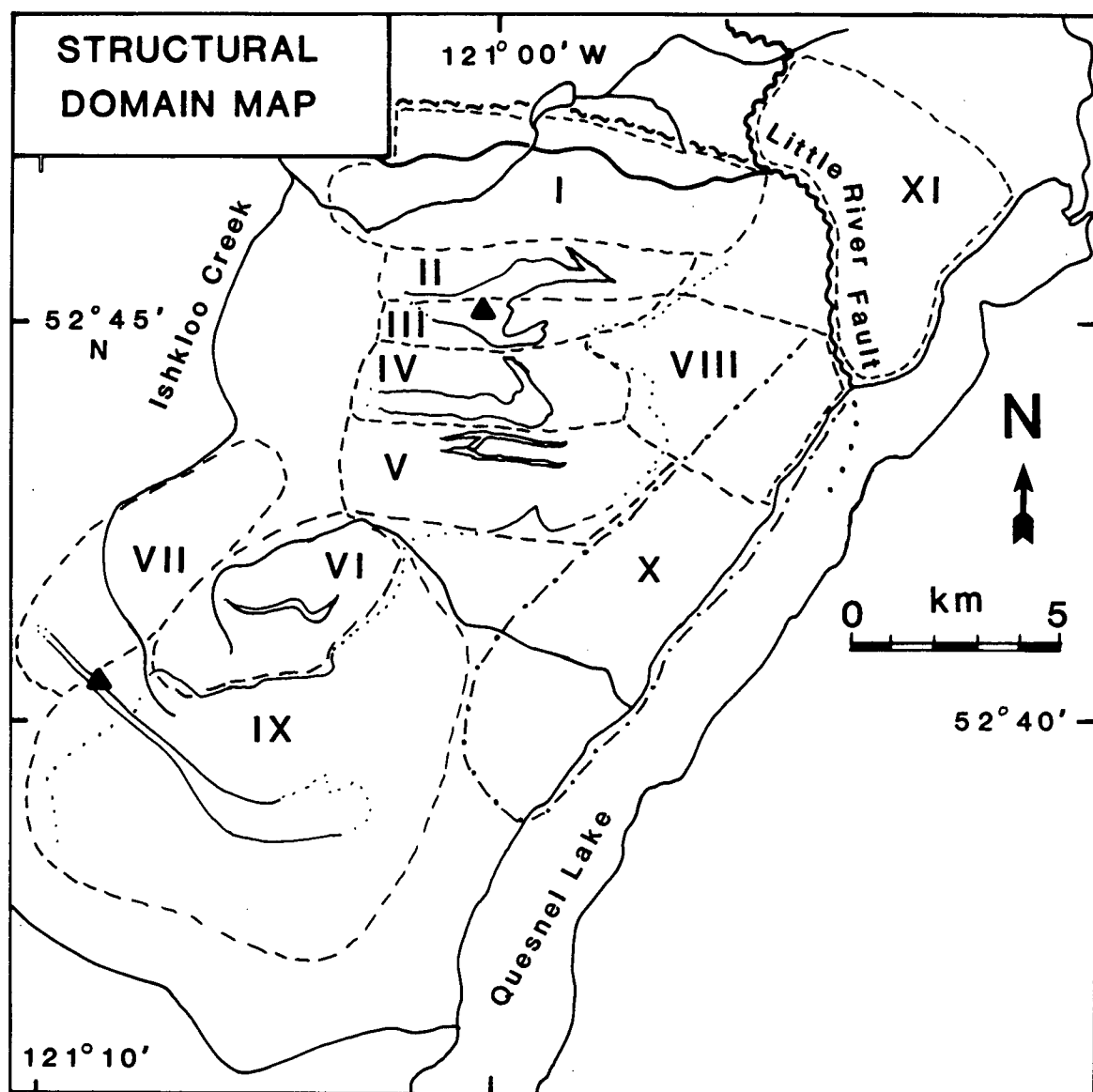
Figure 12. Structural domain map of the Three Ladies Mountain area showing domains referred to on stereographic projections. Refer to Plate I for geology and to Plates IV-VI for structural detail.

3.2.2 <u>DEFINITION OF TERMS</u>

Structural elements plotted on stereographic projections include those shown on Plate I, and Plates IV, V, and VI. Planar features are plotted on π-diagrams as poles to surfaces.

Bedding is plotted only where it can be distinguished from metamorphic layering, as in the low-grade rocks above the Little River Fault. For the high-grade schist and gneiss, compositional layering and foliation are combined as "foliation", as they are generally parallel in the field and when plotted separately their distributions overlap entirely. "Foliation" refers to the dominant metamorphic foliation in an outcrop, which is generally parallel to compositional layering, and may include foliation related to either F1 or F2 structures. Where foliation could be identified as axial planar to a particular fold phase, it is plotted in the category of "axial planes". "Axial planes" are either measured axial surfaces, axial planar foliations, or crenulation cleavage, or approximations to axial planes of folds with no easily measurable axial surfaces. "Fold axes" are measured hinge lines of folds, or approximated by measuring lineations apparently parallel to hinge lines. Where fold phases could be distinguished, axial planes and fold axes are separated into groups of F1, F2 (mainly westerly-overturned folds), F3, F4, and "pre-F2" folds

(including easterly-overturned F1B folds as well as isoclinal and rootless F1A folds). "Lineations" measured in the field include intersection lineations (usually a combination of F1 and F2 structures), crenulations, and mineral orientation lineations such as quartz rods, preferred dimensional orientation of micas, and alignment of elongate hornblende. Quartz rod lineations are parallel to F1 fold axes where they can be distinguished from other lineations. Kinks and crenulations are F3 or F4 structures. Most lineations are parallel to F1 or F2 fold axes, which are nearly coaxial in most areas. "Fault surfaces" are surfaces on which movement appears to have taken place, as indicated by offset or slickensides. "Slickensides" are not divided into slickenfibres, slickenlines, or slickensurfaces; these are meaningless distinctions here as the slickensides observed appear to consist of smoothed-over, fibrous-looking lines that form a generally smooth and shiny surface. "Joints" refer mainly to prominent fracture planes in the rocks, most commonly those perpendicular to F2 fold axes.

3.2.3 SUMMARY OF STEREOGRAPHIC PROJECTIONS

In the Three Ladies Mountain area, or Domains I-V, foliation is generally parallel to compositional layering and probably related to to F1 folds. Limbs of F2 folds can be divided into a dominant limb at 075/44N

and a short limb of 135/70N. (Combination stereograms
were constructed from averages for concentrations from
each domain and used to determine the average trends
given here.) Other concentrations in Domain IV indicate
possible F1 limbs, one of which trends north and dips
moderately west, and the other of which trends southeast
and dips steeply southwest. Average F2 fold axis lies
at 334/42, approximately perpendicular to the great
circle which contains poles to foliation, indicating
that F2 folding was cylindroidal and has not been
disturbed by any major deformational event. The wide
spread in points on the stereograms can be accounted for
by F3 and F4 folding. F3 folding is difficult to define
from structural data, and may only be apparent as
changes in dip from one area to another, such as the
steeper dip of foliations at Three Ladies Mountain,
shallower to the north and south. F4 folds, which are
broad warps with a NE trend, have the most effect on the
plunge of F2 axes to NW or SE.

In Domains VI-X, including the Mount Stevenson and
Quesnel Lake area, the foliations are less steep than at
Three Ladies Mountain, but not much, with dominant
attitude of 073/36N. There is no evidence for extending
the Lightning Creek Anticlinorium (Campbell et al. 1973,
Fletcher 1972) through this area, as foliation dips
mainly north everywhere from the Little River (north
boundary of map area) to Grain Creek (southwest of Mount

Stevenson).

Axes of pre-F2 folds and F1 lineations are difficult
to distinguish from F2 structures, but it appears that
in the Three Ladies Mountain area the most northerly
axes and lineations belong to F1, whereas near Mount
Stevenson there is a distinct WNW grouping belonging to
F1 structures. Easterly-overturned, tight (not truly
isoclinal) F1B folds occur mainly in the Mount Stevenson
and Welcome Mountain areas. F1A intrafolial isoclines
occur in every domain (except XI*).

F2 axial planes from the entire area average at
118/58N, and are remarkably consistent considering the
later phases of folding. F2 fold axes from the "upper
sequence" rocks, or Domains I-IV and VII, average at
332/42, whereas F2 fold axes from the "lower sequence"
rocks, or Domains V, VI, and VIII-X, average a little
more westerly and shallower at 315/24. Foliations,
lineations, and fold axes in Domain II, which contains
the north face of Three Ladies Mountain, are unusually
steep. This may be due to later folding or faulting. A
large, asymmetrical F2 S-fold is well exposed in the
Three Ladies Mountain area; the middle limb extends from
the middle peak of Three Ladies Mountain down Marten
Creek, and has vertical foliation as well as foliation
dipping to both sides of vertical, suggesting a refolded
F1 fold.

Structural elements assigned to F3 folding are inconsistent within and between domains, attesting to the relative subordinate nature of these structures, compared with F2 folds. As kinks and crenulations do not occur on every outcrop, there are fewer data points for F3 elements, and no consistent patterns emerged from the stereonets.

Lineations are dominantly F2, parallel to F2 fold axes. For Domains II-IV, lineations group at 340/45; for Domains IV-X, at 315/30; and for Domains I and X, at 336/28 (these are interpreted as having been rotated to lower angles by faults related to the Little River Fault). Quartz rod lineations are associated with F1 folds, particularly easterly-overturned F1B folds in the Mount Stevenson area, where quartz rod lineations average 288/20.

See captions of stereographic projections for more details.

Figure 13. Equal area projections for Domain II. Three Ladies Mountain, northeast ridge. Includes hinge zone of a westerly-overturned F2 synform.

a. Foliations are folded about a calculated axis of 335/48; the dominant fold limb is 070/48N, with the shorter limb at 124/66N, subparallel to the axial plane (compare (e.)).

b., d., and f. Lineations plot at 335/44, fold axes at 332/56, and F2 fold axes at 332/56, all comparable with calculated fold axis shown in (a.). This implies that F2 folding was cylindroidal and that most of the foliations are F1 structures.

c. Poles to axial planes of folds of uncertain affinity show a grouping around 095/64N interpreted as F1 axial planes.

e. Poles to F2 axial planes are spread broadly around 125/66N; spread may be due to later broad warping with NE trend (F4).

Figure 13.

a DOMAIN 2 FOLIATION

b DOMAIN 2 LINEATIONS

c DOMAIN 2 AXIAL PLANES

d DOMAIN 2 FOLD AXES

e DOMAIN 2 F2 AXIAL PLANES

f DOMAIN 2 F2 FOLD AXES
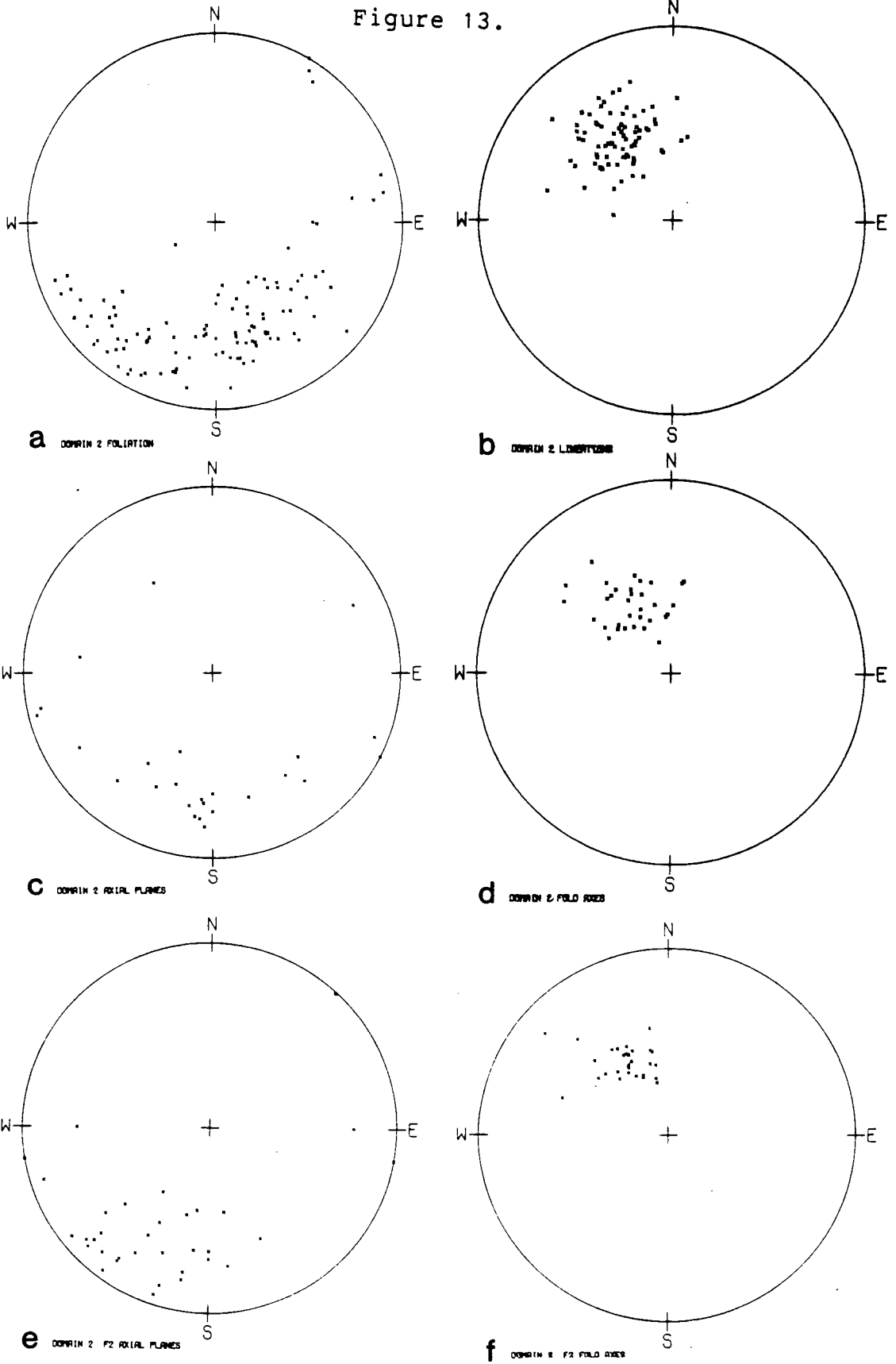
Figure 14. Equal area projections for Domain III. Three
Ladies Mountain north peak and east cirque. Includes F2
antiform and possible F1 closures.

a. Foliations are folded about a calculated axis of 352/53;
dominant limb is at 078/45N, with subordinate limb at
137/68N.

b., d., and f. Lineations plot at 340/50, fold axes at
340/50, and F2 fold axes at 338/45. Domain III has steepest
axes and lineations in entire area.

c. Non-F2 axial planes plot in 3 groups: 088/38N,
interpreted as F1; 150/34N, interpreted as possible F3(?);
and 035/85N, interpreted as F4.

e. F2 axial planes show greater spread than in some other
areas; spread may be due to later broad warping with
NE-trend (F4).

Figure 14.

a DOMAIN 3 FOLIATION

b DOMAIN 3 LINEATIONS

c DOMAIN 3 AXIAL PLANES

d DOMAIN 3 FOLD AXES

e DOMAIN 3 F2 AXIAL PLANES

f DOMAIN 3 F2 FOLD AXES
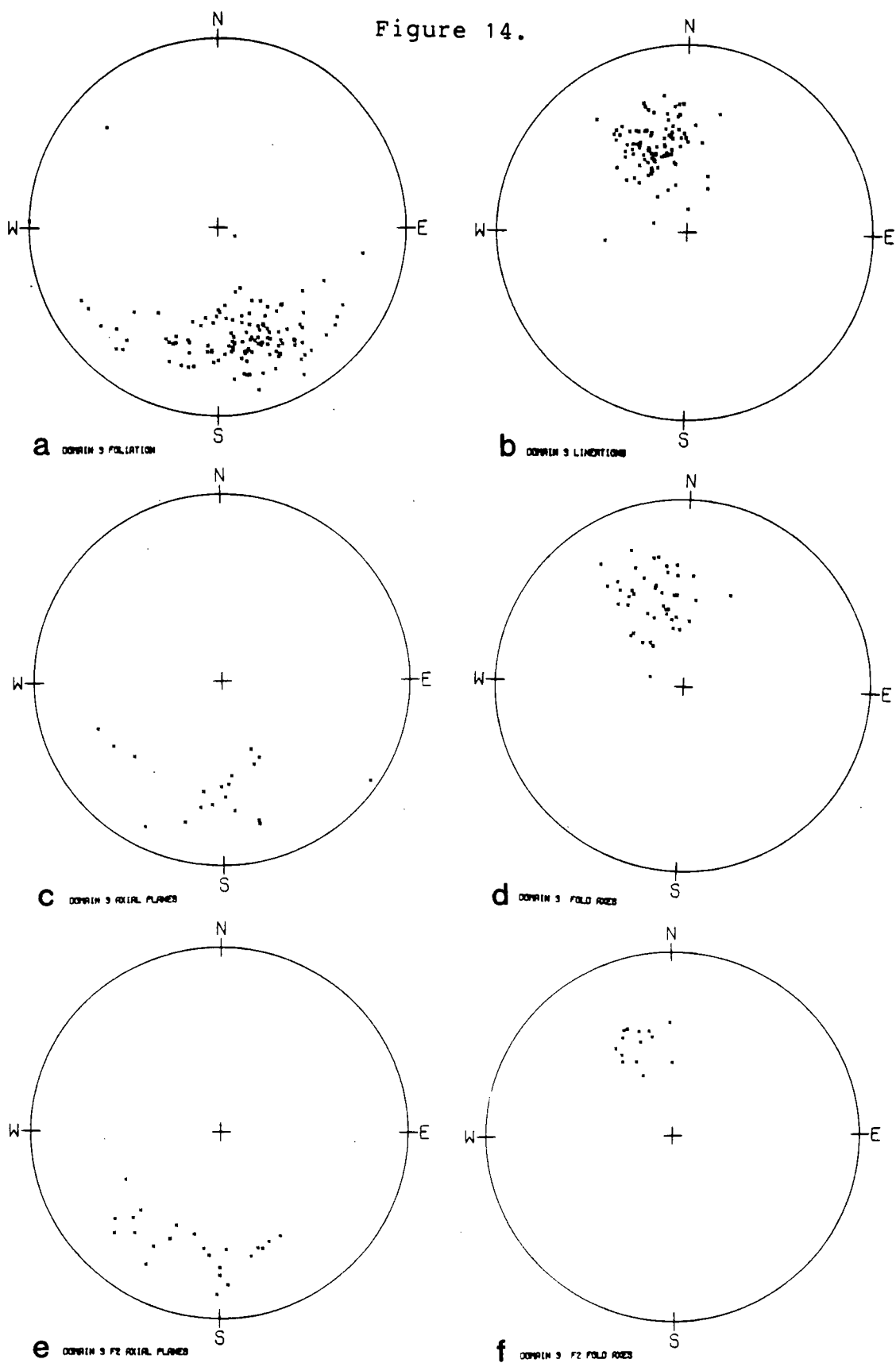
Figure 15. Equal area projections for Domain IV. Three Ladies Mountain middle and south peaks. Includes large synform in carbonate-amphibolite unit.

a. Poles to foliation show 4 concentrations. Limbs at 083/44N and 124/67N are interpreted as F2 and give a calculated fold axis of 323/40, parallel to lineations and fold axes, indicating that F2 folding was dominantly cylindroidal. Limbs at 018/46W and 142/76S (overturned equivalent of 124/67N limb) suggest control from previous F1 antiform.

b. Lineations center around 325/40, parallel to fold axes (d., f.) and to calculated axis in (a.). Wide spread of lineations suggests two groups of F1 lineations now at 350/54 and 287/26.

c. Non-F2 axial planes fall into great circle of poles to foliation folded by F2 folds; interpreted as mainly F1 axial planes.

d., f. Fold axes and F2 fold axes both plot at 324/38, parallel to the dominant lineation.

e. F2 axial planes have orientation of 109/52N.

Figure 15.

a DOMAIN 4 FOLIATION

b DOMAIN 4 LINEATIONS

c DOMAIN 4 AXIAL PLANES

d DOMAIN 4 FOLD AXES

e DOMAIN 4 F2 AXIAL PLANES

f DOMAIN 4 F2 FOLD AXES
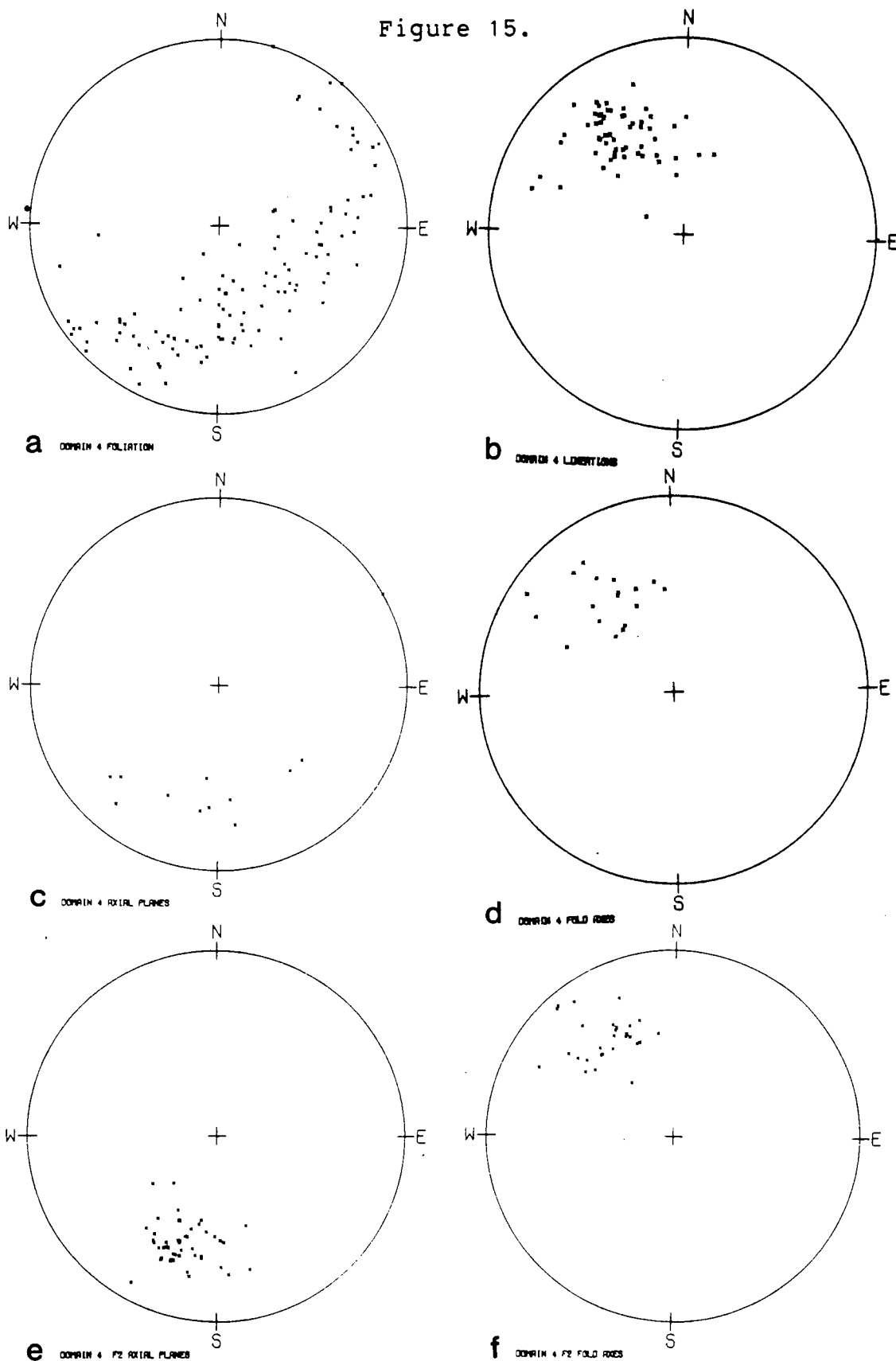
Figure 16. Equal area projections for Domain VIII, Marten Creek to Little River Fault; and Domain X, Quesnel Lake from Devoe Creek to Little River Fault. Both contain F2 antiform in Marten Creek.

a. Domain VIII. Foliation shows up in 3 groups. Limbs of antiform: 072/42N and 125/42S. Foliation rotated by drag on faults related to Little River Fault: 170/20E.

b. Domain VIII. Lineations and fold axes show concentration at 310/33 but a few near Quesnel Lake plunge SE indicating effect of F4 folding and/or drag on Little River Fault.

c. Domain X. Foliations fall into 4 groups. Limbs of Marten Creek F2 antiform: 081/27N and 124/42S. Foliations at 120/58N are approximately parallel to F2 axial planes. A fourth group loosely centered at 000/12E is interpreted as foliations rotated by Little River Fault movement.

d. Domain X. Lineations and fold axes show a broad spread with a dominant concentration at 314/22. Spread to NNW and WNW is attributed to folded F1 lineations. Southeast-plunging lineations and axes near Quesnel Lake are folded by F4 folds and/or rotated by Little River Fault.

e. Domain X. Axial planes are either F1, which fall in two groups subparallel to limbs of F2 folds at 077/37N and 136/46S; or F2, at 134/66N.

f. Domain X. Fault surfaces could be divided into two groups, one at 171/21E, interpreted as related to Little River Fault; and one at 099/23N, which is parallel to some faults at Limestone Point, which may or may not be related to Little River Fault.

Figure 16.

a DOMAIN 8 FOLIATION

b DOMAIN 8 LINEATIONS AND FOLD AXES

c DOMAIN 10 FOLIATION

d DOMAIN 10 LINEATIONS AND FOLD AXES

e DOMAIN 10 AXIAL PLANES

f DOMAIN 10 FAULT SURFACES
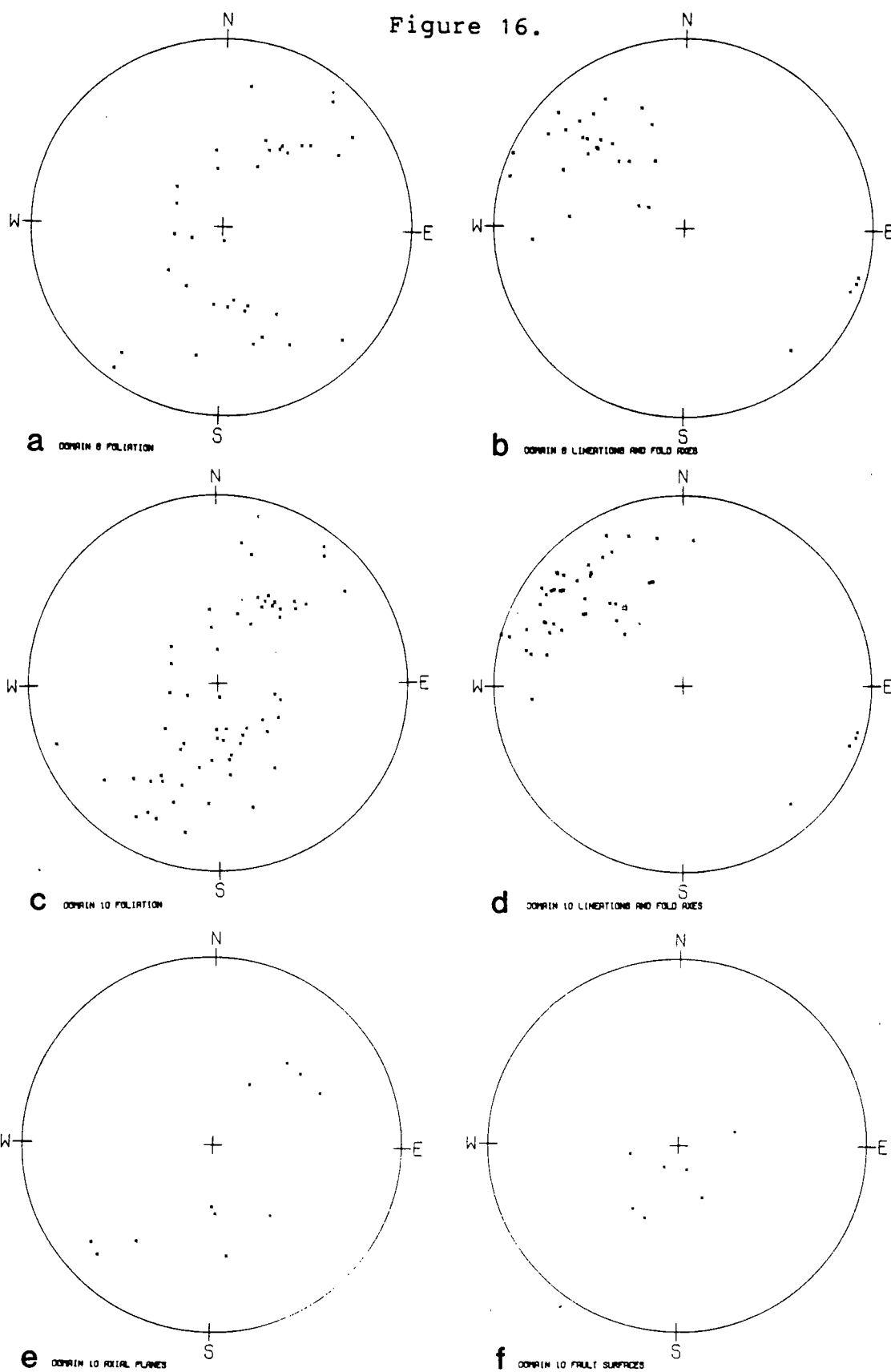
Figure 17. Equal area projections for Domains I, V, and VII, foliations and lineations. All contain areas of relatively homoclinally dipping foliations.

a. Domain I. Foliations center at 072/32N, much less steep than in Domains II and III.

b. Domain I. Lineations center at 333/28, also not as steep as in Domains II and III.

c. Domain VII. Foliations plot at 070/46N. These rocks appear very similar to those in Domain I and may be continuous with them; this would imply a large S-fold with a middle limb of about 124/67N (analogous to Domain IV) between Ishkloo Creek and Three Ladies Mountain, an area which is not well exposed.

d. Domain VII. Lineations and fold axes plot at 320/40, similar to F2 structures in Domain IV.

e. Domain V. Foliations concentrate at 082/42N, forming the dominant limb of the fold shown in Domain IV.

f. Domain V. Lineations plot at 317/34, with a few more northerly and westerly lineations interpreted in the field as F1 lineations.

Figure 17.

a DOMAIN 1 FOLIATION

b DOMAIN 1 LINEATIONS

c DOMAIN 7 FOLIATION

d DOMAIN 7 LINEATIONS AND FOLD AXES

e DOMAIN 5 FOLIATION

f DOMAIN 5 LINEATIONS
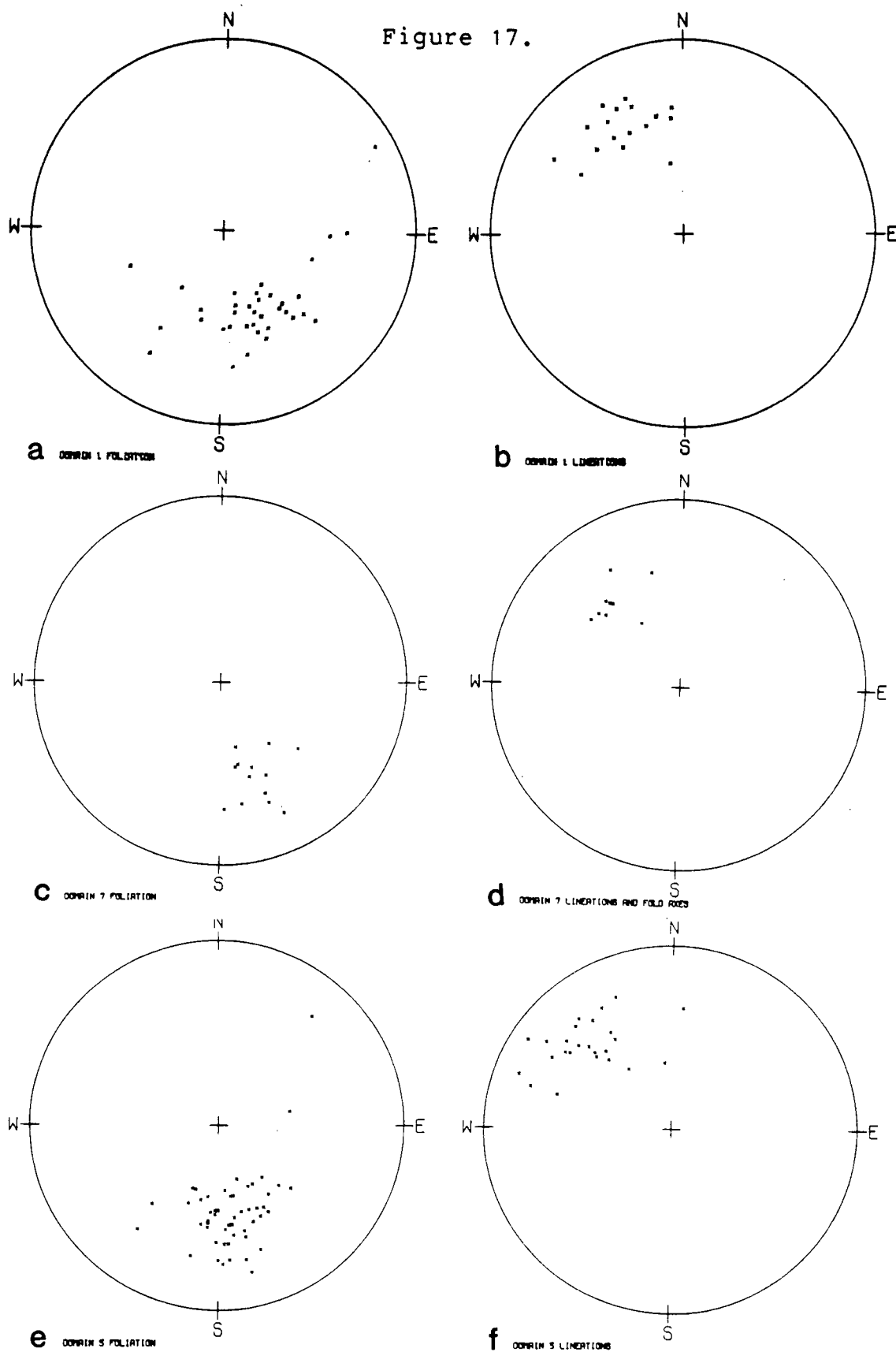
Figure 18. Equal area projections for combinations of structural elements from several domains.

a. Domain V. F2 axial planes plot at 110/47, approximately parallel to those in Domain IV.

b. Domains I-V, IX. Poles to contacts of pegmatite dikes plot around 121/62N, subparallel to F2 axial planes.

c. Domains I-V, IX, and X. F3 axial planes. Three groups emerge: one at 048/56S, approximately perpendicular to F2 fold axes and parallel to the dominant joint set; one at 158/61S; and one at 166/61E. These might be interpreted as conjugate kinks, but actual field relations of these two sets are unknown.

d. Domains II-VI, VIII, and IX. Crenulation lineations plot all over the NE quadrant of the stereonet centering at 054/36. They could be interpreted as related to either F3 or F4 folds.

e. Domains I-V, VI, and IX. Poles to contacts of planar quartz veins fall into two groups; one approximately parallel to metamorphic foliation, and one at 050/90, subparallel to F4 axial planes.

f. Domains I-V, VI, IX, and X. F4 fold axes plunge 035/16. F4 axial planes were too few to plot but average around 040/90.

Figure 18.

a DOMAIN 5 F2 AXIAL PLANES

b DOMAINS 1-5.9 ORIENTATION OF PEGMATITE DIKES

c DOMAINS 1-5.9.10 F3 AXIAL PLANES

d DOMAINS 2-5.8.9 CRENULATION LINEATIONS

e DOMAINS 1-5.8.9 QUARTZ VEINS

f DOMAINS 1-5.8.9.10 F4 FOLD AXES
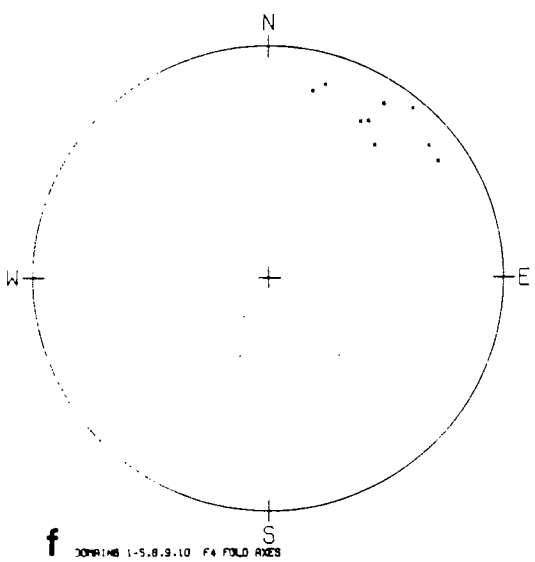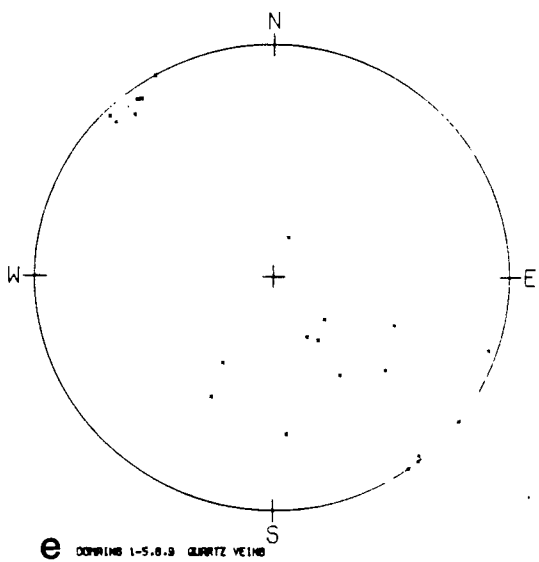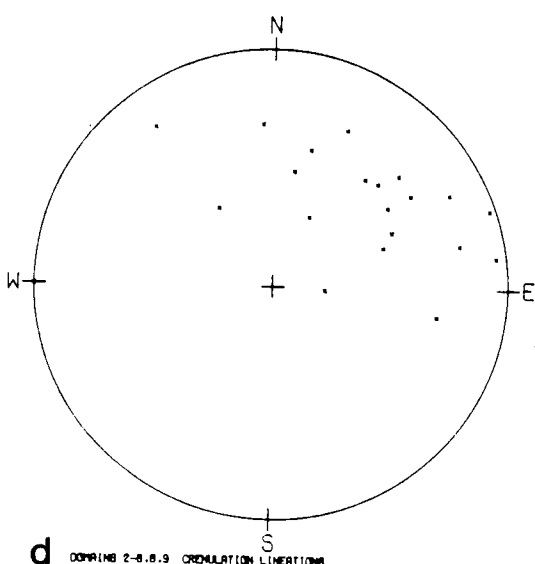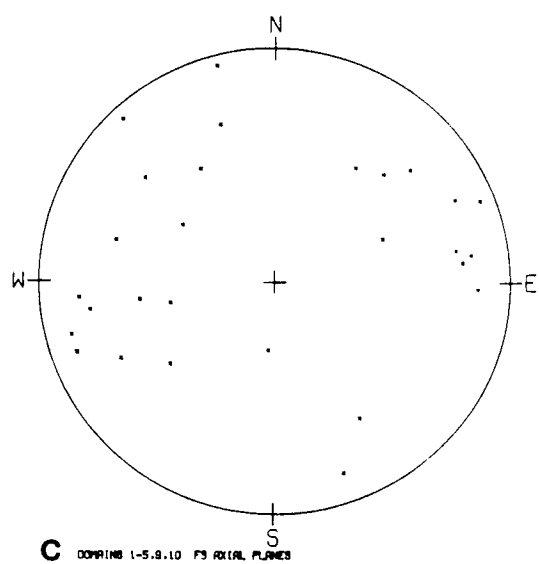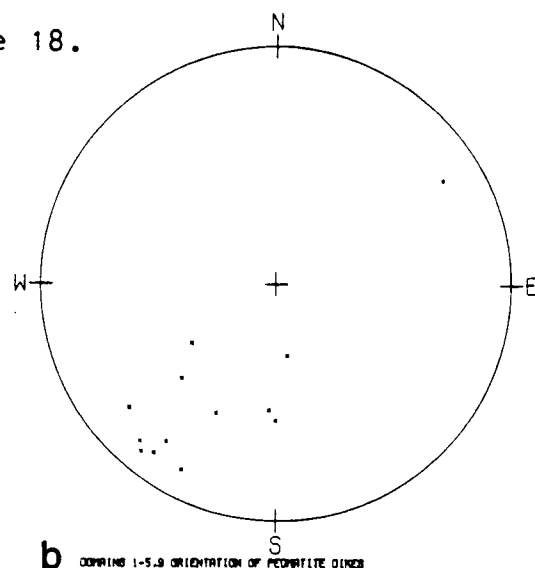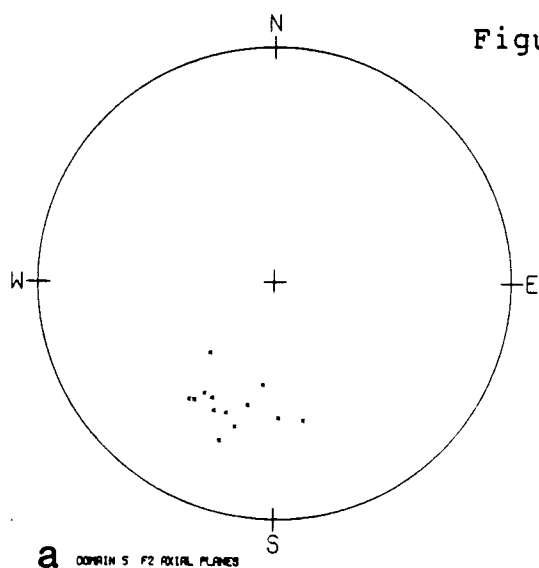
Figure 19. Equal area projections of pre-F2 fold elements for combinations of domains; and F2 fold elements in Domain IX, Mount Stevenson area.

a. Domains II-IV, VI, and X. Axial planes of pre-F2 folds plot in two groups. East-verging F1B folds plot around 177/29W, whereas other F1 folds including F1A isoclines are parallel to foliation at 084/48N.

b. Domains II, III, and V. F1 fold axes show a spread from WNW to NNW and NE.

c. Domain IX. Axial planes of pre-F2 folds can be divided into two groups which are roughly concordant with foliation (see Figure 20 (c.)), one at 041/24N (easterly overturned) and one at 143/43S.

d. Domains VI and IX. F1 fold axes are concentrated at 295/16, more westerly and shallower than F2 axes.

e. Domain IX. F2 axial planes plot at 116/54N, similar to those near Three Ladies Mountain.

f. Domain IX. F2 fold axes plot at 314/25. F2 structures near Mount Stevenson are consistent with but less steeply dipping than those near Three Ladies Mountain.

Figure 19.

a DOMAINS 2,3,4,6,10 AXIAL PLANES OF E-VERDINO AND PRE-F2 FOLDS

b DOMAINS 2,3,5 F1 FOLD AXES

c DOMAIN 9 AXIAL PLANES OF EAST-VERDINO AND PRE-F2 FOLDS

d DOMAINS 6 AND 9 F1 FOLD AXES

e DOMAIN 9 F2 AXIAL PLANES

f DOMAIN 9 F2 FOLD AXES
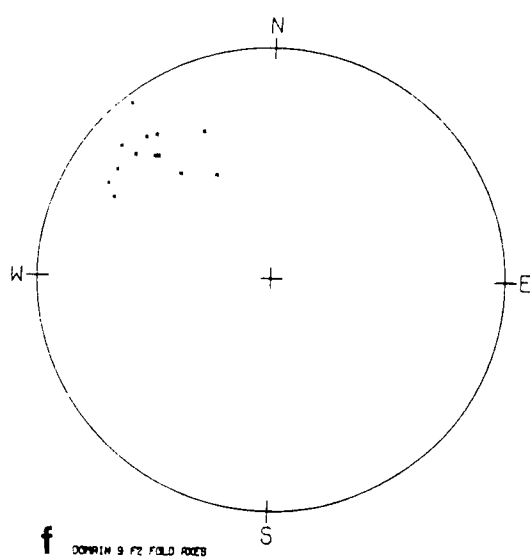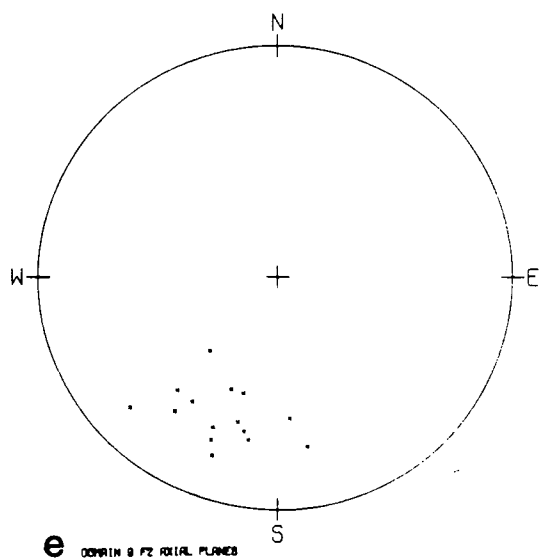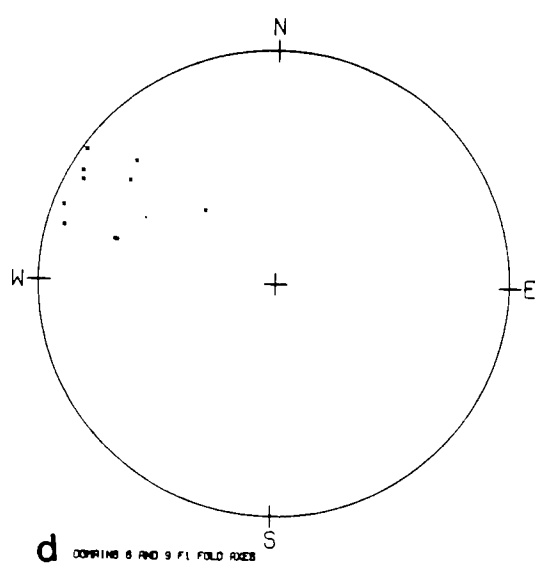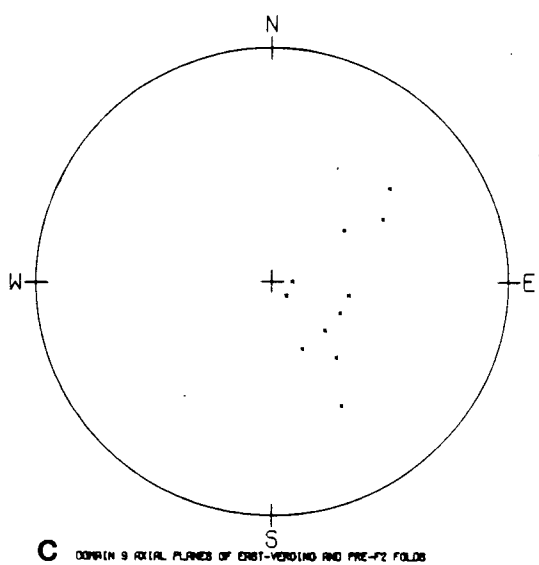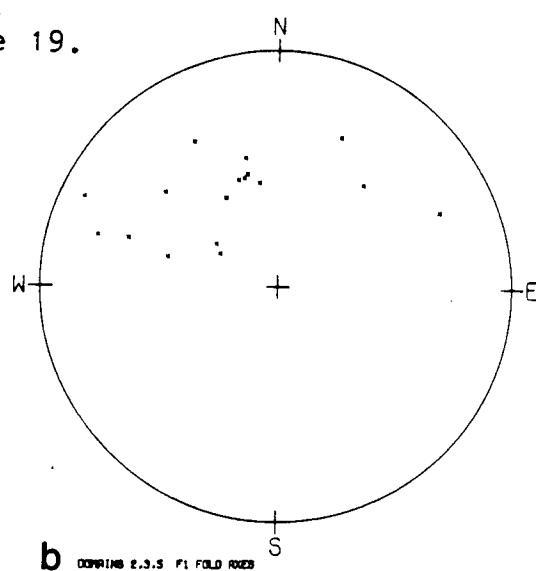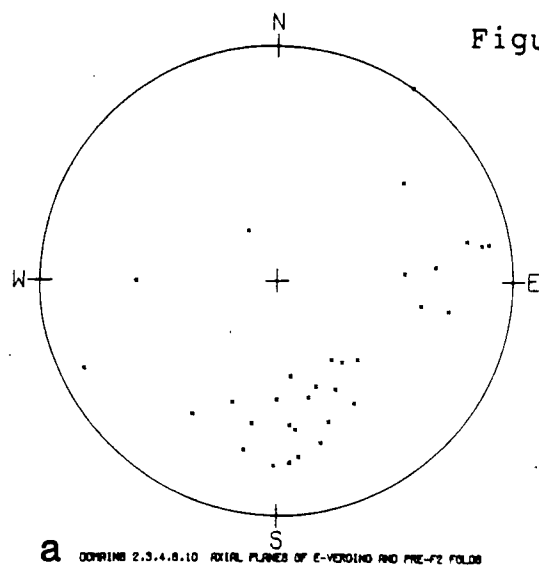
Figure 20. Equal area projections for Domains VI and IX.
Mount Stevenson area.

a. Domain VI. Foliations are concentrated mainly at
076/36N except near fault in upper Long Creek.

b. Domain VI. Lineations and fold axes plot around 315/16
except those plunging SE where folded adjacent to fault in
upper Long Creek.

c. Domain IX. Foliations plot mainly at 073/29N with some
SW-dipping foliations from south of Mount Stevenson.

d. Domain IX. Lineations plot in 3 groups. F1 lineations
plot at 251/16; F2 lineations at 314/22; and F4 lineations
at 028/05. These are all more gently plunging than at Three
Ladies Mountain.

e. Domain IX. Foliation in quartz dioritic gneiss is
generally parallel to foliation in other rocks; the spread
of poles indicates a calculated axis of 314/25, indicating
that the quartz dioritic gneiss is folded cylindroidally by
F2 folds.

f. Domain IX. Fold axes (not F2) plot at 311/27.

65

Figure 20.

a DOMAIN 8 FOLIATION

b DOMAIN 8 LINEATIONS AND FOLD AXES

c DOMAIN 9 FOLIATION

d DOMAIN 9 LINEATIONS

e DOMAIN 9 FOLIATION IN QUARTZ DIORITIC GNEISS

f DOMAIN 9 FOLD AXES
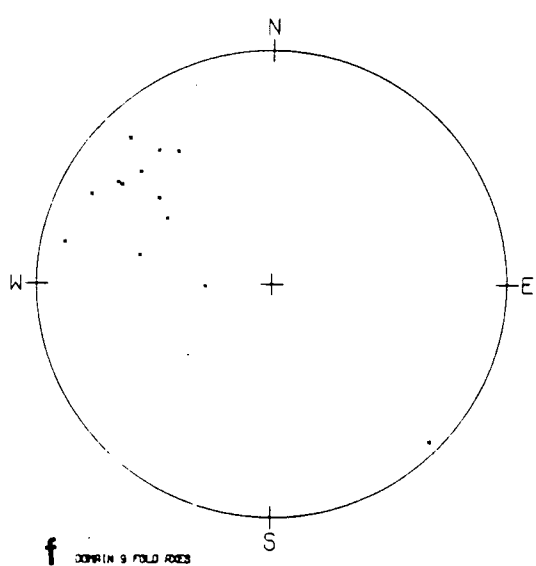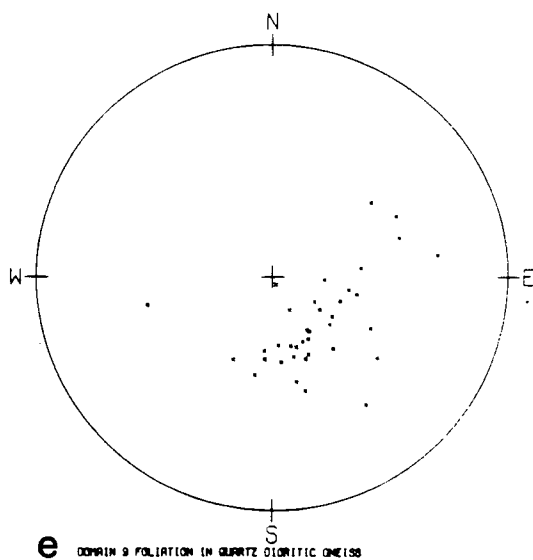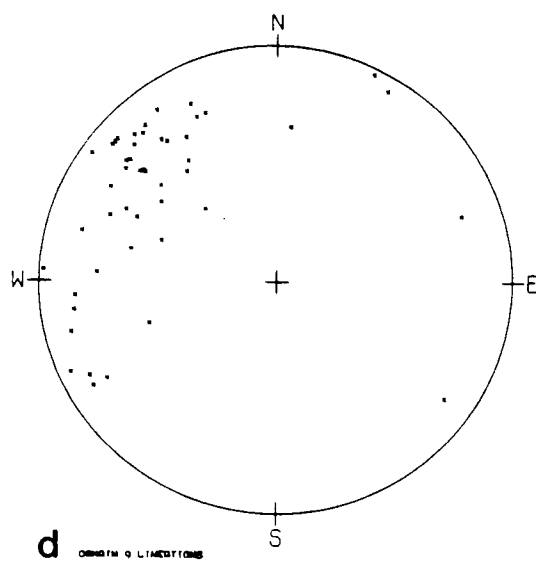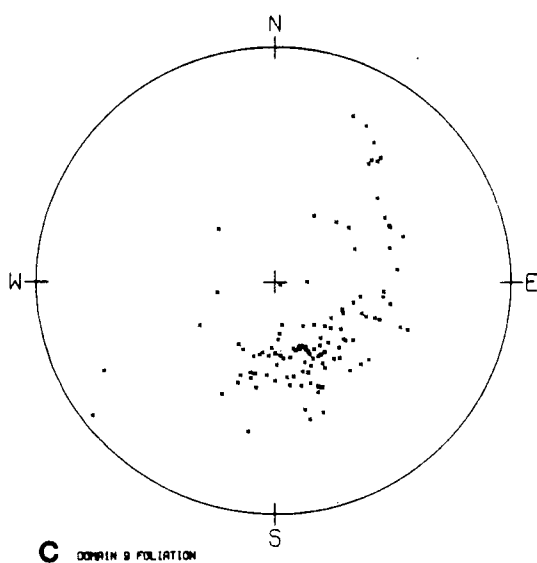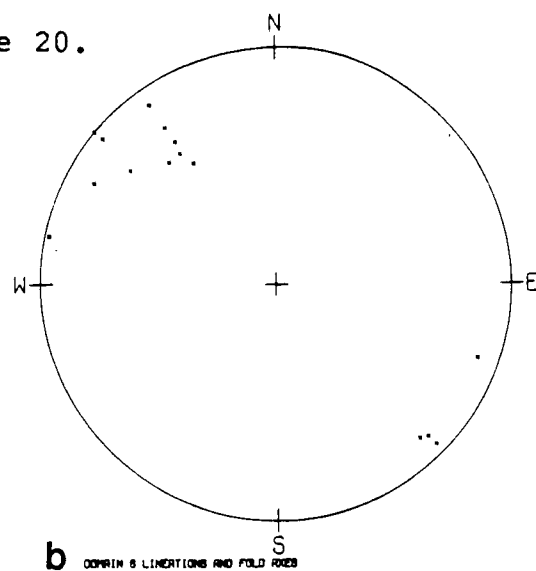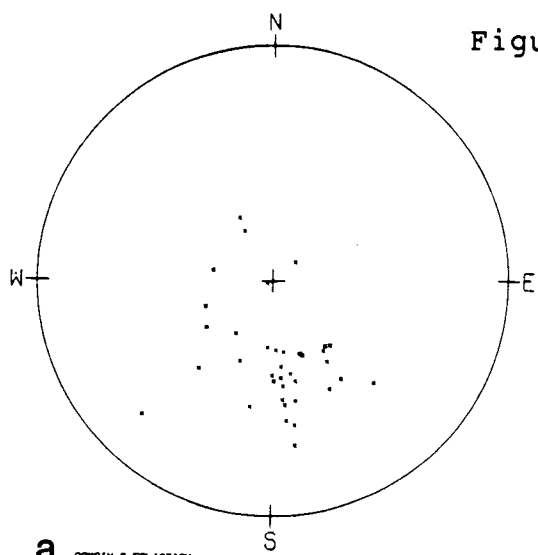
Figure 21. Equal area projections of fault surfaces, slickensides, and joints.

a. Domains I-V. Three Ladies Mountain. Fault surfaces dip shallowly east, and are interpreted as related to the Little River Fault.

b. Domains I-V. Three Ladies Mountain. Slickensides point mostly toward 118 with low plunge; field evidence such as displacement and drag indicates movement of top down to SE.

c. Domains VI and IX, Mount Stevenson. Fault surfaces dip shallowly in every direction.

d. Domains VI and IX. Slickensides point to NE, SE, and SW.

e. Domains I-V, VIII-XI. Fault surfaces are generally shallowly-dipping, and if related, center around 178/16E, which is parallel to part of the Little River Fault near Quesnel Lake. Because the Little River Fault is curved, all of these fault surfaces may be related to it.

f. Domains I-V, VIII, and IX. Poles to joint surfaces are concentrated in the northwest quadrant, indicating that most joints measured are perpendicular to F2 fold axes (perpendicular to 324/45) at 054/45S. Some overlap with fault surfaces is expected as some of these joint planes show displacment and drag indicating movement of top down to southeast.

Figure 21.

a DOMAINS 1-5 FAULT SURFACES

b DOMAINS 1-5 SLICKENSIDES

c DOMAINS 8 AND 9 FAULT SURFACES

d DOMAINS 8 AND 9 SLICKENSIDES

e DOMAINS 1-5,8,9,10,11 FAULTS

f DOMAINS 1-5,8,9 JOINTS
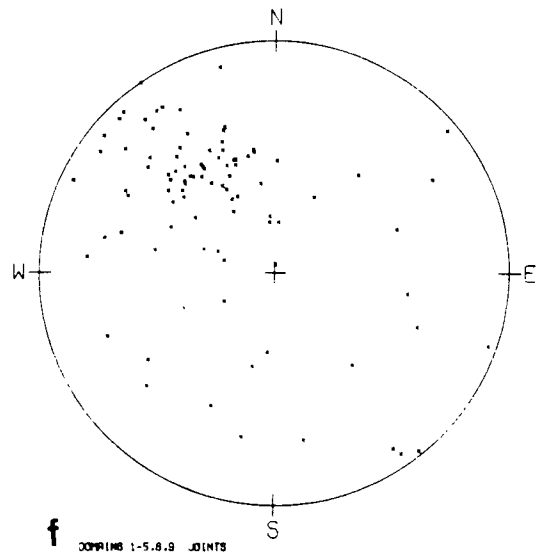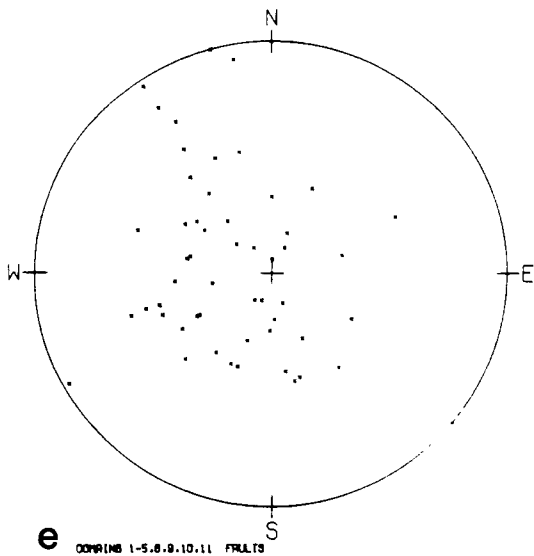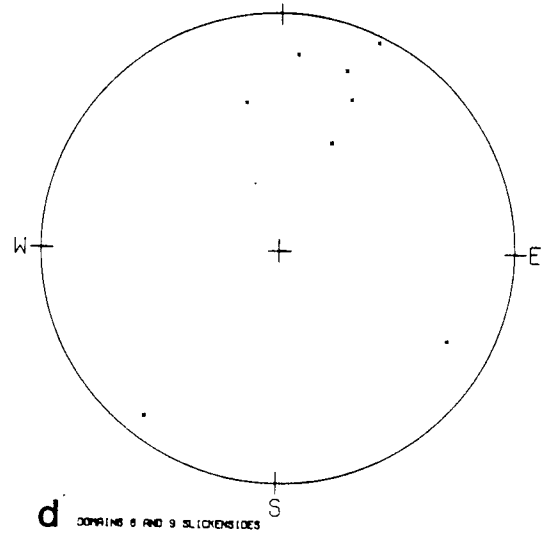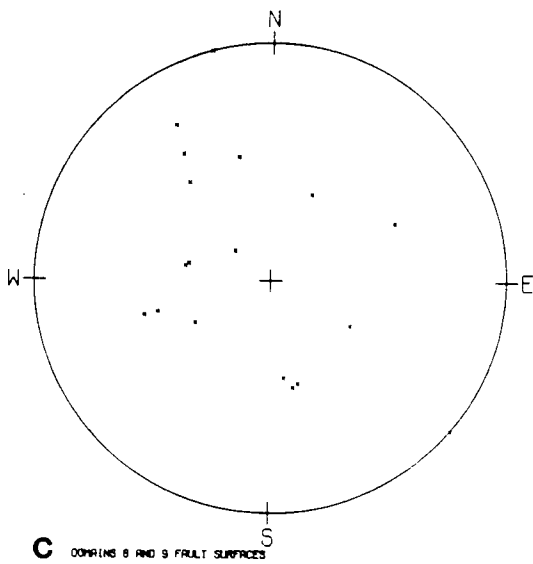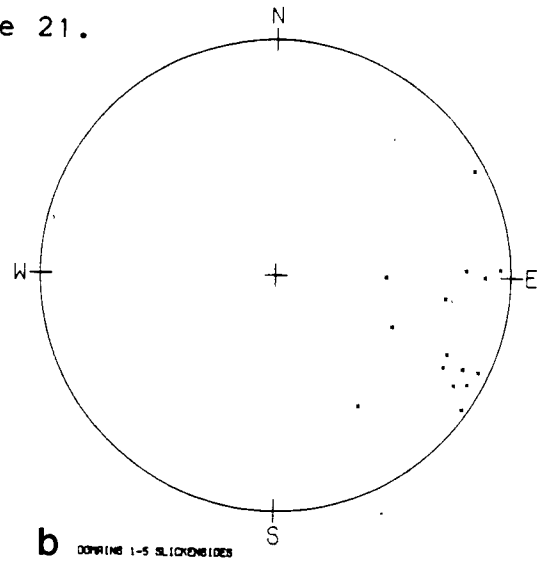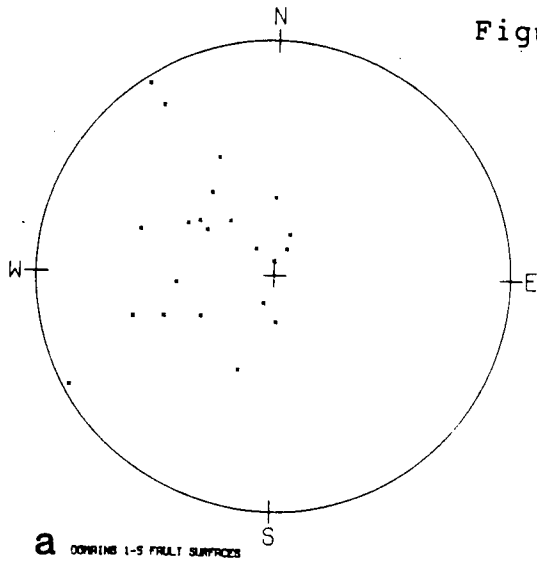
Figure 22. Equal area projections of structural elements in hanging wall of Little River Fault, Domain XI.

a. Bedding and compositional layering in marble plot at 097/21N.

b. Bedding and compositional layering in phyllite and quartzite plot at 108/24N, not too different from bedding in marble.

c. Foliation in phyllite/quartzite is axial planar to "F2" folding at 139/60N.

d. Fold axes and lineations plot mainly at 342/12, more shallow than in the underlying Snowshoe Group schist. These are mainly "F2" structures. Spread to SE indicates change of plunge due to NE-trending F4 warping.

e. Axial planes of F3 kinks in phyllite plot at 174/60N, whereas F2 axial planes in marble plot at 118/69N.

Additional measurements taken in 1982 were not plotted on these stereonets but confirm F2 axial planes consistent with those in the Snowshoe Group; and the presence of a broad F4 anticline trending NE on Service Ridge, which intersects with an F2 antiform at "6287'", forming a domal interference pattern.

Figure 22.
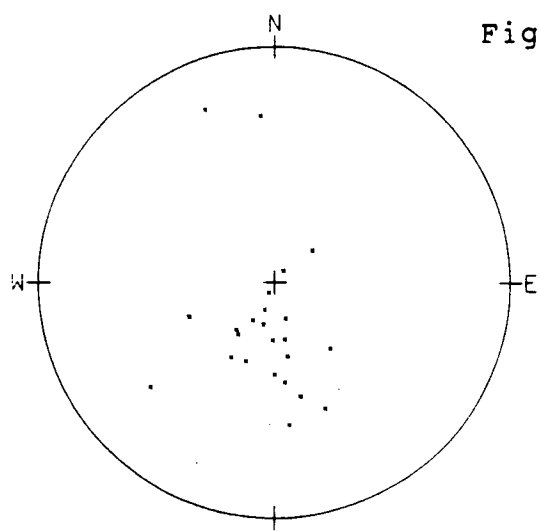
a DOMAIN 11 BEDDING AND COMPOSITIONAL LAYERING IN MARBLE
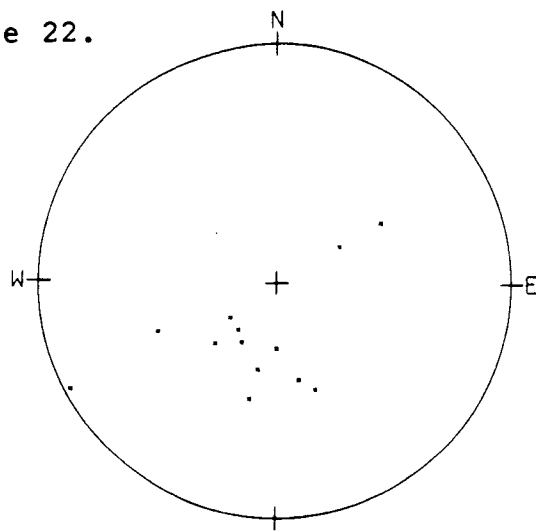
b DOMAIN 11 BEDDING AND COMPOSITIONAL LAYERING IN PHYLLITE/QUARTZITE
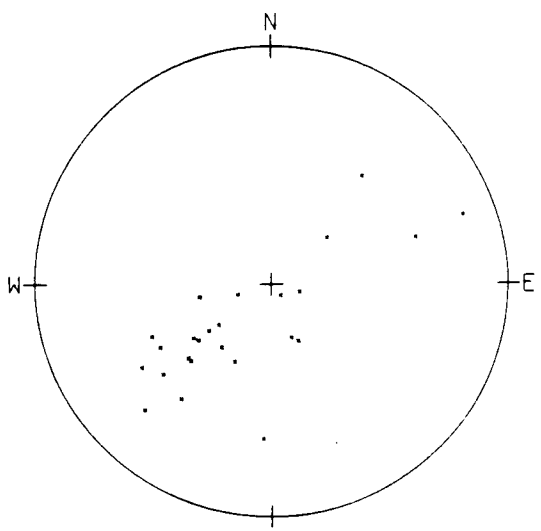
c DOMAIN 11 FOLIATION IN PHYLLITE/QUARTZITE
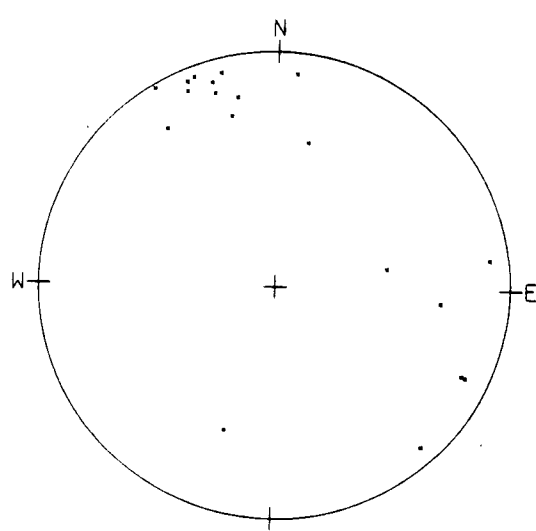
d DOMAIN 11 FOLD AXES AND LINEATIONS
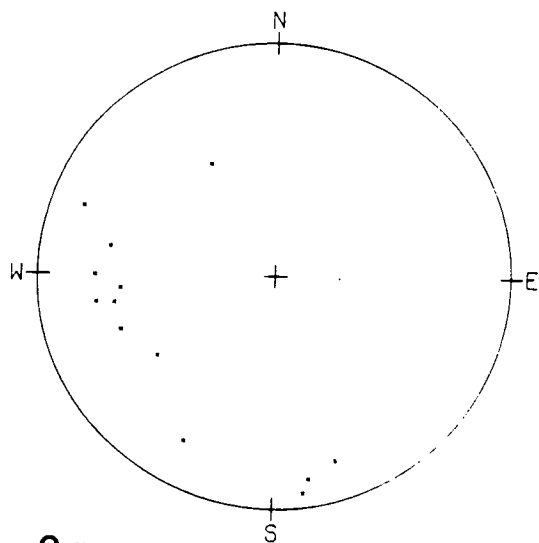
e DOMAIN 11 AXIAL PLANES

3.2.4 <u>SUMMARY OF FOLDING</u>

Metamorphic rocks in the Three Ladies Mountain area were folded first by folds which are now tight to isoclinal and subparallel with F2 folds; quartz rods developed during early folding. F2 folding was accomplished mainly by a combination of buckling in more competent layers and shear folding in less competent layers, producing flattened flexure folds transitional between true similar folds and pure flexural slip folds Dominant southwesterly-overturned F2 fold geometry across the entire study area suggests maximum compressive strain in a northeast-southwest direction, and a sense of shear implying northeast over southwest translation. Alignment of minerals parallel to fold axes implies elongation in a northwest-southeast direction.

The nearly coaxial orientation of F1 and F2 folds, and possibly F3 folds, implies fairly constant orientation of strain directions and maximum compressive stress during progressive deformation over a time period which spanned an entire metamorphic episode. F4 folds, which are perpendicular to dominant earlier trends, may have formed late during uplift.

3.3 DEFORMATION: FAULTING

3.3.1 LITTLE RIVER FAULT

One major fault zone (Little River Fault) and numerous minor faults were identified in the Three Ladies Mountain/Mount Stevenson area.

The Little River Fault, which separates higher grade schist and gneiss in the footwall from lower grade metasedimentary rocks in the hanging wall, was mapped by Klepacki (1981) near Maeford Lake, immediately north of the present map area. In this study, the continuation of the fault was traced from the saddle west of Service Mountain south down Service Creek, and thence west of Limestone Point into Quesnel Lake. Klepacki (1981) found that in the Maeford Lake area the Little River fault dips shallowly to the east, whereas toward Quesnel Lake the dip is more variable, although still generally east-dipping. Where it intersects Quesnel Lake, the orientation of the fault is about 170/20 E. The fault surface appears to be convexly curved rather than planar. This curvature is seen in the shape of the rounded ridge east of Three Ladies Mountain, believed to have formed as the fault surface was exhumed by erosion (see Figure 23).

The fault trace itself is poorly exposed. Where it crops out at Quesnel Lake, it is marked by a brittle zone several tens of meters wide featuring fractured,
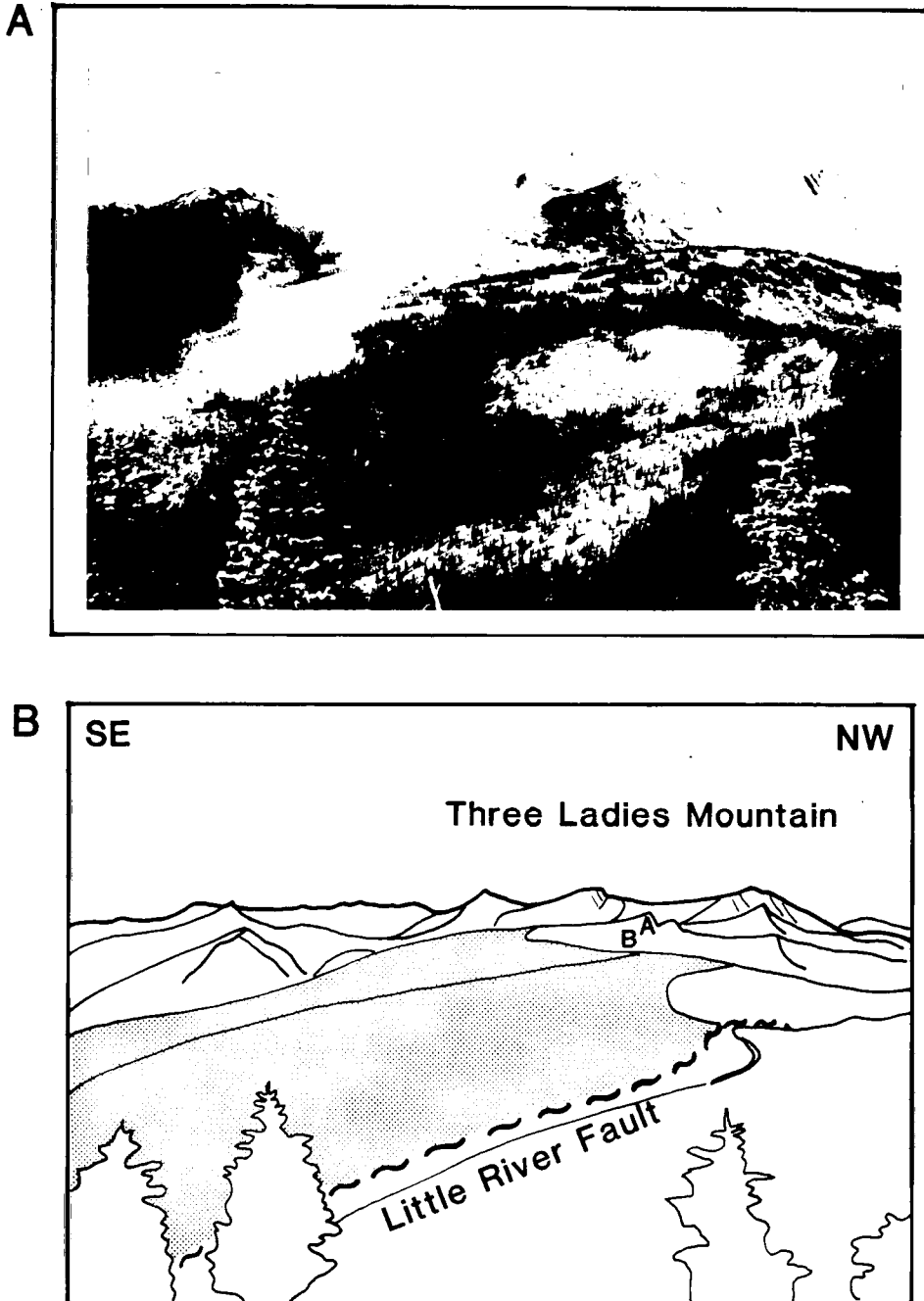
Figure 23.   A.   View of Three Ladies Mountain from Service
Mountain.

B.   Sketch of view in A showing trace of Little River Fault
and exhumed tectonic denudation surface (stippled).   A and B
refer to Figure 24 A and B, respectively.

non-cohesive, phacoidal, graphitic rocks barely
recognizable as original schist, quartzite, or
pegmatite. Microscopic strain markers were not
investigated.

The footwall rocks include coarse-grained Bralco
marble (Struik 1983) and underlying metamorphic rocks of
Snowshoe Formation (late Proterozoic to Paleozoic) and
probable Paleozoic granitoid gneisses. The hanging wall
rocks, some of which were mapped by Klepacki (1981) as
Yankee Belle Formation, consist of a series of marble
layers intercalated with phyllite and fine-grained
quartzite. These are mapped as late Proterozoic to
Cambrian Cariboo Group, undivided. Although the ages of
the two sets of rocks may be similar, the Snowshoe
Formation and Cariboo Group cannot be correlated (Struik
1982).

The Little River Fault crosscuts complex fold
structures on both sides of the fault. The Snowshoe
Group rocks in the footwall were folded at least once
and intruded by at least two types of granitoid sills
prior to F2 folding, whereas the hanging wall rocks show
very little evidence for pre-F2 structures. Only a few
isoclinal folds were observed in the marble on Service
Mountain parallel to layering, and bedding is still
identifiable in some of the phyllitic units, crosscut by
later (F2 and F3) cleavages. Although the structural
and metamorphic history in the footwall rocks appears to

have begun earlier and is more complex than in the hanging wall rocks, the similarities in F2 and later fold episodes are notable considering the difference in metamorphic grade and proposed stratigraphic packages across the fault.

The designation "F2" is used for folds which are characterized on both sides of the fault by northeast-dipping axial planes, consistent southwest vergence, and an association with maximum metamorphic recrystallization. Usage of F2 in this sense equals F1 folds as mapped by Klepacki (1981). Plunge of F2 axes in the footwall rocks is steep to the northwest except near Quesnel Lake, where it is near horizontal or to the southeast; plunge of F2 axes in the hanging wall is generally shallower, to the northwest west of the ridge, and to the southeast or variable near Quesnel Lake (see Figure 9, and Plates I and IV). These reversals in plunge are due to a combination of drag on the Little River Fault and superimposed F4 folding.

In the footwall, prograde metamorphism associated with F2 folding reached amphibolite facies, with staurolite-kyanite zone on the ridge, and sillimanite zone at Quesnel Lake. F3 kink-folding was accompanied or followed by retrograde metamorphism indicated by growth, perhaps mimetic, of chlorite along F3 axial planes. Prograde metamorphism associated with F2 folding reached greenschist facies in the hanging

wall with the development of recrystallized marble and chlorite-sericite phyllite on the ridge, and chlorite-sericite-biotite phyllite at Quesnel Lake. Recrystallization during F3 folding was at approximately the same grade, resulting in two different cleavages outlined by chlorite in some phyllites. "Retrograde" metamorphism associated with F3 folding was characterized in both footwall and hanging wall rocks by growth of chlorite, suggesting that both packages of rock were in approximately the same metamorphic P/T regime around the time of completion of F3 folding. At least some relative displacement bringing the lower grade rocks closer to the higher grade rocks had therefore occurred either postkinematic to or, more likely, synkinematic with F3 folding. On the eastern flank of Service Mountain, axial planes of some F3 folds trend around 010/30 E, approximately parallel to minor fault surfaces believed to be related to the Little River Fault.

Evidence from kinematic indicators in the Snowshoe Group (below the projection of the trace of the Little River Fault toward Three Ladies Mountain) indicates that movement in the hanging wall was east-southeast relative to the footwall. Minor structures believed to be related to movement along the Little River Fault, such as slickensides (see stereographic projections and Plate VI) and drag features associated with repeated fault

surfaces, show consistent orientation toward the southeast. Many minor fault zones are found near-parallel to the unusual rounded meadow slope east of Three Ladies Mountain to Quesnel Lake, which could be an exhumed fault surface related to the Little River Fault (see figure S10). Minor numerous faults are observed with various orientations ranging from parallel to joint planes which are perpendicular to F2 fold axes, to northeast dipping to eastward dipping. It looks as though any available surface--joint planes, foliation planes, and axial planes--took up part of the movement. Slickensides on joint-parallel faults show movement to have been down toward 118 (ESE), confirmed by drag of F2 fold axes and lineations in the same direction, near the joint surfaces showing the displacement Small displacements are common, no more than ten meters. However, on surfaces spaced less than one meter to ten meters apart for at least 500 m below what may have been the original, major fault surface (now just above Three Ladies Mountain), the combined displacement could be very large. The joint-parallel faults are particularly evident in the carbonate-amphibolite unit that makes up the north slope of Three Ladies Mountain. In some places, marble has been remobilized and smeared into fractures perpendicular to F2 fold axes and lineations (see Figure 24). The marble consists of fine-grained, finely-laminated calcite, with thin graphitic horizons
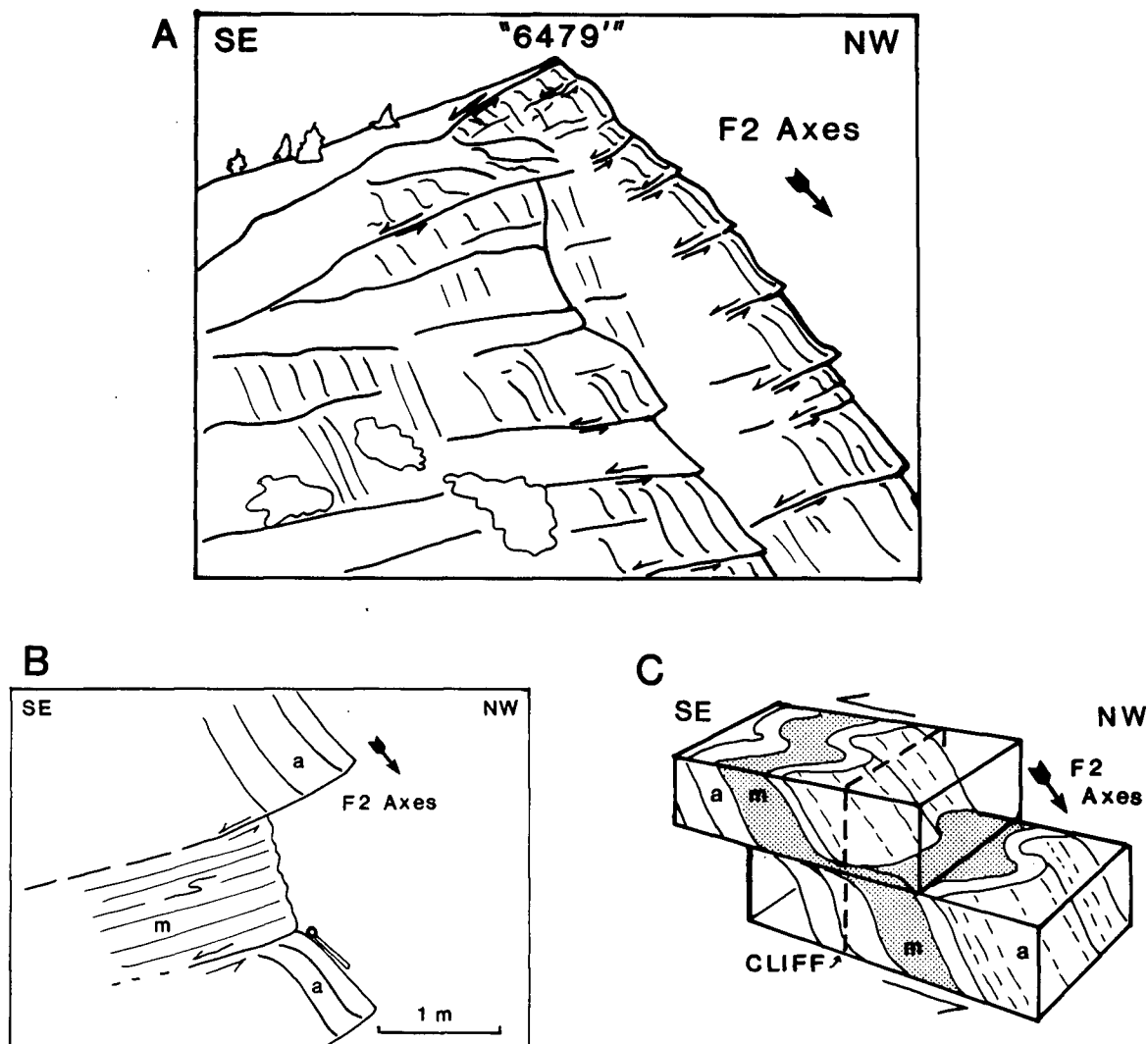
Figure 24.   Structures below but related to Little River Fault; for location see Figure 23 B.

A.   Multiple joints perpendicular to F2 fold axes in folded quartzite and pelite showing drag features of top down to southeast.   Cliff height is about 20 m.

B. 150 m below A.   Marble (m) (1-2 m thick) is smeared along fracture perpendicular to dominant fold structures in amphibolite unit (a).

C.   Schematic block diagram showing how marble (m; stippled) intercalated with amphibolite (a) could have been smeared along fault surface as upper block was displaced to southeast.

which are folded such that the axial planes are perpendicular to F2 fold axes and parallel to the shear zone.

Closer to Quesnel Lake, these minor fault surfaces show variable attitudes, but retain ESE slickensides and drag features. The average attitude of faults in the whole area is about 170/20 E, parallel to some fault surfaces measured in the fault zone, and consistent with the attitude of the fault trace near Limestone Point.

Displacement on the Little River Fault is unknown. The most recent movement was hanging wall down toward the east and southeast relative to the footwall. This could have been merely the latest episode of displacement due to differential uplift.

The metamorphic difference across the trace of the Little River Fault could be as much as 200°C and 2 kb, indicating a possible throw of as much as about 6 km. This is based on an assumption of a typical Barrovian P-T path, with the kyanite/sillimanite zone rocks at approximately 5 to 7 kb and 500° to 600°C, and the adjacent chlorite and biotite zone rocks at approximately 3 to 4 kb and 300° to 400°C (see section on metamorphic petrology). The continuation of the Little River Fault from where it disappears into Quesnel Lake is unknown, although the shape of its surface suggests it continues south along the North Arm of Quesnel Lake, at least as far south as Marten Creek.

The difference in metamorphic grade across the North Arm of Quesnel Lake has been ascribed to a late normal fault (Campbell and Campbell 1969), but it is probably due to earlier movement on the Little River Fault. Topographic evidence, such as the contrast in elevation between Three Ladies Mountain and Mount Watt, suggests that if there is a late normal fault in the North Arm of Quesnel Lake, it has downdropped the west side by a few hundred meters, not uplifted it, as implied by Campbell and Campbell (1969).

No definite premetamorphic faults were identified in the Three Ladies Mountain/Mount Stevenson area. Premetamorphic movement on the Little River Fault itself would be difficult to establish. There is no evidence for a recrystallized mylonitic zone near the Little River Fault. Two possible tectonic slides, parallel to foliation, have been mapped along attenuated limbs of F2 folds where marker units (carbonate-amphibolite) are truncated by apparently continuous layers of foliated micaceous quartzite and pelitic schist (see map Plate I). Northeast of Three Ladies Mountain, the amphibolite plus carbonate unit is folded synformally, and then lost in the pelitic plus quartzitic unit that continues all the way up to the base of the Bralco marble. Near Three Ladies Mountain middle peak, it looks as though a band of pelite has been transposed into the axial plane of the large F2 fold, and crosscut the adjacent layer of

amphibolite plus carbonate. An alternative explanation for these structures is that they represent hinge zones of F1 folds, refolded by the F2 folds.

3.3.2 DISCUSSION OF LITTLE RIVER FAULT

Struik (1982) proposed a premetamorphic fault, called the Pleasant Valley Thrust, separating known Cariboo Group stratigraphy on the northeast side (hanging wall) from Snowshoe Group units on the southwest side (footwall). The Pleasant Valley Thrust is said to delineate the eastern margin of Snowshoe Group rocks from north and east of Wells and Barkerville to east of the North Arm of Quesnel Lake. It is defined mainly on the basis of contrast between major lithostratigraphic packages, and is difficult to identify in the field, although it is supposed to be a major terrane boundary. Struik (1983) proposes that the northern contact of the Bralco marble at Maeford Lake is a high-angle fault which may be part of the Pleasant Valley Thrust. The rocks to the north of this fault have been mapped by Klepacki (1981) as schist and marble of Cariboo Group, also in the footwall of the Little River Fault. Mapping in this study interpreted this fault as a late normal fault with little displacement, which has resulted in a small topographic scarp (on the order of tens of meters) at Maeford Lake; rocks on the north (down) side are obsured by cover, or outside the limits mapped here. Although this fault appears to intersect the Little River Fault on the ridge west of Service Mountain, it is not clear from field relations whether either fault offsets the other. However,

present topography suggests that the Little River Fault surface was raised slightly to the southwest, and has been eroded away. It is possible that this small normal displacement is a reactivation of an older fault.

Struik (1983) shows the continuation of the Pleasant Valley Thrust into the hanging wall of the Little River Fault north of Limestone Point. Here the Pleasant Valley Thrust trace is mapped (by Struik) along the lower part of Service Creek between the marble and clastic rocks of Limestone Point (footwall) and the phyllites and marbles above (hanging wall). Mapping in the same area revealed mainly sparse outcrops of nondistinctive calcareous phyllite, a difference in metamorphic grade from biotite zone to chlorite zone, and minor fault surfaces near-parallel to bedding and foliation in breccia in the marble at Limestone Point (110/25 N). Such evidence might support slight syn- or postmetamorphic movement on a surface parallel to layering somewhere in the vicinity of Limestone Point, but does not necessarily confirm or deny the existence of the Pleasant Valley Thrust as mapped by Struik (1983). Geometrically it would be difficult to justify continuing a high-angle fault from the footwall into nearly adjacent hanging wall rocks, considering the direction and possible large magnitude of movement on the Little River Fault which is supposed to postdate the higher-angle fault.

The chlorite-biotite zone rocks of the Cariboo Group (?) were presumably at higher levels in the crust at the time of metamorphism than were the staurolite to sillimanite zone rocks of the Snowshoe Group, unless the isotherms were steeply inclined to the earth's surface. Structural evidence indicates that the low-grade rocks in the hanging wall of the Little River Fault slid over or down relative to the higher-grade rocks in the footwall, implying that the hanging wall was structurally higher than the footwall prior to the latest movement on the Little River Fault. This evidence requires that nearly unmetamorphosed late Proterozoic to Cambrian sediments must have been emplaced above prefolded late Proterozoic to Paleozoic sediments which had been intruded by quartz dioritic and granodioritic bodies in the early Paleozoic. Although the Cariboo Group may in fact be younger than the Snowshoe Group, it is older than the orthogneisses intruded into the Snowshoe Group. The Cariboo Group (?) was not intruded by these bodies, so was probably not immediately adjacent to the Snowshoe Group in the early Paleozoic. Rocks of the Cariboo Group (?) could have been thrust over rocks of the Snowshoe Group from east to west (or Snowshoe Group underthrust from west) at some time prior to peak metamorphism, probably synkinematic with F2 folding, as suggested by Struik (1982).

This type of east-over-west movement could have occurred partly on the proposed surface of the Pleasant Valley Thrust, along which the Cariboo Group and Snowshoe Group are now juxtaposed (Struik 1982). In the Three Ladies Mountain area, the dominant southwest vergence of F2 fold structures, lack of vergence reversals over a large area, and layer-parallel tectonic slides along attenuated limbs of F2 folds attest to a strong component of progressive simple shear strain in a northeast over southwest direction during prograde metamorphism. These observations are consistent with the observations and interpretations of Murphy (1984) and Brown (1978), who propose that northeastward underthrusting during accretion of terranes in the early mid-Jurassic caused consistently southwest-verging structures (F2 folds) in the continental margin sequence being underthrust from the southwest. Large lithostratigraphic packages, including continental margin sediments of Kaza Group, Cariboo Group, and Snowshoe Group, formed large nappes separated by faults and/or ductile shear zones, which together define "a broad shear zone accommodating shear strains associated with northeastward underthrusting" (Murphy 1984). The Pleasant Valley Thrust (Struik 1982) may have been of this type, active during F2 folding and metamorphism; the "premetamorphic mylonite zone" (Fletcher 1972) at Penfold Creek and other portions of "Campbell's

Enigmatic Line" may also have been active during the underthrusting proposed by Murphy (1984).

The Little River Fault, however, is not a thrust fault, at least in its latest stage, but rather a low-angle normal fault along which the hanging wall rocks slid down relative to the footwall, as suggested by the minor structures already mentioned. Movement displacing the Cariboo Group rocks down relative to the Snowshoe Group rocks probably began around the time of F3 folding and associated retrograde metamorphism. Movement continued through uplift, most likely in the Tertiary, as it postdated cooling of late Cretaceous (86 Ma) pegmatite (see section on geochronology (Chapter III)). Most of the uplift in the Columbia Mountains (which include the Cariboo Mountains and Quesnel Highland) was completed by Miocene time (Wheeler and Gabrielse 1972). In the area which is now the Intermontane Belt, a widespread erosion surface with low relief (about 500 m) was covered by Miocene lavas. A similar erosion surface covered much of the Quesnel Highland at higher elevations, and is now block-faulted to various levels. Although this surface has been deeply dissected by glacial erosion, it is still recognizable as an upper elevation limit in each block. The Three Ladies Mountain/Mount Stevenson area is a single block raised above the level of the surrounding hills west of the North Arm of Quesnel Lake. As

evidence, all three peaks of Three Ladies Mountain and Mount Stevenson reach a height close to 2200 m, whereas in the Goose Range, across Ishkloo Creek to the west and Grain Creek to the southwest, all of the "B" peaks (Barker, Borland, Browntop, Badger, and Brew) are within 15 m of 2045 m. The peaks to the southeast of the North Arm of Quesnel Lake are much higher, such as Mount Watt (2529 m). North of the Little River is a plateau at about 1800 m which rises gently to the east, until it is abruptly terminated by the Mathew River Fault and the high Cariboo Mountains beyond (2600 m).

The topography near the top of Three Ladies Mountain, which appears to approximate the level of the old erosion surface, has been strongly influenced by the Little River Fault surface and minor structures associated with it in the underlying rocks. If this interpretation is correct, then most of the movement on the Little River Fault was pre-Miocene, and post-Late Cretaceous. The timing of events involved in the formation of metamorphic core complexes elsewhere in the Cordillera was also late Cretaceous (post-Laramide orogeny) to middle Tertiary (Coney 1980).

Metamorphic core complexes, according to Crittenden et al. (1980), are characterized by cores of older metamorphic and plutonic basement overprinted by gently-dipping gneissic fabric, and overlain by less-metamorphosed, younger, commonly attenuated rocks.

These are separated from the basement rocks by
"decollement" zones characterized by apparently steep
metamorphic gradients, brecciation, and structures
indicative of detachment involving low-angle (commonly
listric) normal faulting (Coney 1980). These detachment
zones formed during uplift following major compressional
events such as the Cretaceous to Tertiary Sevier and
Laramide orogenies in the United States and the Jurassic
Columbian orogeny in Canada, but prior to extensional
events such as Basin and Range style faulting and
rifting in the mid to late Tertiary.

In a descriptive sense, the Little River Fault in
the Three Ladies Mountain area displays characteristics
that are similar to detachment surfaces of typical
metamorphic core complexes. These features, as well as
the timing of the movement on the Little River Fault,
between late Cretaceous pegmatite and Miocene erosion,
suggest a relationship to the tectonic processes which
led to formation of other metamorphic core complexes.

However, many differences between the Three Ladies
Mountain area and the typical core complexes of the
southwestern United States caution against lumping the
Little River Fault with other detachment zones. For
instance, the rocks in the hanging wall are not as young
as Tertiary, and may be approximately the same age as
the footwall rocks (late Proterozoic to Paleozoic), nor
are they undeformed nor completely unmetamorphosed.

There are also no mylonitic fabrics in the footwall schists and gneisses that can be proven to be related to Tertiary movement on the Little River Fault. Mylonitic fabrics have been observed in the footwall carbonate by Klepacki (1981). Ductile strain occurred during compressional tectonic events in the mid-Jurassic, whereas brittle features related to the Little River Fault are clearly younger than mid-Jurassic folds, and are also postmetamorphic.

Sliding of hanging wall rocks down along the Little River Fault occurred during uplift and tilting of the underlying footwall rocks, but did not involve much rotation, as crosscut F2 structures retain similar orientations on either side of the fault. Variations in orientation of pre-fault and fault-related structures are due to later northeast-trending folds (F4) and normal faults. The latest fold phase (F4) was accompanied by locally-occurring, axial-plane mica crenulations with near-vertical axial planes and gentle northeast plunge. F4 folds may imply minor compression in a northwest-southeast direction, but later northeast-trending normal faults, which appear to displace a Miocene erosion surface, imply extension in the same northwest-southeast direction.

3.3.3 OTHER FAULTS

Other than low-angle faults believed to be related to the Little River fault system, various higher-angle faults occur throughout the area. Most of the high-angle faults in the Three Ladies Mountain area are discontinuous and show relatively small displacements; they probably formed during uplift. Late, east-west striking, steeply north-dipping faults were observed in the Three Ladies Mountain area, none of which showed any more than a few meters of identifiable displacement; however, as they are nearly parallel to foliation, and lithologies are similar over hundreds of meters of thickness, actual displacement could be much greater. Some northeast-trending faults, parallel to F4 axial planes, near Mount Stevenson, are associated with quartz veins; sparse occurrences of molybdenite, pyrite, and chalcopyrite occur in small rusty zones.

North-northeast-trending fractures and faults, parallel to F4 axial planes, are common and influence topographic features including U-shaped glacial valleys such as Cariboo Lake, Ishkloo Creek Valley, and the North Arm of Quesnel Lake. Displacement on these faults is mostly down to the west, probably on the order of a few hundred meters, deduced from the assumption of a faulted pre-Miocene erosion surface. The large metamorphic displacement across the North Arm of Quesnel Lake is due mainly to earlier movement down to the

southeast along the Little River Fault. The age of the
north and northeast-trending faults is inferred to be
late Tertiary, and pre-Pleistocene.

Northwest-trending, high-angle faults with
displacement of unknown direction but magnitude less
than a few hundred meters also appear as topographic
lineaments; they may follow F2 axial plane foliation.
If there is any northwest-trending, high-angle fault in
Long Creek, it is of this type. Continuity of
lithologic units, foliated gneiss bodies, and structural
trends across the lower Long Creek valley absolutely
rules out the possibility of major strike-slip faulting
in this location. No evidence for strike slip faulting
was observed anywhere in the study area.

4. METAMORPHISM

4.1 INTRODUCTION

Most of the high-grade metamorphic rocks in the southern Omineca Belt are included in the Shuswap Metamorphic Complex, which is loosely defined as a metamorphic and plutonic complex bounded by the sillimanite isograd. The Shuswap Complex has been divided by Okulitch (1984) into three major parts: (1) the Monashee Complex, which contains gneisses older than 2 Ga, surrounded by the Monashee Decollement; (2) the northwestern Shuswap Complex, which is an area of sillimanite grade paragneiss of late Proterozoic to early Paleozoic depositional age, and possible minor mid-Paleozoic granitoid gneiss; and (3) the Okanagan Plutonic and Metamorphic Complex.

Although not formally part of the Shuswap Metamorphic Complex, and separated from it by about 20 km, the area of high-grade metamorphic rocks of the Snowshoe Group west of the North Arm of Quesnel Lake can be viewed as a window into the "northwestern Shuswap Complex" as defined by Okulitch (1984). Struik (1984) includes the Snowshoe Group in the "suspect" Barkerville Terrane, which lies between definite North American strata such as the Kaza Group and Cariboo Group to the northeast, and the suture zone between the Omineca Belt and Quesnellia. The suture crosses Quesnel Lake about 10 km south of Mount Stevenson (Okulitch 1984). The relationship between Barkerville Terrane and the Shuswap

Metamorphic Complex has not yet been clarified. The sillimanite isograd in the Three Ladies Mountain area as well as the sillimanite isograd defining the western boundary of the Shuswap Complex do not coincide with major lithologic or tectonic contacts, but are part of a normal metamorphic progression from low grade to high grade rocks within an apparently continuous lithostratigraphic succession. This implies that rocks in the Barkerville Terrane are transitional into the Shuswap Metamorphic Complex at least on its west side. This is not true of the northeastern boundary of the northwestern Shuswap Complex, where steep metamorphic gradients have been shown to coincide with faults or shear zones (Fletcher 1972; Pigage 1978; Engi 1984). The northeastern boundary of the sillimanite zone in the Three Ladies Mountain area is also a fault zone. Here, the Little River Fault crosscuts metamorphic isograds at a high angle rather than parallels them, and places chlorite and biotite zone rocks directly on staurolite-kyanite and sillimanite zone rocks. The Little River Fault is not continuous along strike with the northeastern boundary of the Shuswap Metamorphic Complex, whereas the Matthew Fault, which lies about 10 km to the northeast, probably is. The Little River Fault is discussed in a separate section.

The regional metamorphic progression in the Three Ladies Mountain/Mount Stevenson area follows a typical Barrovian sequence from greenschist facies to amphibolite facies, with

maximum metamorphic recrystallization synkinematic and postkinematic to second-phase deformation during the mid-Jurassic Columbian Orogeny. Timing of formation of the oldest metamorphic foliation is unclear. Possible evidence for pre-Jurassic deformation and/or metamorphism rests entirely on a few observations that quartz dioritic sills folded by first-phase folds apparently truncate metamorphic foliation in the adjacent metasedimentary rock. Prograde metamorphism involving growth of index minerals such as garnet, staurolite, kyanite, and sillimanite (and rarely preserved chloritoid) took place primarily during and after second-phase folding in one relatively continuous metamorphic-deformational cycle. Recrystallization of muscovite accompanied later folding, followed by retrograde growth of chlorite.

Metamorphic isograds mapped in the Three Ladies Mountain/Mount Stevenson area follow the general pattern shown by Fletcher (1972) and Campbell (1978) with a few differences resulting from subdivision of metamorphic zones and recognition of the Little River Fault (see Plate III). Pelitic rocks of the Snowshoe Group in this area are mainly in the staurolite-kyanite zone of the Barrovian series in amphibolite facies, with slightly lower grade rocks to the west near Ishkloo Creek and first sillimanite zone rocks to the east near the North Arm of Quesnel Lake. To the northwest, metamorphic grade in the Snowshoe Group decreases to garnet and then biotite zone a few kilometers west of

Ishkloo Creek. Metamorphic grade also decreases to the northeast, southeast, and southwest; the original distribution of isograds is disrupted by faults in the northeast and southeast, and is obscured by retrograde metamorphism and cover in the southwest toward Grain Creek. The relationship of metamorphism to the suture zone between the Snowshoe Group rocks and Quesnellia has been studied by Rees (1981).

4.2 <u>METAMORPHIC ZONES IN PELITES</u>

4.2.1 <u>INTRODUCTION</u>

Ten metamorphic subdivisions or zones have been defined in the Three Ladies Mountain/Mount Stevenson area on the basis of metamorphic textures and mineral assemblages in pelites. Plate III is a map showing metamorphic zones and sample localities. Zones (1) through (8) are in pelites of the Snowshoe Group, and represent divisions of the Barrovian series in amphibolite facies. Zones (9) and (10) are in phyllites of the hanging wall of the Little River Fault, and are divisions of greenschist facies. For each zone, distinctive mineral textures are summarized as supporting evidence for a suggested metamorphic history. Illustrations showing representative textures accompany the text (Figures 26 to 32). Schematic AFM diagrams for zones (3) through (8) are shown on a P-T petrogenetic grid in Figure 25.

The minerals that characterize the zones are referred to by their abbreviations, which are given in Appendix I.
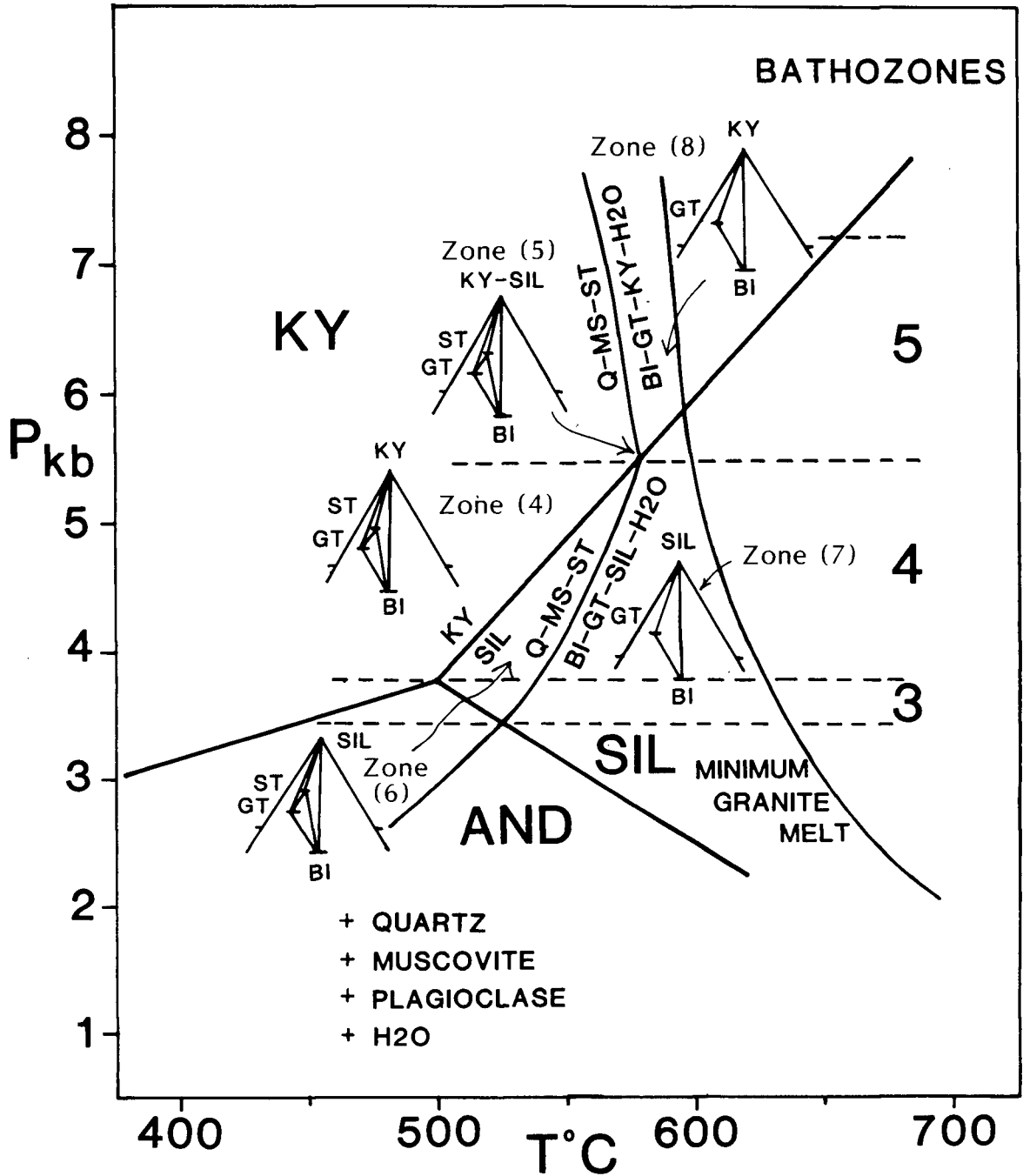
Figure 25. Pressure/temperature diagram illustrating AFM assemblages for metamorphic zones in the Three Ladies Mountain/Mount Stevenson area in relation to bathozones as defined by Carmichael (1978), and modified by Archibald et al. (1983).

4.2.2 METAMORPHIC ZONES

ZONE (1). RETROGRADE GARNET ZONE

QZ-BI-MS-PL-GT (GT replaced by CH) ± CH, OP, AP, RU, ZR, CA, EP, SP

Garnets are completely retrograded to chlorite. No other index minerals are present. Garnets contain vague straight S_i parallel to S_1 but not to S_2. Foliation (S_1) defined by muscovite and perhaps biotite was overgrown by garnet. Further metamorphic crystallization formed S_2, defined by biotite. Renewed deformation cracked garnets and kinked biotite, also kinked and smeared muscovite, which appears to be later than biotite. Retrograde reactions involve biotite and garnet altering to chlorite and sericite. Red-brown, titanium-rich biotite is replaced by pale-green, rutilated (sagenitic) chlorite with prominent pleochroic haloes from zircon.

Highest metamorphic grade achieved was at least garnet-biotite zone, and could have been much higher.

ZONE (2). GARNET-BIOTITE ZONE

QZ-BI-MS-PL-GT ± CH, OP, ZR, RU, SP, KS, CA

Garnets range from 2 to 6 mm in diameter, with possible zoning and some rotational texture. Most are severely retrograded to chlorite on the rims, and to chlorite plus sericite between rim and core (see Figure 26). Cores show straight inclusion pattern, with some rotational texture (S-pattern) toward the rims. Inclusions are quartz, opaques, and K-feldspar, which is interpreted as relict clastic grains. Some retrograded garnets have deformed chlorite rims, with undeformed inner retrograde zones. Garnet grew on layering or first foliation (S_1), was then rotated while growing synkinematically with formation of S_2, which is defined by muscovite and biotite. Large, postkinematic porphyroblasts of red-brown biotite are kinked and crosscut by muscovite, which grows along kink direction and is either also kinked or mimetic on polygonal arcs. Some retrograde chlorite is also kinked, and crosscut by muscovite, and later retrograde chlorite is undeformed within garnet outlines.
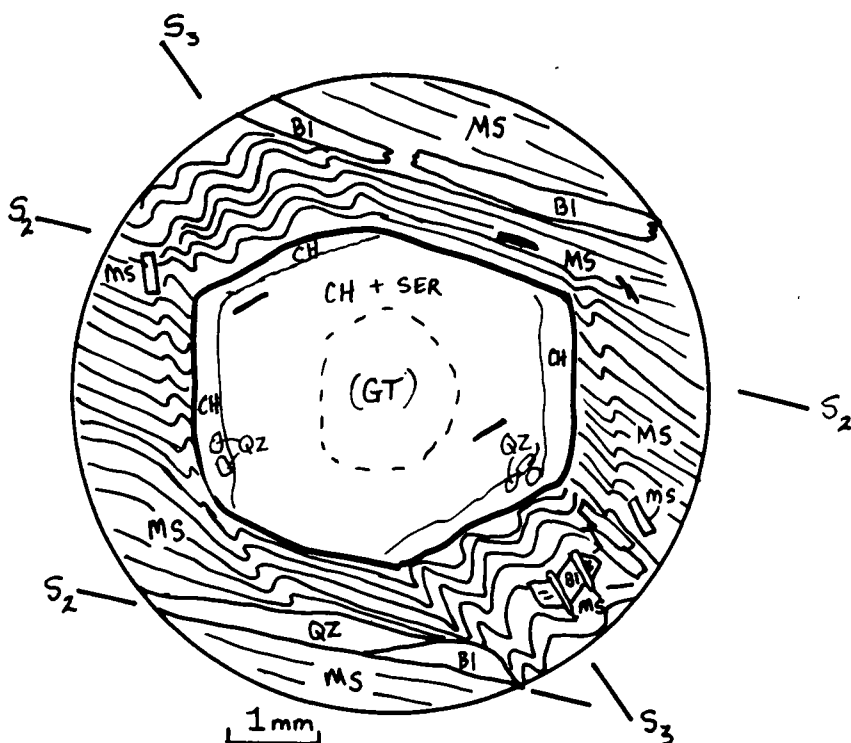
Figure 26. Garnet zone (2), sample 82-376. Main
metamorphic foliation (S_e) of biotite and muscovite,
wrapping around garnet, was subsequently folded by F3 folds
(S_3 with minor additional muscovite recrystallization;
retrograde chlorite and sericite after garnet are
postkinematic.

ZONE (2a).   "GARNET" ZONE

Subset of Zone (3) or Zone (4)

QZ-BI-MS-PL-GT-TO ± CH, OP, ZR, AP, SP, RU

This zone is distinguished on the basis of garnet textures and mineral association, and is not recognizable as a separate zone in the field. The samples were collected from within the staurolite and staurolite-kyanite zones. Garnets range from 2 to 14 mm, with S_i parallel to S_e (S_2), defined by straight trails of quartz and opaques. These samples escaped the rotation and further porphyroblast growth so common in other pelites in the same areas. It is possible that they were less pelitic initially and so fewer reactants (less Al_2O_3, H_2O) were available to recrystallize at the higher grades. Most of these samples are associated in the field with the uppermost Snowshoe Formation quartzite and pelite, and close to outcrops with staurolite and/or kyanite. This texture may be compositionally controlled.

ZONE (3). STAUROLITE ZONE

QZ-BI-MS-PL-GT-ST-TO ± CH, OP, ZR, RU, AP

Five subgroups are based on textures in garnets:
(a) Garnets are about 5 mm and have textural zoning.
Straight S_i in core is defined by quartz and opaques,
surrounded by a rotational zone with S-shaped inclusion
trails, and a clear rim free from inclusions.
(b) Garnets have straight S_i in core, but no obvious
rotational zone; however, they have been rotated after
cessation of growth.
(c) Garnets contain folded or crenulated S_i , so are
helicitic, but not rotational.
(d) Garnets are broken and retrograded, as is
staurolite.
(e) Staurolite contains tiny, idioblastic garnets, with
no garnets in matrix (see Figure 27).

All the garnets in this zone are texturally zoned,
indicating at least two periods of growth, or changing
conditions during growth. Most cores contain only
straight S_i of dominantly quartz. Rapid growth during
renewed shear and rotation led to syndeformational,
"snowball" textures in the intermediate zone of the
garnet. Finally, some garnets continued to crystallize
without inclusions, resulting in clear rims. Some
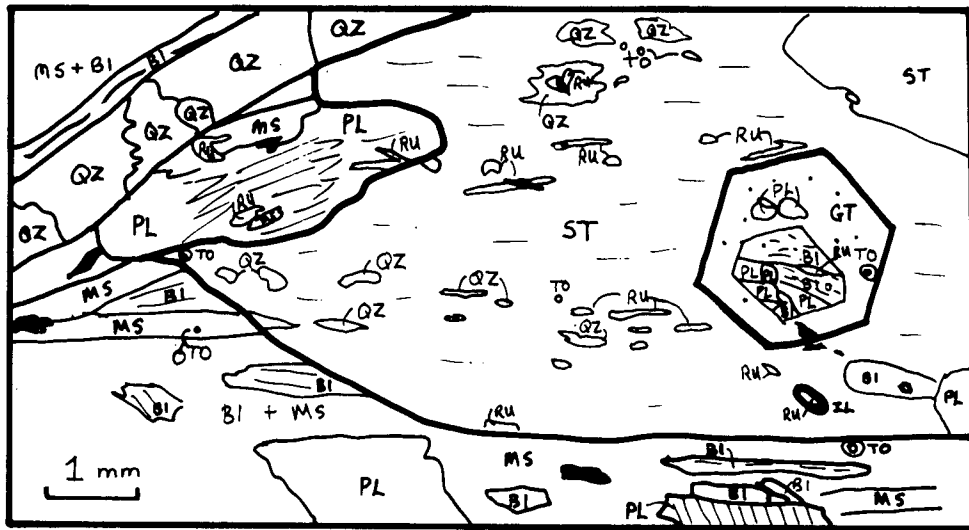
Figure 27. Staurolite zone (3), sample 81-344. Large staurolite porphyroblast includes idioblastic garnet and trails of rutile and quartz (S_i) parallel to $S_e(S_2)$.

staurolites, as well as garnets, show S-shaped inclusion patterns, indicating synkinematic rotation during growth. S_i may be parallel to S_e , either at edges of grains showing rotational textures or all through postkinematic grains. Staurolite growth outlasted that of garnet in some rocks. It contains garnets and folded (helicitic) internal trails of opaques. Garnet rims appear to be contemporaneous with biotite crystallization foliation (S_2) in some places. Later foliation (S_3) is defined by muscovite and is at a slight angle to S_2; it may represent flattened and kinked S_2 that has been only partly recrystallized. Both staurolite and plagioclase porphyroblasts contain inclusion trails related to S_2. Finally, some biotite and most garnet rims have retrograded to chlorite. Presence of staurolite may be partly controlled by composition of the host pelite. One locally mappable unit contains the largest percentage of staurolite porphyroblasts (>10%), as well as large plagioclase porphyroblasts, uncommon in other pelites (for example, samples 80-69, 80-135, 82-344).

ZONE (4).   STAUROLITE-KYANITE ZONE

QZ-BI-MS-PL-GT-ST-KY-TO ± CH, OP, GR, ZR, AP, RU, SP, EP

Pelitic schists in this zone show the greatest
variety of textures which record the crystallization
history of the rocks. Garnet, staurolite, and kyanite
reach their maximum size and modal abundance in this
zone, and the recorded deformational history is more
complex than for the other zones. This may be a
consequence of increased reaction rates and shearing due
to increasing temperatures during progressive
deformation, leading to rapid crystallization and large
size of porphyroblasts, which tend to preserve the
textural history.

Garnets range in size from 1 to 15 mm, averaging
2 to 5 mm, and make up 5-25% (average 10%) of a sample
of pelitic schist. They are idioblastic to
subidioblastic, rounded, or skeletal, or atoll-shaped,
and contain up to 40% inclusions. Minerals included in
garnet are quartz, ilmenite and other opaques, graphite,
and minor chloritoid, staurolite, chlorite, and
tourmaline. It is possible that some chlorite and/or
staurolite included in garnet have replaced former
chloritoid inclusions.

All garnets show some degree of rotation, with S_i not parallel to S_e . Most garnet textures in the staurolite-kyanite zone are similar to those in the staurolite zone. Patterns of inclusion trails and textures within garnet may be categorized as follows (number of examples for each shown in parentheses):

- Straight S_i (3)
- Straight S_i only in core (8)
- Helicitic (folded or crenulated S_i) (2)
- Snowball or rotational (S-shaped pattern) (9)
- Texturally zoned (9)
- Atoll (3), mostly near ST-KY-SIL transition zone (5)
    (see Figures 28, 29, and 30)

Chloritoid occurs only as inclusions in a large garnet (Figure 28), between the inner core and the outer zone, within the rotational zone of the garnet, implying that folding was taking place during chloritoid growth. This rock, which is now in the staurolite-kyanite zone, must have crystallized along a prograde P-T path that included formation of chloritoid, such as a typical medium to high-pressure Barrovian sequence. The chloritoid inclusions in this sample are large enough to determine complete optical properties, and to distinguish them from chlorite inclusions in the same garnet (see Appendix I). Many chlorite inclusions in garnet may be replacements of earlier chloritoid grains. In one rock (81-315), abundant small inclusions of staurolite in a garnet may have replaced
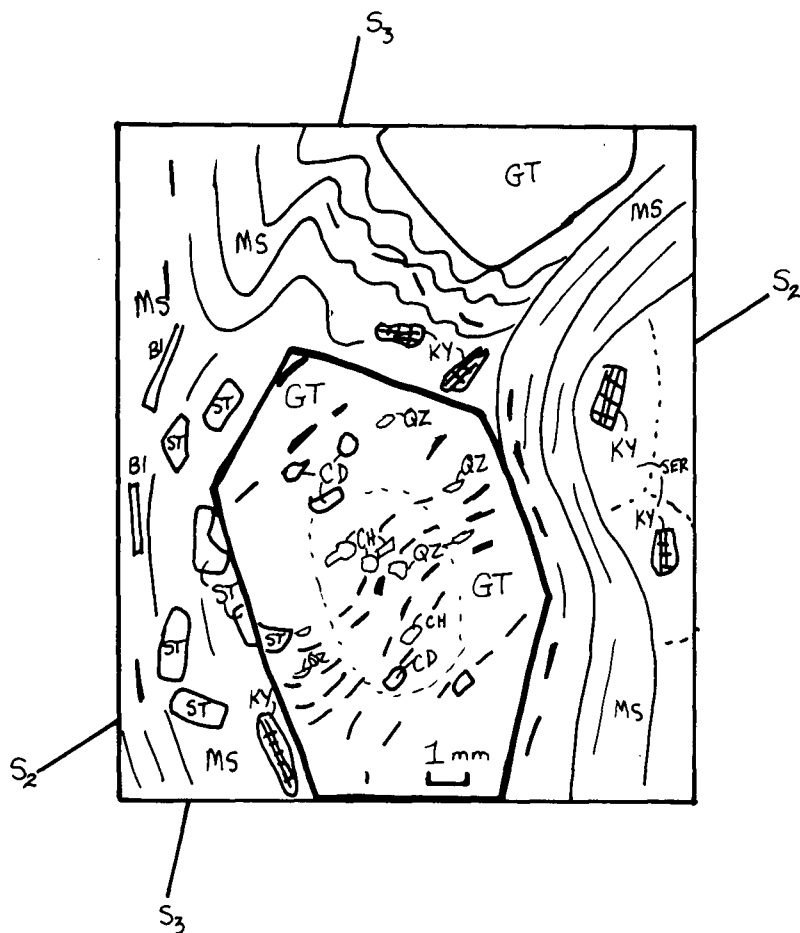
Figure 28. Staurolite-kyanite zone (4), sample 79-13. Staurolite-kyanite-garnet-muscovite schist contains chloritoid (CD) inclusions in 'snowball' (rotational) garnet synkinematic with F2 folding, indicating prograde metamorphic growth of garnet. Green chlorite (CH) is included in garnet core. Staurolite and kyanite are postkinematic to S_2 but prekinematic to S_3, and some kyanite is replaced by retrograde sericite.
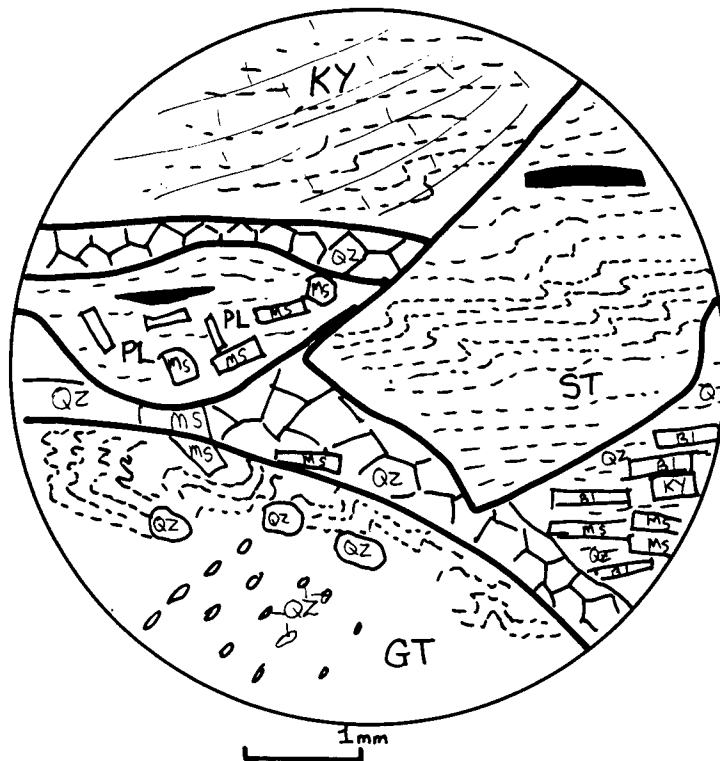
Figure 29. Staurolite-kyanite zone (4), sample 81-234. Garnet rims, staurolite, and kyanite are all helicitic, including folded trails of graphite. S_i is parallel to S_e.

former chloritoid, as this texture is unusual for staurolite, which is usually porphyroblastic.

Staurolite continues into the staurolite-kyanite zone, where it is as important a porphyroblast as kyanite. Staurolite forms idioblastic to subidioblastic porphyroblasts up to 3 cm long by 1 cm wide, but is commonly < 1 cm. It includes grains of quartz, graphite, ilmenite, rutile, biotite, kyanite, garnet, tourmaline, and zircon. Inclusion trails may be parallel to the outside foliation, folded (helicitic), or rotational (S-shaped). Some staurolites are texturally zoned, showing two growth periods, that are distinct in terms of deformation. The cores contain many inclusions that define a vague foliation, and the rims are clear, and apparently post-kinematic. Staurolite may include kyanite, or kyanite may include staurolite, in some cases in the same thin section, so staurolite and kyanite are interpreted as contemporaneous. Poikiloblastic staurolite may include smaller staurolite grains as well as kyanite, attesting to a long growth period, or wide stability field for staurolite.

Kyanite commonly occurs in two different settings in the staurolite-kyanite zone: (1) It is common as porphyroblasts up to 2 cm long in pelitic schist along with staurolite and garnet. Kyanite is somewhat aligned on foliation and lineation, but is neither strongly oriented nor completely random. It tends to be synkinematic with respect to F2 folding, but some is bent, kinked, and has undulose

extinction, probably as a result of F3 or later deformation. Some grains contain S-shaped inclusion trails, and generally S_i is parallel to S_e. Inclusions are quartz, graphite, ilmenite, rutile, muscovite, biotite, and tourmaline. Near the kyanite to sillimanite zone transition, kyanite grains are rounded and embayed by quartz; in some cases the core has been replaced by quartz and biotite, leaving part of the rim. (2) Kyanite is more sparsely distributed as large, tabular crystals (up to 2 cm wide by 10 cm long) within unfoliated quartz-muscovite segregations occurring in pelitic schist or micaceous quartzite, throughout the staurolite-kyanite and kyanite zones.

In the same area, near the kyanite to sillimanite boundary, large garnets are also beginning to break down to "atoll garnets" (Figure 30). The rim of the garnet remains as a ring-shaped grain, whereas the intermediate zone, which probably contained S-shaped inclusion trails, has been replaced by quartz and biotite. In some cases the core has been the last part of the interior of the garnet to break down.

The outermost zone of the garnet would still be in equilibrium with the pelite matrix, whereas the interior would be unstable if exposed to the matrix, and able to react with it or with the inclusions (in some of these garnets, the mid-zone contains up to 40% inclusions). The components of the interior part of the garnet would then be available for further reactions, including those producing
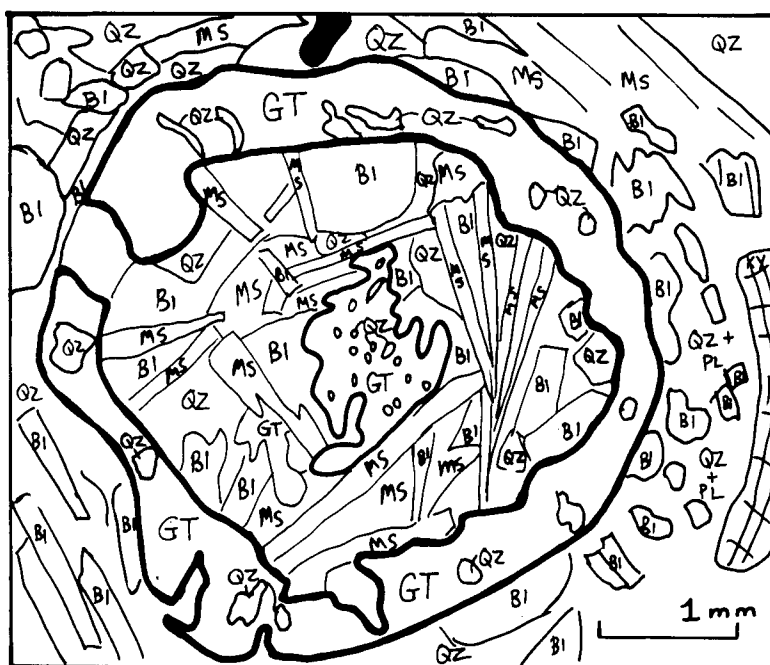
Figure 30. Staurolite-kyanite-sillimanite zone (5), sample
81-279. Atoll, or ring-shaped, garnet near
kyanite-sillimanite isograd; interior of garnet has been
replaced by muscovite, biotite, and quartz.

new garnets. Such a reaction might be that of the breakdown of staurolite and formation of sillimanite:

$$QZ + MS + ST = BI + GT + SI + H_2O \qquad\qquad (1.1a)$$
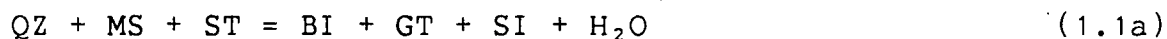
There must also be a garnet breakdown reaction, such as

$$MS + GT = SI + BI + QZ. \qquad\qquad (1.2)$$

These reactions could occur simultaneously as long as different garnet compositions were involved. If the cores of the relict garnets were the last part to break down, Mn would be released after the new garnets had started to grow. Then the rims of the newly regenerated garnets would be higher in Mn than expected for sillimanite zone. This is the case in some of the analysed garnets (see section on garnet zoning).

Most of the larger opaque inclusions in porphyroblasts in the staurolite-kyanite zone are lath-shaped ilmenite (confirmed with probe data). Other Ti-rich minerals are rare, such as sphene, which only occurs in slightly calcareous schists. Rutile occurs as inclusions within staurolite and kyanite, but not in garnet (except in the kyanite zone). Where rutile comes in contact with quartz, whether inside a grain of staurolite or kyanite, or at the rim next to the matrix, it is replaced by ilmenite. This is a common texture throughout both the staurolite zone and

staurolite-kyanite zone. Some striking examples occur where an elongate grain straddles the contact between the porphyroblast and the schist matrix, and the part included within the staurolite or kyanite is clearly rutile, and the part projecting into the matrix is opaque ilmenite, with the transition coinciding exactly with the rim of the porphyroblast. See the section on the GRAIL geobarometer for an illustration and interpretation of this texture.

The ilmenite-rutile textures suggest that the staurolite zone and kyanite zone were formed in P-T conditions below those for the pressure-sensitive reaction

$$ALM + RUT = ILM + KY/SI + QZ, \qquad\qquad (1.3)$$

known as the GRAIL geobarometer (Bohlen et al. 1983).

Tourmaline is commonly zoned in pelites from blue-green to olive green. In thin sections of pelites cut perpendicular to the dominant F2 fold axis, tourmaline end-sections (0001) are more abundant than those parallel to the c-axis, indicating some synkinematic orientation of tourmaline, implying either rotation or growth during peak metamorphism. Grain size is too small to see tourmaline in most hand specimens.

ZONE (5). STAUROLITE-KYANITE-SILLIMANITE ZONE

Also referred to as "Transition Zone".

QZ-BI-MS-PL-GT-ST-KY-SI-TO ± CH, OP, RU, ZR, AP

This zone is defined by the "sillimanite-in isograd", or first appearance of fibrolite in thin sections. Kyanite and staurolite are still present, but are apparently breaking down to sericite, or quartz, biotite, and garnet.

Tourmaline in this zone shows complex zoning with more than three concentric colour-zones, in contrast to the usual two. In sample 80-33, colour-zoning concentric to the c-axis is as follows, from core to rim: (1) bluish-green to brown, (2) olive green, (3) pale yellowish olive, (4) olive green. Cation zoning in one grain of this sample is shown in probe data (see Appendix II). Probe data indicate a variation from higher Mg than Fe in the core, to lower Mg than Fe in the rim, as well as higher Na in the core than in the rim, but lower Ca in the core than in the rim. There is no Mn in this tourmaline, negligible K, and constant Ti from core to rim. This zoning pattern is continuous with no abrupt transitions.

Tourmaline in this zone may contain inclusions of quartz, zircon, or opaques, and may also crosscut biotite. In another sample (81-279), tourmaline inclusions inside kyanite have only one zone, and contain inclusions that are parallel to inclusion trails in the kyanite, which are

parallel to the outside foliation. Tourmaline in the matrix
of this rock shows two colour-zones, implying that the rim
of the matrix tourmaline is contemporaneous with kyanite
growth.

Garnet textures are markedly different from those in the
staurolite-kyanite zone. Although some relict garnets up to
3 mm remain, most garnets are now < 1 mm in diameter and
comprise less than 5% of the rock. Larger, relict garnets
contain straight S_i perpendicular to S_e, are zoned, and
include kyanite, staurolite, biotite, and rutile in the
outer portions. Small, new garnets have few inclusions, and
are associated with fibrolite near embayed staurolite (see
Figure 31).

These textures have preserved evidence for two
uncompleted reactions:

KY = SIL   (1.4)

QZ + MS + ST = BI + GT + SI + H_2O.   (1.1a)
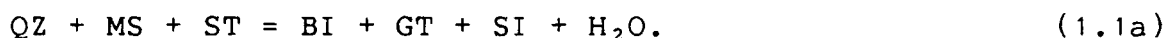
P-T conditions were probably near the intersection of these
reactions. See the section on staurolite breakdown for
estimated temperatures and pressures of this intersection.

Figure 31. Staurolite-sillimanite zone (6), sample 80-30.
Fibrolitic sillimanite forming at the expense of staurolite.
Note small size of garnets (<1 mm).

ZONE (6).   STAUROLITE-SILLIMANITE ZONE

QZ-BI-MS-PL-GT-ST-SI ± CH, OP, ZR, RU, AP, KS, EP

Staurolite is still present, but skeletal and embayed;
kyanite is no longer present. Fibrolite surrounds
staurolite, which appears to be breaking down. Garnets are
tiny, < 2 mm, look new, and are associated with new biotite.
A few relict garnets are broken and embayed.

That kyanite has disappeared before staurolite is
suggestive of a P/T path in Bathozone 4 (Carmichael 1978).

ZONE (7).   SILLIMANITE ZONE

QZ-BI-MS-PL-GT-SI ± CH, OP, RU, ZR, SP, ST

This corresponds to the classic "first sillimanite zone". As muscovite is present in all pelites, conditions are below those of the reaction $MS + Q = SI + KS + H_2O$. Garnets are small (< 1 mm) except relicts (3 to 6 mm), and comprise 1-5% of the rock. They tend to be blocky to rounded, subidioblastic, or oval. Garnets contain less than 5% inclusions, which are quartz, opaques, and biotite. Sillimanite is in the form of fibrolite knots, which are bundles of tiny, acicular sillimanite grains, commonly associated with biotite.
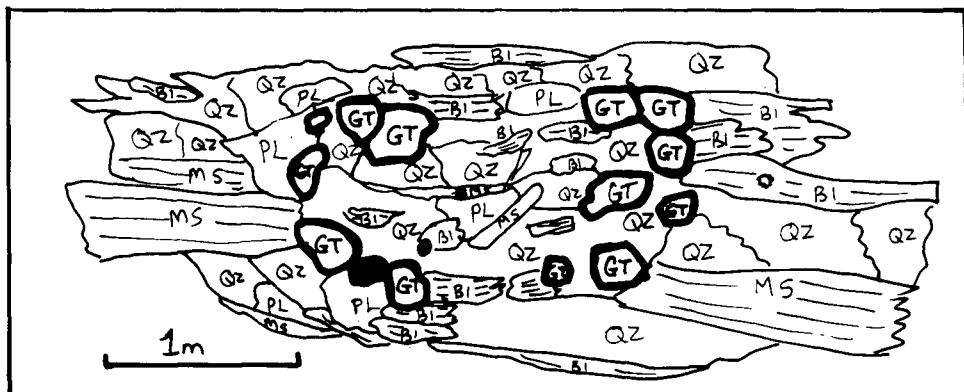
Figure 32. Sillimanite zone (7), sample 80-31. Tiny garnets outline a former garnet porphyroblast replaced by quartz, plagioclase, biotite, and muscovite. Similar textures, involving both garnet and kyanite, were observed in the kyanite zone (8).

ZONE (8). KYANITE ZONE

QZ-BI-MS-PL-GT-KY ± CH, OP, RU, ZR, AP, ST, TO, KS

Garnets 2-5 mm are relict, embayed, and include quartz, opaques, rutile, biotite, muscovite, and staurolite. Garnets < 2 mm have rare inclusions of quartz, opaques, biotite, and rutile. All are very small and in some places appear to be growing in an old garnet shape, as a ring of little garnets (see Figure 32). In some rocks, tiny garnets contain no inclusions. Kyanite in this zone is also tiny, occurring along layers with garnets. Big kyanites are pseudomorphed by sericite; staurolite is reacting out. This is the only zone in which garnets include biotite or rutile.

Textures suggest regenerated forms of garnet, biotite, and kyanite in this zone, although all were also present in Zone (4). Such textures are consistent with an interpretation that the discontinuous reaction

QZ + MS + ST = BI + GT + KY + H_2O (1.1b)
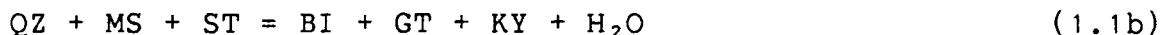
has taken place in Bathozone 5 (Carmichael 1978).

ZONE (9).   BIOTITE-CHLORITE ZONE

QZ-MS-CH-BI-OP

This zone is restricted to the hanging wall of the Little River Fault near Limestone point, in phyllitic rocks interlayered with with carbonates. Foliation is mainly defined by muscovite and chlorite. Biotite is rare; where it occurs it is red-brown and porphyroblastic, postkinematic to the main muscovite-chlorite foliation, but also kinked and retrograded to chlorite.

ZONE (10). CHLORITE ZONE

This zone also occurs in the hanging wall of the Little River Fault, but structurally higher, on Service Mountain, in phyllitic rocks interlayered with carbonates. The following assemblages are present:

Q-MS-CHL ± CA, TO, ZR, OP (IL, HE, MG)

Q-MS ± GP, OP

Q-MS-CA-GP ± OP, PY

The pelitic rocks in this zone may show two distinct phyllitic cleavages, axial planar to F2 and F3 folds. Either one of these cleavages may be dominant in a particular outcrop, which makes them difficult to distinguish with certainty, as both were formed in chlorite grade greenschist facies conditions, and are defined by muscovite-chlorite crystallization foliation.

The more quartz-rich units tend to preserve the F2 axial planar cleavage, whereas interlayered phyllite may show F3 axial planar cleavage nearly perpendicular to it (see Figure 9).

4.3 GARNET ZONING

4.3.1 DESCRIPTION OF ZONING PROFILES

Garnets from eight samples were analyzed on the electron microprobe (data shown in Appendix II). All garnets analyzed can be characterized by the mineral formula

$$(Fe,Mg,Ca,Mn)_3Al_2Si_3O_{12}.$$
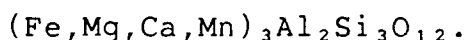
They are dominantly almandine (28 to 37 Wt.% FeO) with lesser amounts of pyrope (1 to 4 Wt.% MgO), spessartine (0.1 to 4.5 Wt.% MnO), and grossular (1 to 8 Wt.% CaO). Zoning profiles of garnets are shown in Figures 33 to 41. The staurolite zone (Zone 3) is represented by sample 82-389; the staurolite-kyanite zone (Zone 4) by sample 81-279; the staurolite-kyanite-sillimanite zone (Zone 5) by samples 80-33, 80-119, and 81-278; the staurolite-sillimanite zone (Zone 6) by sample 80-19; the sillimanite zone (Zone 7) by sample 80-31; and the kyanite zone (Zone 8) by sample 81-325.

Although the number of analyzed samples is limited, certain patterns have emerged that may have general significance. Observations and interpretations made here have been supplemented by textural evidence from additional samples.

In the samples analyzed, Fe is lower in the core of the garnet and increases toward the rim in all but one sample. The maximum difference between core and rim is 5 Wt.% (32 to 37) in 81-279. The exception is sample 81-325, in which the garnets are very small (<0.5 mm); Fe is relatively constant with slightly higher values in the core (all within 1 Wt.% (34 to 35 Wt.%). Some of the larger garnets near the kyanite to sillimanite transition show a drop in Fe values near the rim (81-278, 81-279).

Mg varies less strongly than does Fe. In the lower grade samples it is lowest in the core of the garnet, and higher near the rim, with a slight drop right at the rim (81-278, 81-279, 82-389). Mg is highest in the core of garnets in rocks from the high-grade side of the kyanite to sillimanite transition (80-19, 80-119, 80-33, and 80-31) and in the kyanite zone (Zone 8) (81-325).

Mg and Fe zoning patterns in garnet are related in that in the lower grade rocks Mg and Fe are both lower in the core and higher in the rim, but in sillimanite zone (Zones 6 and 7) they are opposite, with Mg higher in the core whereas Fe is still lower. In kyanite zone (Zone 8) both Fe and Mg show slightly higher values in the core of the garnet, but the variation is small.

Mn zoning patterns also vary from the low-grade to the high-grade rocks. The larger garnets from the staurolite and staurolite-kyanite zones (82-389, 81-279,

81-278) have higher Mn in the core, lower Mn toward the rim, and higher Mn on the rim itself. This kind of pattern is fairly typical of garnets that retain prograde textural zoning. The higher Mn on the rim of these large, zoned garnets may be due to retrograde metamorphism of the rim of the garnet.

This is probably not the case in some of the higher-grade garnets, however, in which the Mn zoning profiles show lower Mn in the cores grading out to higher Mn in the rims (80-19, 80-119, 81-325). Not all of the higher-grade garnets follow this pattern; small garnets from samples 80-31 and 80-33 show normal zoning patterns with Mn higher in the core, and Fe lower in the core.

Ca zoning patterns in garnets from rocks in the staurolite and staurolite-kyanite zone (82-389, 81-279) show extreme zoning with higher Ca in the core and lower Ca in the rim. This may be compositionally controlled or reflect a prograde metamorphic cation preference. Ca values in the higher-grade rocks are fairly low and constant.

Presence of Ti in garnets is directly related to nearby ilmenite inclusions and is considered to be insignificant.

82-389 GARNET 2
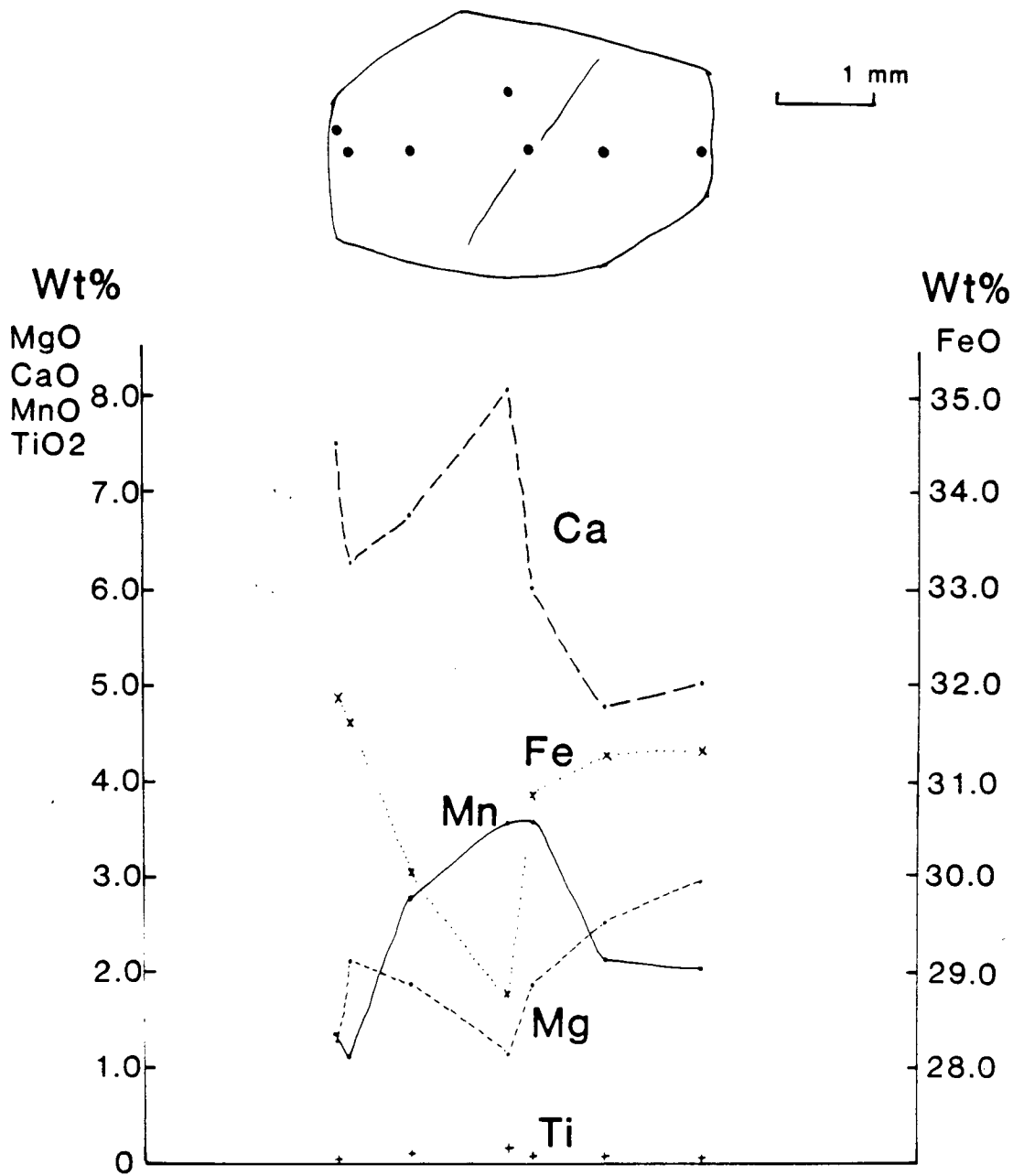
Figure 33. Garnet zoning profile for Garnet 2 from sample 82-389, staurolite zone.
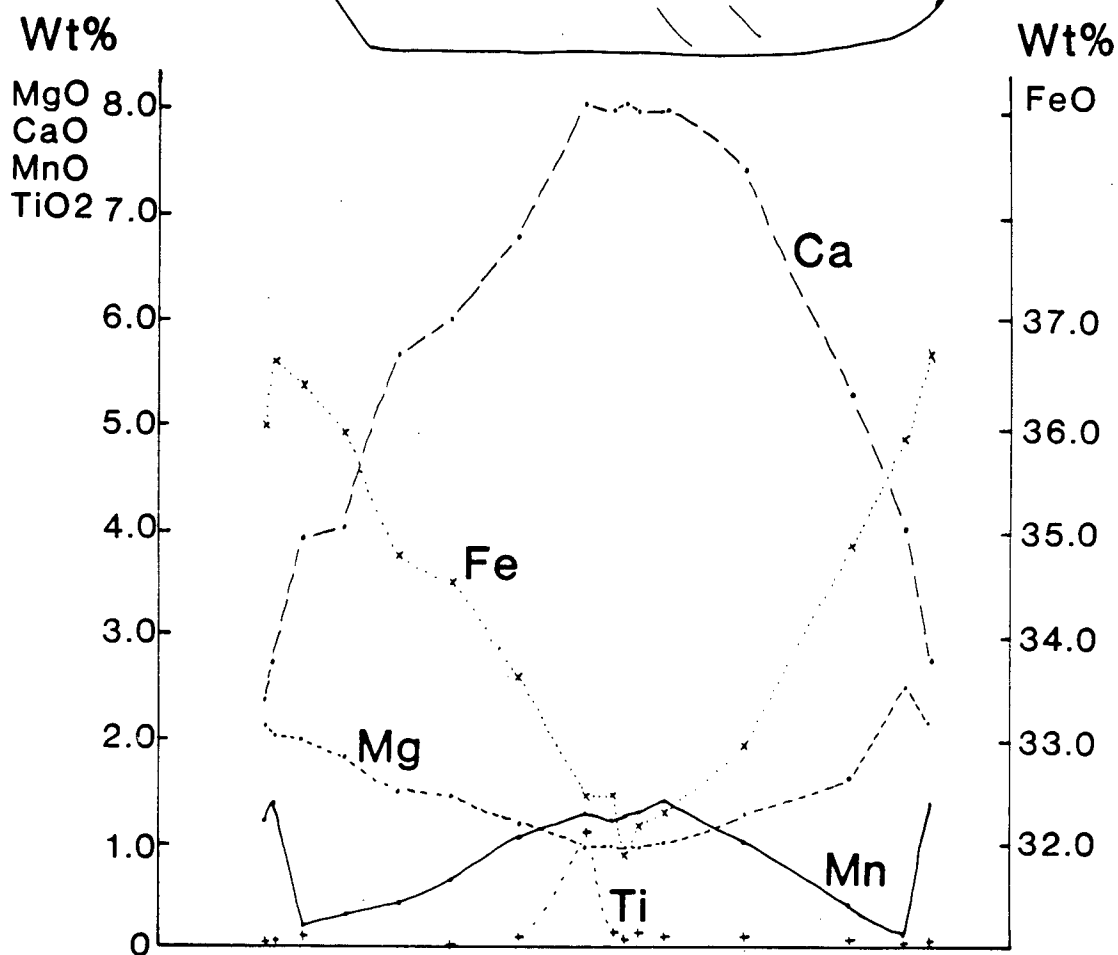
Figure 34. Garnet zoning profile for Garnet 3 from sample 81-279, staurolite-kyanite zone.

81-278   GARNET $(Fe,Mg,Ca,Mn)_3Al_2Si_3O_{12}$
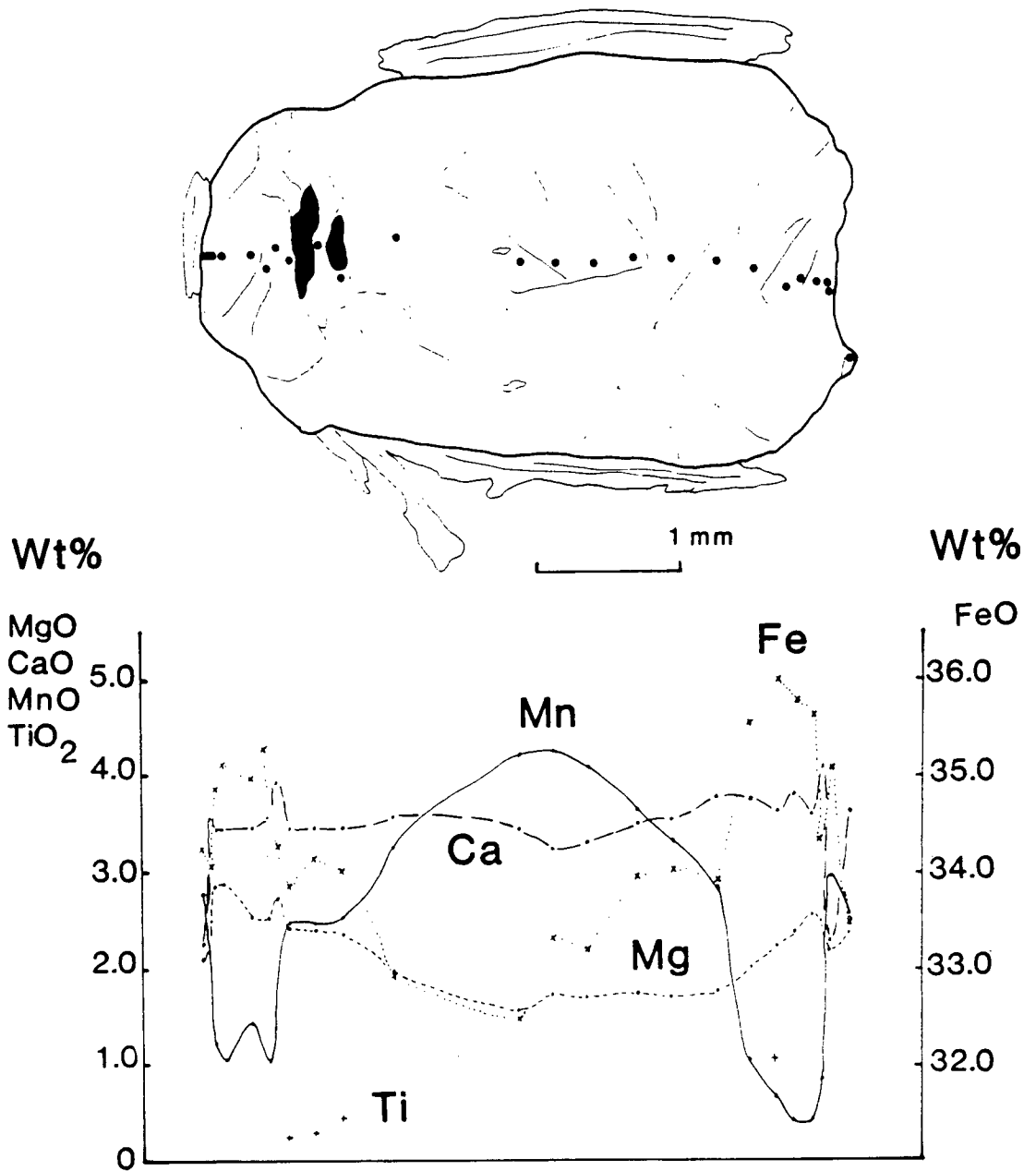
Figure 35.   Garnet zoning profile for Garnet 4 from sample
81-278, staurolite-kyanite-sillimanite zone.

80-33 GARNET 1

0.65 mm
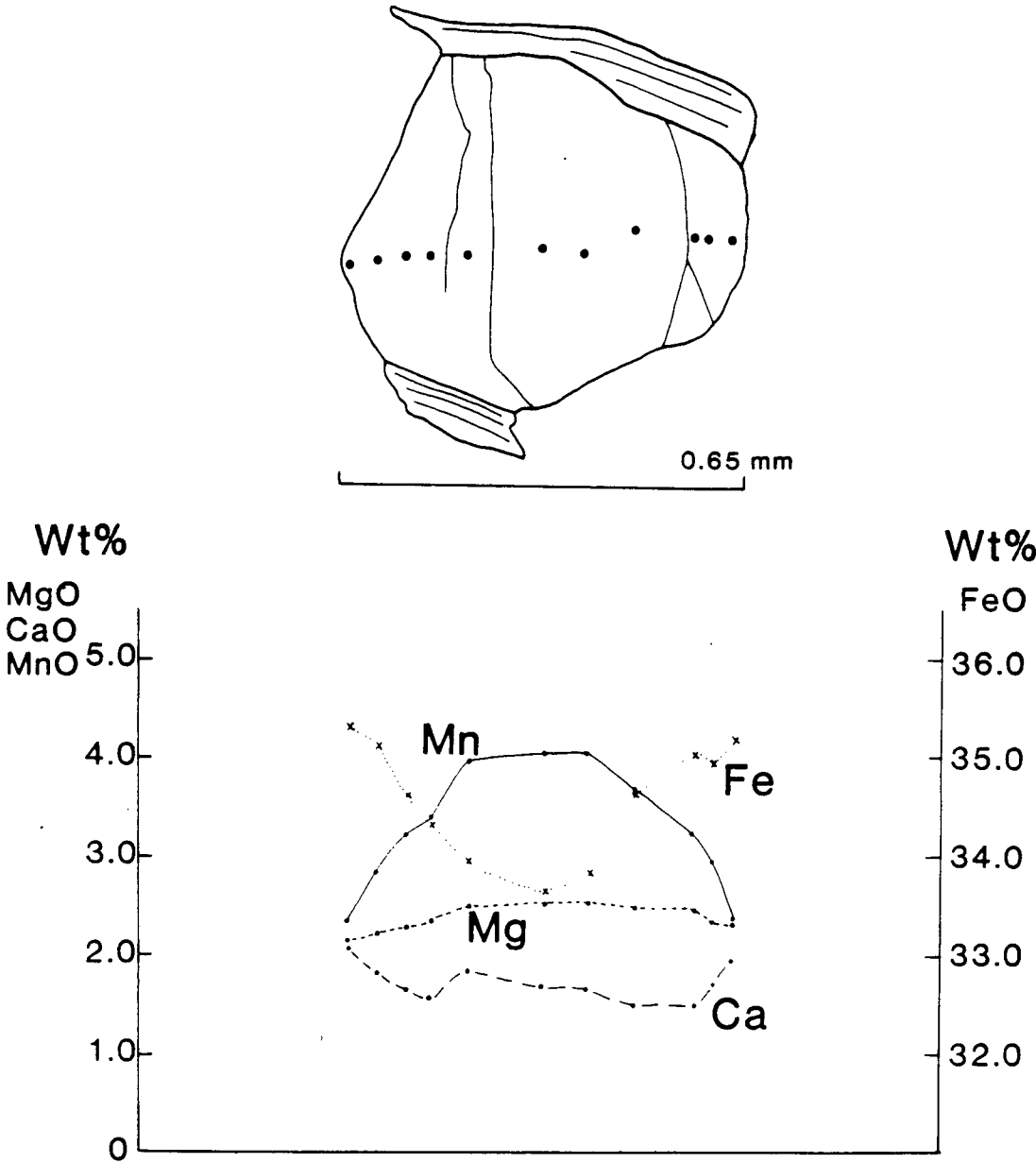
Figure 36. Garnet zoning profile for Garnet 1 from sample 80-33, staurolite-kyanite-sillimanite zone.
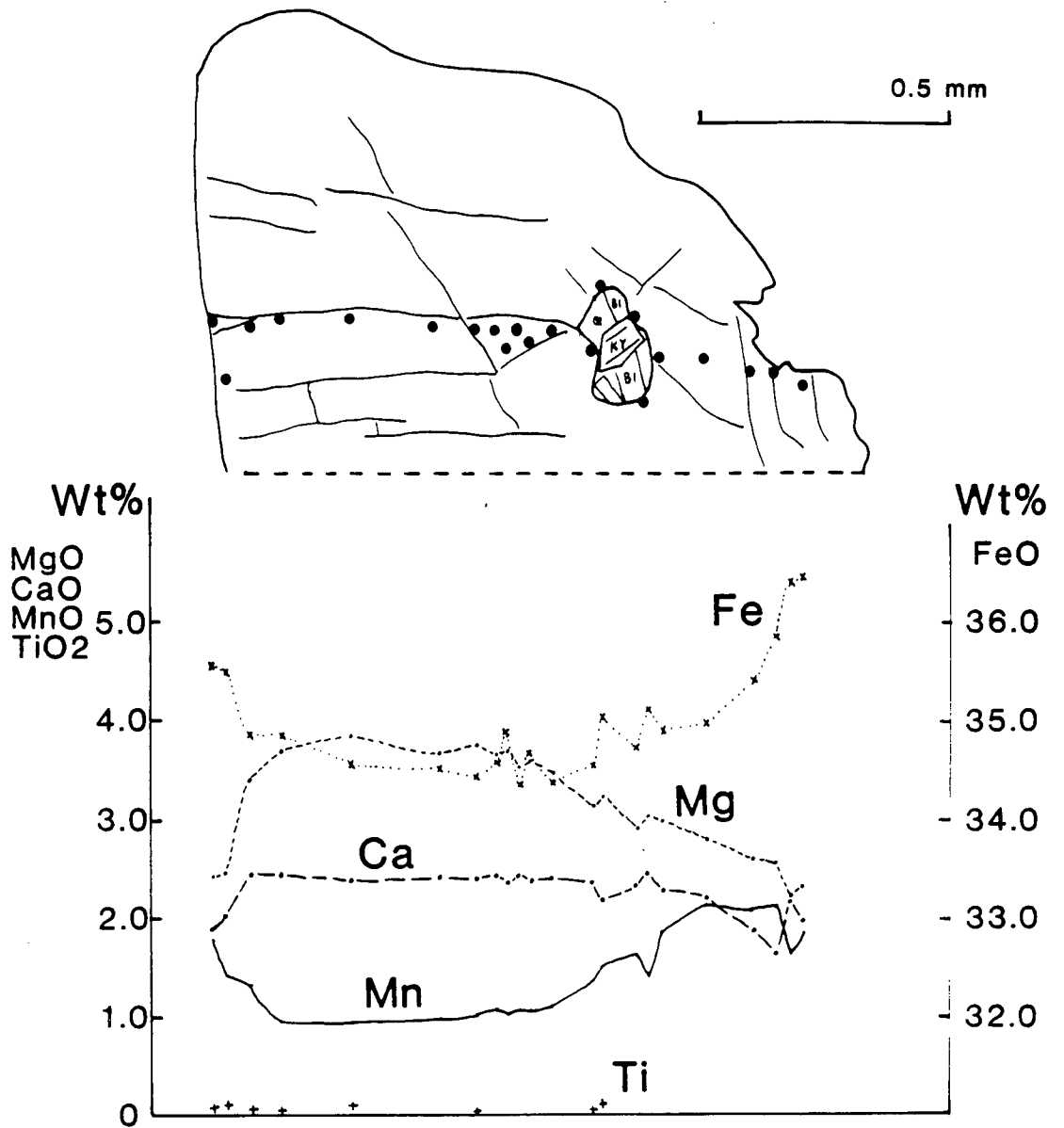
Figure 37. Garnet zoning profile for Garnet 1 from sample 80-119, staurolite-kyanite-sillimanite zone.
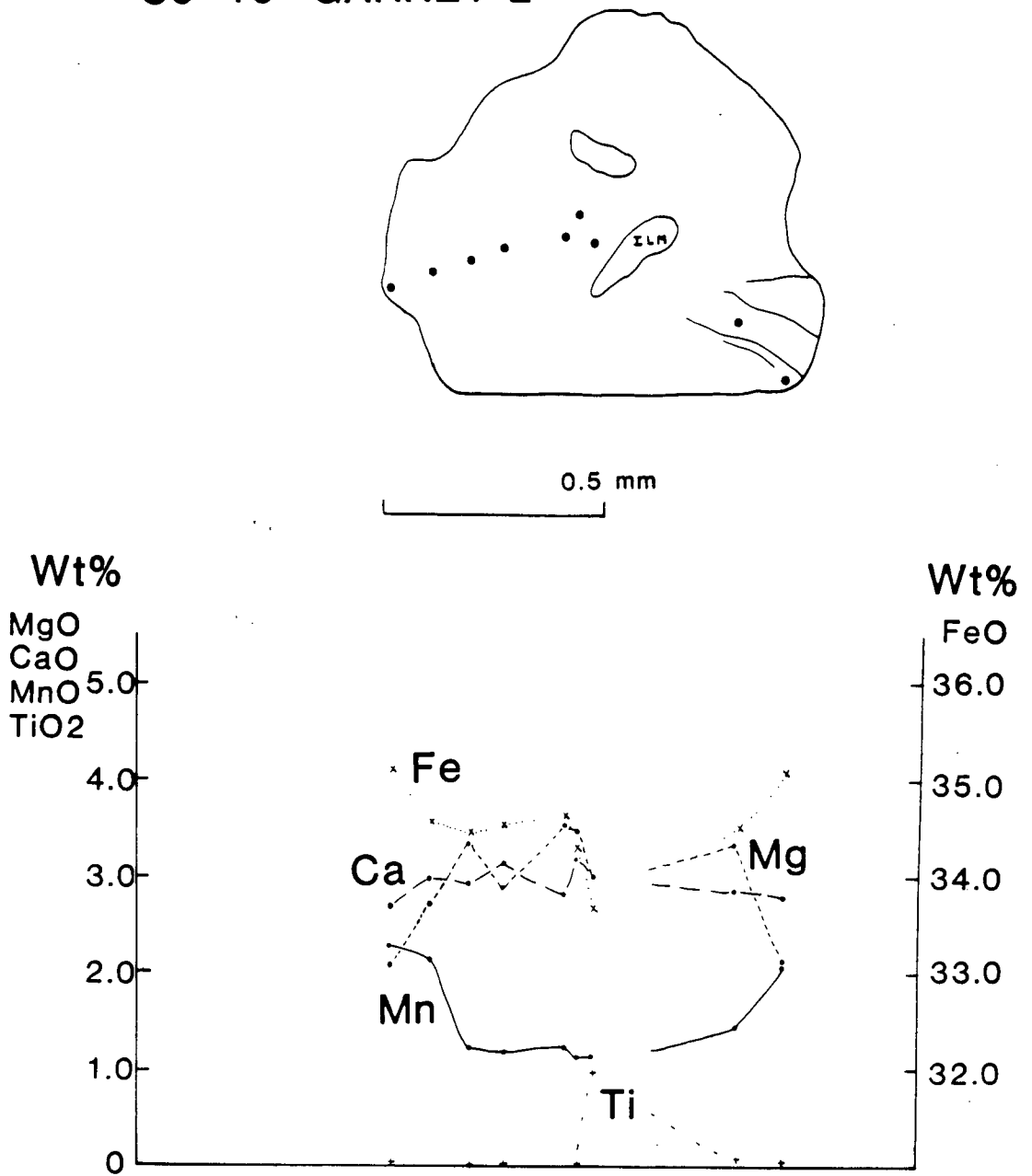
Figure 38. Garnet zoning profile for Garnet 2 from sample 80-19, staurolite-sillimanite zone.

80-31 GARNET 3

0.1 mm
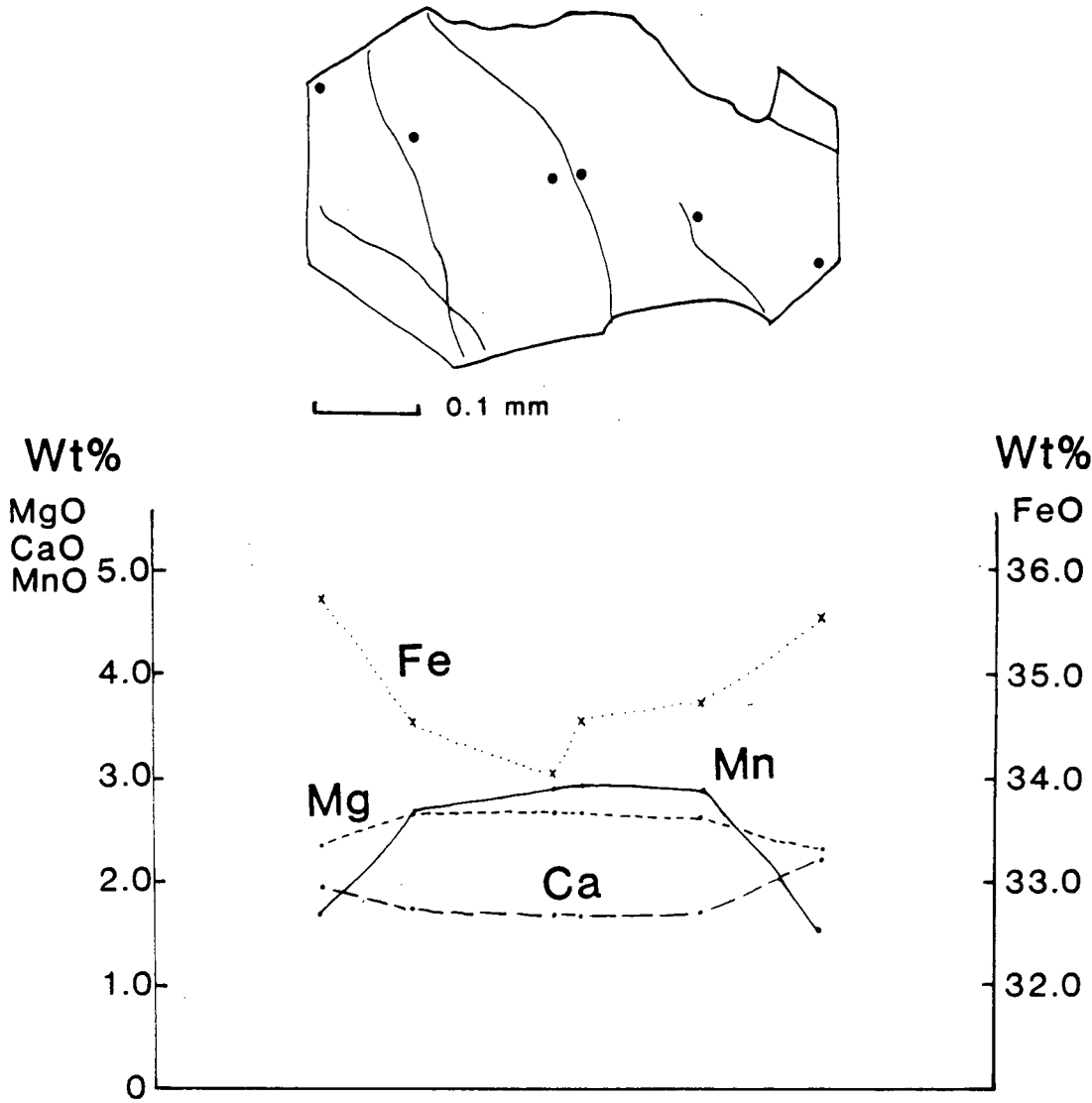
Figure 39. Garnet zoning profile for Garnet 3 from sample 80-31, sillimanite zone.
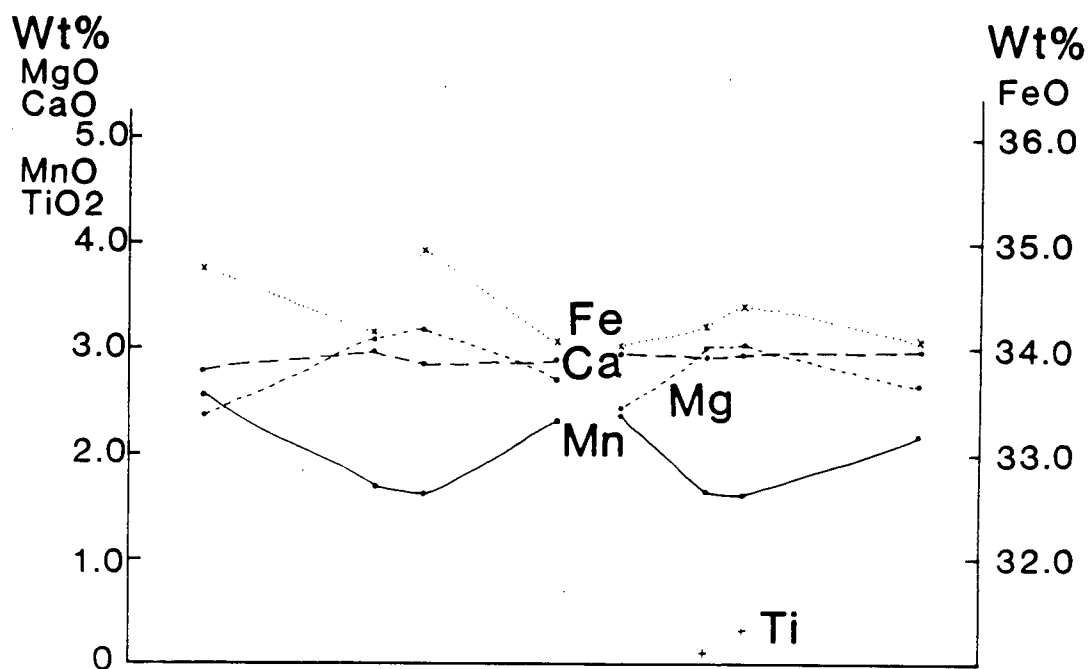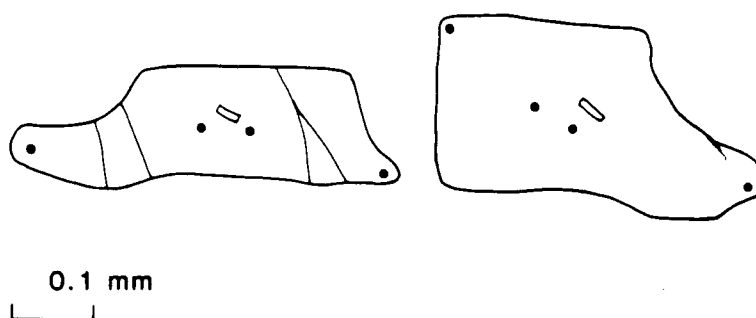
Figure 40. Garnet zoning profiles for Garnets 3.1 and 2 from sample 81-325, kyanite zone.
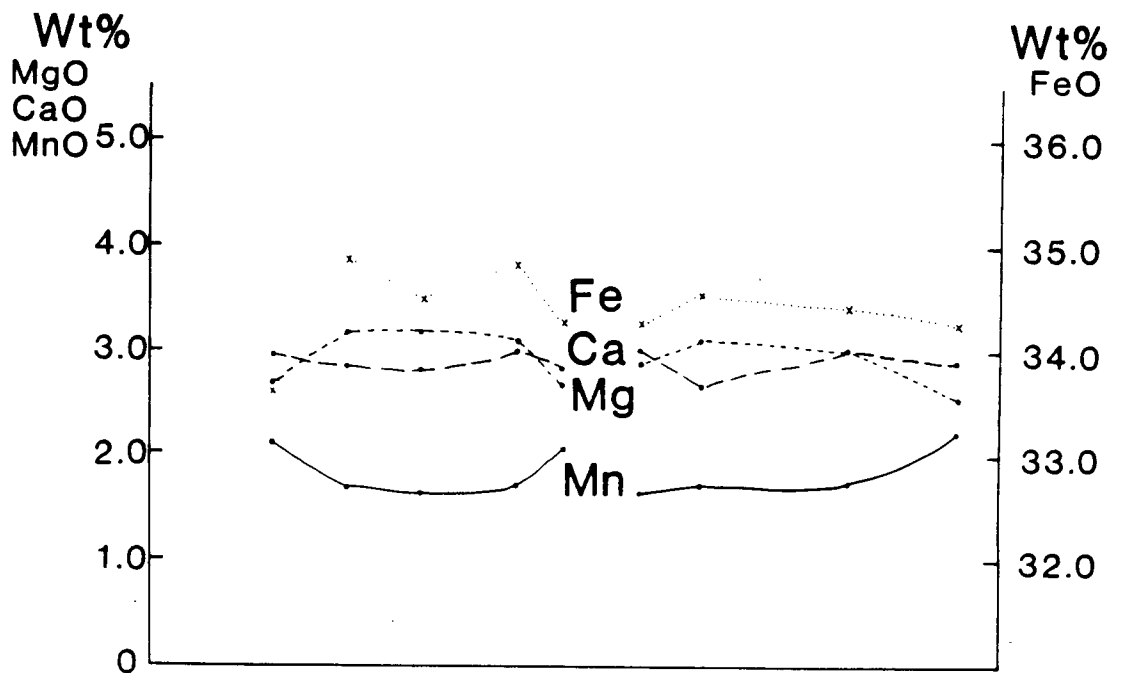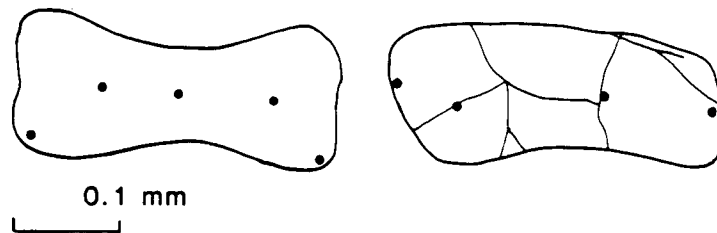
Figure 41. Garnet zoning profiles for Garnets 4 and 1 from sample 81-325, kyanite zone.

4.3.2 <u>DISCUSSION OF GARNET ZONING</u>

As mentioned in the section on the staurolite-kyanite zone, textures in garnets from rocks near the kyanite to sillimanite transition suggest breakdown of larger, texturally zoned garnets and formation of smaller, apparently homogeneous garnets. Atoll garnets attest to the breakdown of the intermediate zone of the garnet first, starting with the area richest in inclusions, which is the rotational zone of the garnet. Both atoll garnets and whole garnets from sample 81-279 appear to be of the same generation because of similar size and inclusion patterns, but they represent different stages of breakdown. The whole garnet shown in Figure 34 contains more Ca and Mn in the core than the rim, and is normally zoned for a garnet which has retained some of its prograde history into staurolite-kyanite zone conditions. It exhibits a rotational pattern in the mid-zone of the garnet, which is typical for garnets in this metamorphic zone. An atoll garnet observed in the same sample shows complete breakdown of this mid-zone to biotite, quartz, and muscovite, and incipient breakdown of the core, whereas the rim is clear of inclusions and apparently stable. Rims of some atoll garnets appear to be in the process of breaking up into smaller, more idiomorphic grains. A similar texture has been observed in the kyanite zone (Zone 8) where tiny garnets are arranged around a ring

as if mimicking the former rim of a larger garnet which has broken down (see Figure 32). The interior of larger garnets may be unstable in the presence of inclusions. Alternatively, the breakdown of garnet of appropriate composition may be due to a combination of reactions, including

$$MS + GT = 2 \; SIL + BI + QZ. \tag{2.4}$$

The inner cores are the last part of the garnet to break down, thus releasing Ca and Mn--the Ca going into plagioclase rather than garnet, and the Mn going to the rims of the new garnets that have nucleated on the relict grains of the old rim, producing reverse Mn zoning in the small garnets. Farther from this transition, the higher grade garnets show normal zoning. The new garnets may also be acquiring components from the breakdown of staurolite,

$$QZ + MS + ST = BI + GT + KY/SIL + H_2O \tag{2.1}$$
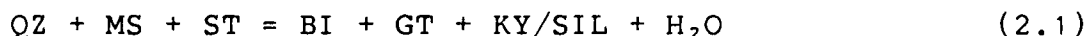
which is consistent with textures observed in thin section.

Whatever combination of reactions is responsible, the staurolite-out isograd is accompanied by a distinct change in garnet textures, as well as changes in the stable aluminosilicate. Below the staurolite-out

isograd, garnets are large, texturally and compositionally zoned and retain evidence of their prograde metamorphic and structural history. Above the staurolite-out isograd, small, clear garnets appear homogeneous but show reverse Mn zoning. At Three Ladies Mountain, kyanite porphyroblasts become unstable along with large garnets, fibrolite appears, and staurolite persists for a short distance into the sillimanite zone. East of Mount Stevenson, on the other hand, large garnet and kyanite porphyroblasts are replaced above the staurolite-out isograd by much smaller grains of kyanite (rather than fibrolite) and tiny garnets with reverse Mn zoning. Such evidence is consistent with a change from Bathozone 4 to Bathozone 5 (Carmichael 1978). defined by the intersection between the reactions

$$KY = SIL \qquad\qquad (1.4)$$

and

$$QZ + MS + ST = BI + GT + KY/SIL + H_2O. \qquad\qquad (2.1)$$
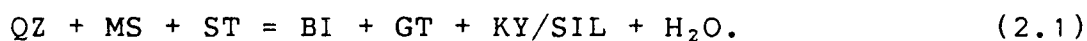
This intersection is discussed in the section on staurolite breakdown, and would be located in the field somewhere near lower Long Creek between Three Ladies Mountain and Mount Stevenson.

4.4 STAUROLITE BREAKDOWN

For defining the bathograd between bathozones 4 and 5, Carmichael (1978) has chosen a staurolite breakdown reaction

$$ST + MS + QZ = GT + BI + KY/SIL + H_2O \qquad (2.1)$$
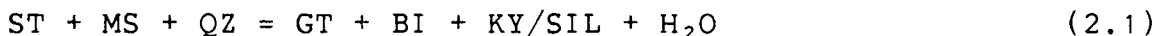
from field and textural evidence, and located it on a P/T diagram within reasonable conditions for the host pelites based on other indications of metamorphic grade. This reaction is a reasonable representation of changes in assemblages observed across the staurolite-out isograd in rocks from the Three Ladies Mountain/Mount Stevenson area.

Carmichael (1978) shows the intersection of reaction (2.1) with KY = SI at 4.75 kb and 540°C, but states that the experimental data for staurolite are inconsistent with these conditions of staurolite stability, and would indicate a higher temperature for the breakdown of staurolite. Archibald et al. (1983) place the intersection at about 5.5 kb and 580°C, having revised Carmichael's curve using an analysis of experimental data on staurolite by Pigage and Greenwood (1982). Higher temperatures for staurolite breakdown were calculated by Pigage and Greenwood (1982) for the reaction

$$6ST + 12.5QZ = 4ALM + 23KY/SIL + 6H_2O. \qquad (2.2)$$
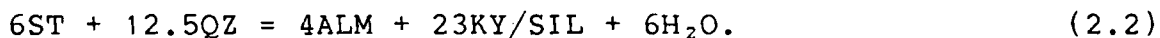
Experimental data for staurolite are inconsistent with field

evidence for the location of this reaction in P/T space. According to Pigage and Greenwood (1982), experimental data for staurolite with a composition of $Fe_2Al_9Si_{3.75}O_{22}(OH)_2$ are internally consistent, but still put the intersection between this reaction (2.2) and KY = SIL at 6.5 kb and 680°C. As this temperature is approaching that of granite melt, it appears high for breakdown of staurolite. Lang and Rice (1985) give values for $\Delta H°f$ and $S°_{298}$ for staurolite which are consistent with the range of best data chosen by Pigage and Greenwood (1982), so these values have been used in calculations in this study.

Staurolite in rocks from the Three Ladies Mountain area is a binary solution of Fe^{2+} and Mg end-members, with XFe ≃ 0.85.

The reaction

$$ST + MS + QZ = GT + BI + KY/SIL + H_2O, \qquad (2.1)$$
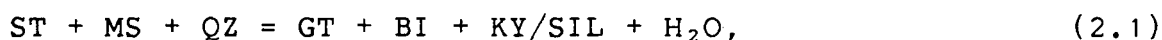
described by Carmichael (1978) as defining the bathograd between bathozones 4 and 5, involves six components and seven phases, and so cannot be calculated in the Fe end-member system. Data for Mg-staurolite are poorly known, and have not yet been found to be consistent with other sets of data. Instead of calculating reaction (2.1), two other staurolite breakdown reactions involving Fe end-member phases were considered:

$$25QZ + 3ST = 46KY + 8ALM + 12H_2O \qquad (2.2)$$

$$17ALM + 25MS + 3ST = 96KY + 25BI + 12H_2O. \qquad (2.3)$$
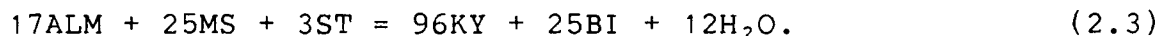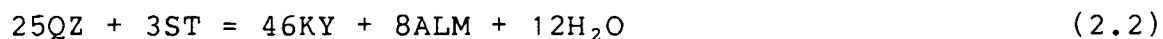
(Note that staurolite formula of $Fe_2Al_9Si_{3.75}O_{22}(OH)_2$ has been multiplied by four in order to have an integral value for Si for computing purposes, so coefficients appear unusually high.)

These reactions were calculated and then displaced assuming the oversimplification that measured values of XFe in staurolite, biotite, and garnet approximate activities of these phases, and that all other phases are pure, and using the thermodynamic data compiled by Lang and Rice (1985) (Table I).

Expressions for activity assume ideal site mixing, as follows:

Almandine ($Fe_3Al_2Si_3O_{12}$) $a_{alm} = (X_{Fe}^{Gt})^3$

Biotite ($KFe_3Si_3AlO_{10}(OH)_2$) $a_{bi} = (X_{Fe}^{Bi})^3$

Staurolite ($Fe_8Al_{36}Si_{15}O_{88}(OH)_8$) $a_{st} = (X_{Fe}^{St})^8$

$$\Delta G_r = \Delta G_r^\circ + RT \ln K_{displ} \qquad (2.4)$$

where

$$K_{(2.2)} = \frac{(a_{alm})^8}{(a_{st})^3} = \frac{(X_{Fe}^{Gt})^{24}}{(X_{Fe}^{St})^{24}} \qquad (2.2a)$$

$$K_{(2.3)} = \frac{(a_{bi})^{25}}{(a_{st})^3 (a_{alm})^{17}} = \frac{(X_{Fe}^{Bi})^{75}}{(X_{Fe}^{St})^{24} (X_{Fe}^{Gt})^{51}} \qquad (2.3a)$$

Results are presented graphically in Figure 42. Both reactions are displaced to lower temperatures as expected. Reaction (2.2) is only displaced by about 20°C, whereas reaction (2.3), involving muscovite and biotite, as well as breakdown of garnet, is displaced by over 250°C, so the effect of Mg in biotite is significant. Temperatures and pressures of intersection of these reactions with KY = SIL (P = 7-7.3 kb, T =670-690°C) still appear too high, but are beginning to approach reasonable values. Water activity <1 would displace these reactions to lower temperatures. However, reduction of XH_2O to 0.88, assuming equilibrium

TABLE I. MINERAL DATA

MINERAL	FORMULA			ABBREVIATION		
$\Delta H^{\cdot} f$ (J/mol)	$S^{\cdot}$ 298K (J/m-K)	a (J/m-K)	b (J/m-K^2)		c (J/m-K)	Vs (J/bar)

MINERALS

A-QUARTZ   SI(1)O(2)   A-QTZ
    -910648.00   41.33800   46.94000   .034309   -1129700.   23.2400

ALMANDINE   FE(3)AL(2)SI(3)O(12)   ALM
    -5277200.00   298.700   408.15   .14075   -7837000.   115.28

FE-BIOTITE   K(1)FE(3)AL(1)SI(3)O(12)H(2)   FE-BIO
    -5155504.   398.3   445.30   .1246   -8079000.   154.32

MUSCOVITE   K(1)AL(3)SI(3)O(12)H(2)   MS
    -5972275.   287.9   408.19   .11037   -10644000.   140.71

KYANITE   AL(2)SI(1)O(5)   KY
    -2581097.   83.68   173.189   .02852   -5389900.   44.09

SILLIMANITE   AL(2)SI(1)O(5)   SIL
    -2573574.   96.776   167.46   .030922   -4884400.   49.90

FE-STAUROLITE   FE(8)AL(36)SI(15)O(96)H(8)   FE-ST
    -47497890.   1770.0   3467.6   .6704   -93880000.   897.6

ANORTHITE   CA(1)AL(2)SI(2)O(8)   AN
        205.4   264.83   .061898   -6460100.   100.79

GROSSULAR   CA(3)AL(2)SI(3)O(12)   GROS
        254.7   435.207   .071182   -11429900.   125.3

GASES
STEAM   H(2)O(1)   H2O
    -241818.   188.72   30.54   .01029

Data from Lang and Rice (1985).

Activities used for displaced reactions are as follows.
XFe ST = (0.85) ' = -0.56465
XFe BI = (0.54) ' = -0.8028
XFe ALM = (0.79) ' = -0.30712
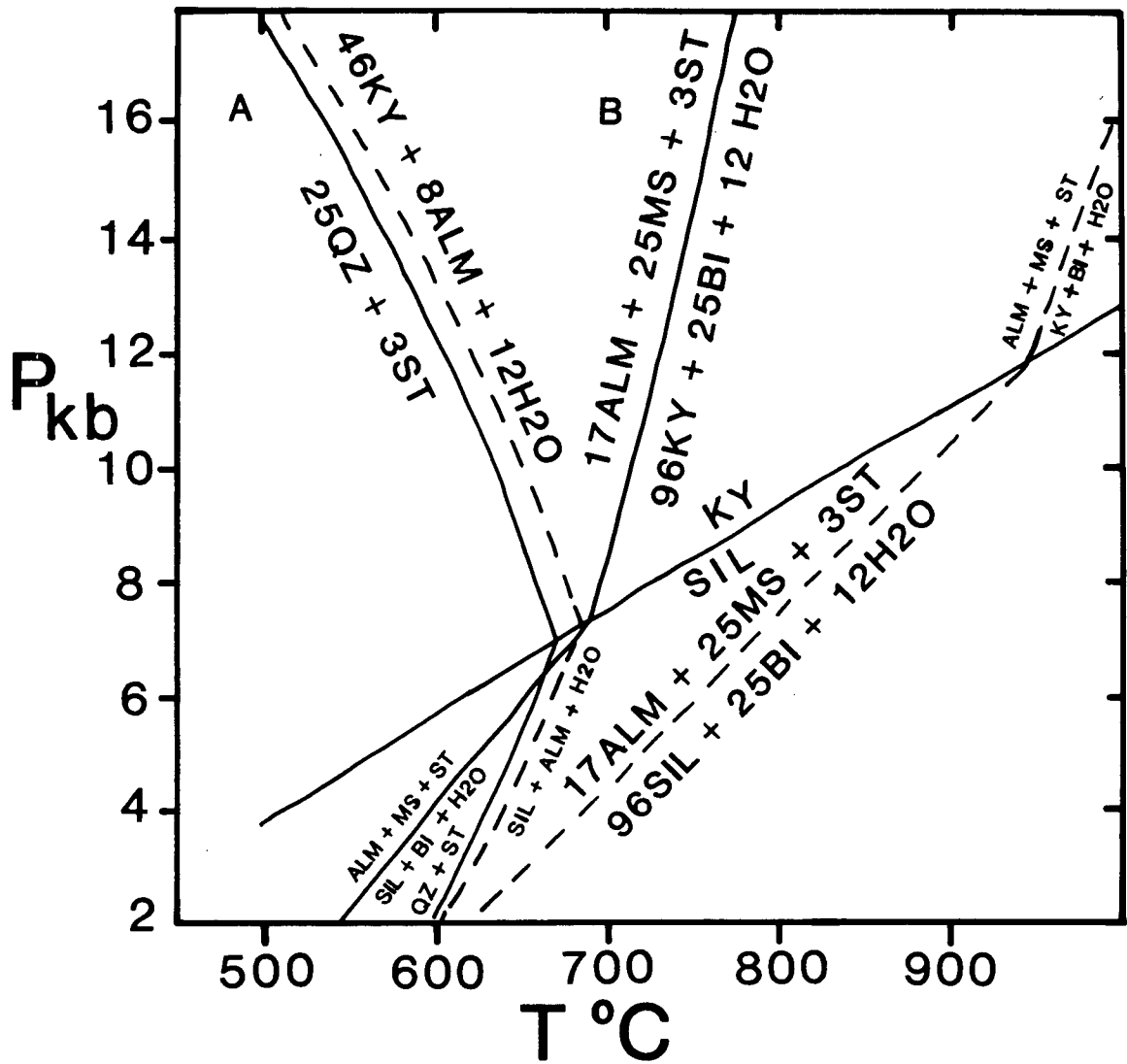
Figure 42. Calculated staurolite breakdown reactions using
thermodynamic data from Lang and Rice (1985) and measured
staurolite XFe = 0.85, garnet XFe = 0.79, and biotite XFe =
0.54. Dashed curves indicate Fe end-member reactions.
Intersection of reaction (A) with KY = SIL is displaced from
7224 bars and 683°C to 6985 bars and 670°C; intersection of
reaction (B) with KY = SIL is displaced from 11825 bars and
945°C to 7333 bars and 689°C. Reduction of XH₂O to 0.88
displaces both curves by only 10°C.

with graphite, only displaces these reactions by about 10°C. Use of a more comprehensive and consistent database (including data for Mg-staurolite) and less simplified activity models for solid solution phases may result in a more realistic petrogenetic grid involving staurolite reactions.

Analysis of rocks from the Three Ladies Mountain area indicates that staurolite breakdown is accompanied by textural and compositional changes in garnet (suggesting discontinuous reaction involving garnet) and also involves muscovite and biotite. Therefore, neither reaction (2.2) nor (2.3) alone is completely adequate for describing staurolite breakdown in these rocks, However, according to the displacement of the reactions shown in Figure 42, they would occur nearly simultaneously near the kyanite to sillimanite transition. Reaction (2.1), suggested by Carmichael (1978), cannot be balanced exactly with the minerals of this study, as the XFe (St) is almost equal to the XFe (Gt). However, simultaneous equilibrium among muscovite, quartz, garnet, staurolite, biotite, and kyanite must also satisfy equilibria (2.2) and (2.3).

4.5 GARNET-BIOTITE GEOTHERMOMETRY

Ferry and Spear (1978) first introduced a calibrated geothermometer based on the Fe-Mg cation exchange reaction between garnet and biotite. Subsequently, several authors have offered corrections for taking into consideration the effects on calculated temperature of Ca and Mn components in garnet (Newton and Haselton (1981); Pigage and Greenwood (1982); Ganguly and Saxena (1984)). Calculated temperatures can vary by over 100°C depending on which solution models are used, especially those involving manganese. Engi (1984) and Lang and Rice (1985) favor the correction by Newton and Haselton (1981) as giving the most realistic and consistent temperatures.

Eight samples were chosen from those least affected by retrograde metamorphism. One garnet-biotite temperature was calculated for each sample using averaged analyses of several points on garnet rims and biotite grains. Averaged microprobe analyses are presented in Appendix II; note that standard deviations among different biotite grains in the same section are approximately the same as those from one grain (biotite from sample 80-19 is given as an example).

Garnet-biotite temperatures were calculated for garnet rims and also for cores paired with matrix biotite in some samples; temperatures were also calculated for garnet with biotite inclusions from sample 80-119. The methods used were those of Ferry and Spear (1978; T1), Newton and Haselton (1981; T2), and Ganguly and Saxena (1984; T3).

The following formulas were used for calculating garnet-biotite temperatures (Lang and Rice 1985):

$$T1 \ (K) = \frac{2089 + 0.00956*P \ (bar)}{0.7820 - \ln K}$$

Ferry and Spear (1978)

$$T2 \ (K) = \frac{(1661 - 0.755*T1 \ (K))X_{Ca}^{Gt} + 2089 + 0.00956*P \ (bar)}{0.7820 - \ln K}$$

Newton and Haselton (1981)

$$T3 \ (K) = \frac{W_{FeMg}(X_{Fe}^{Gt} - X_{Mg}^{Gt} - 0.8)/R}{0.7820 - \ln K}$$
$$+ \frac{1510*(X_{Ca}^{Gt} + X_{Mn}^{Gt}) + 2089 + 0.00956*P \ (bar)}{0.7820 - \ln K}$$

Ganguly and Saxena (1984)

where W_{FeMg} = 11.34 kJ and R = 8.314 $JK^{-1}mol^{-1}$

Table II (A and B) shows the temperatures given by these three methods at 5000 and 6000 bars. Four of the samples (80-119, 80-33, 81-278, 81-279) were chosen from as close to the kyanite-sillimanite transition as possible.

Average rim temperatures for samples from the area as a whole as well as from the kyanite-sillimanite isograd are shown. Garnet rim temperatures using the method of Newton and Haselton (1981) average around $525 \pm 18°C$ at 5 kb and $528 \pm 18°C$ at 6 kb for the whole area and $521 \pm 25°C$ at 5 kb and $525 \pm 25°C$ at 6 kb for the kyanite to sillimanite transition zone. Uncorrected Ferry and Spear (1978) gives temperatures about 35°C lower, whereas the method of Ganguly and Saxena (1984) gives temperatures about 35° higher. Note that variation of temperature among samples from a single mapped isograd exceeds variation across the whole area from staurolite zone to sillimanite zone. If the sillimanite-in isograd corresponds to the reaction KY = SI, then the best fit temperature and pressure are those given by Ganguly and Saxena (1984) at 557°C and 5 kb.

Note that there is not much difference in rim temperature between samples from the staurolite zone, kyanite zone, and sillimanite zone, but that core "temperatures" (using matrix biotite) are lower than rim temperatures in the staurolite zone sample, and higher than rim temperatures in the sillimanite zone, kyanite zone, and kyanite to sillimanite transition zone.

TABLE IIA. GARNET-BIOTITE TEMPERATURES

SAMPLE	82-389 RIM	82-389 CORE	81-279 RIM	81-278 RIM	80-33 RIM	80-33 CORE	80-119 RIM	80-119 INC1	80-119 INC2
MET. ZONE	ST	ST	ST-KY	ST-KY-SI	ST-KY-SI	ST-KY-SI	ST-KY-SI	ST-KY-SI	ST-KY-SI
XMgGt	0.100	0.081	0.087	0.089	0.085	0.095	0.090	0.123	0.119
XFeGt	0.690	0.657	0.806	0.770	0.801	0.779	0.811	0.778	0.799
XCaGt	0.175	0.188	0.075	0.078	0.061	0.047	0.063	0.067	0.050
XMnGt	0.035	0.073	0.032	0.064	0.053	0.080	0.036	0.033	0.033
SUM	3.030	3.063	3.028	3.030	2.966	2.958	3.006	2.992	3.012
Mg/Fe Gt	0.145	0.124	0.108	0.115	0.106	0.121	0.112	0.157	0.149
Mg/Fe Bi	1.253	1.253	0.760	0.978	0.785	0.785	0.761	1.213	1.143
K[1]	0.116	0.097	0.142	0.118	0.135	0.155	0.147	0.130	0.130

T ($^{\circ}$C) at P = 5 kb

T1 (FS[2])	454	416	508	459	494	533	517	441	484
T2 (NH[3])	521	486	537	488	517	552	542	466	504
T3 (GS[4])	562	544	567	532	555	605	573	491	528

T ($^{\circ}$C) at P = 6 kb

T1 (FS[2])	458	419	511	462	497	537	521	444	488
T2 (NH[3])	524	489	541	491	521	555	546	469	507
T3 (GS[4])	565	547	570	535	559	609	576	495	532

[1]K = (Mg/Fe Gt)/(Mg/Fe Bi)
[2]FS = Ferry and Spear (1978)
[3]NH = Newton and Haselton (1981)
[4]GS = Ganguly and Saxena (1984)

TABLE IIB. GARNET-BIOTITE TEMPERATURES

SAMPLE	80-19 RIM	80-19 CORE	80-31 RIM	80-31 CORE	81-325 RIM	81-325 CORE	AVERAGE RIMS	AVERAGE RIMS
MET. ZONE	ST-SI	ST-SI	ST-SI	ST-SI	KY	KY	ST-KY-SI[5]	ALL ZONES
XMgGt	0.089	0.131	0.094	0.106	0.108	0.122		
XFeGt	0.784	0.753	0.806	0.772	0.758	0.758		
XCaGt	0.076	0.091	0.058	0.047	0.085	0.082		
XMnGt	0.051	0.026	0.041	0.076	0.049	0.038		
SUM	3.005	3.025	3.025	3.030	3.040	3.055		
Mg/Fe Gt	0.114	0.173	0.117	0.138	0.142	0.160		
Mg/Fe Bi	0.856	0.893	0.823	0.823	1.003	1.003		
K[1]	0.133	0.194	0.142	0.167	0.142	0.160		

T (°C) at P = 5 kb

	80-19 RIM	80-19 CORE	80-31 RIM	80-31 CORE	81-325 RIM	81-325 CORE	AVERAGE RIMS	AVERAGE RIMS
T1 (FS[2])	489	609	509	558	508	544	494 (±26)	492 (±24)
T2 (NH[3])	519	647	532	577	542	577	521 (±25)	525 (±18)
T3 (GS[4])	558	682	564	630	582	613	557 (±18)	562 (±15)

T (°C) at P = 6 kb

	80-19 RIM	80-19 CORE	80-31 RIM	80-31 CORE	81-325 RIM	81-325 CORE	AVERAGE RIMS	AVERAGE RIMS
T1 (FS[2])	493	613	513	562	512	548	498 (±26)	496 (±24)
T2 (NH[3])	522	651	536	581	545	580	525 (±25)	528 (±18)
T3 (GS[4])	561	686	568	634	586	617	560 (±18)	565 (±15)

[1] K = (Mg/Fe Gt)/(Mg/Fe Bi)
[2] FS = Ferry and Spear (1978)
[3] NH = Newton and Haselton (1981)
[4] GS = Ganguly and Saxena (1984)
[5] Average of 4 samples at KY=SI isograd: 80-33, 80-119, 81-278, 81-279.

148

Overall, garnet-biotite geothermometry estimates temperatures between about 490° and 570°C at pressures between 5 and 6 kb. Presence of sillimanite in the rocks indicates that either the pressure was somewhat lower (4 kb?) at the same T, or that the temperatures given by all of these methods, except perhaps Ganguly and Saxena (1984) are too low at the kyanite-sillimanite isograd by approximately 50°C. No temperature gradient from staurolite zone to sillimanite zone was demonstrated using garnet-biotite geothermometry. Assuming that changes in metamorphic assemblages in pelites are due to changes in pressure and temperature conditions during metamorphism, either the garnet-biotite geothermometer does not adequately estimate metamorphic temperatures, or the temperature gradient required between staurolite zone and sillimanite zone is smaller than the resolution possible with this method so far, or less than about 50°C.

4.6 GEOBAROMETRY: GRAIL

A new geobarometer referred to as "GRAIL" has been calibrated by Bohlen et al. (1983) for the reaction

$$3 \text{ IL} + \text{SI/KY} + 2 \text{ QZ} = \text{AM} + 3 \text{ RU}. \qquad\qquad (3.1)$$

The almandine plus rutile assemblage is on the high-pressure side of the reaction (see Figure 43). This geobarometer can only be applied indirectly to the metamorphic rocks of the Three Ladies Mountain area as the univariant assemblage ilmenite + aluminosilicate + quartz + almandine + rutile is nowhere observed to be stable. However, textures involving subsets of this assemblage have been useful in limiting the pressure conditions over most of the area to those pressures below the GRAIL reaction.

Of thirteen pelite samples containing both ilmenite and rutile, seven are in staurolite-kyanite zone (Zone 4). In these seven samples, rutile is only present as small inclusions within porphyroblasts of staurolite and/or kyanite, whereas ilmenite is present both as inclusions in porphyroblasts such as garnet, staurolite, and kyanite, and as individual laths in the matrix pelite. The same textures were noted in one sample from the staurolite zone (Zone 3) and two samples from the staurolite-kyanite-sillimanite zone (Zone 5). Where rutile comes in contact with quartz, whether within a porphyroblast or near the rim, it is replaced by ilmenite. This texture is illustrated in
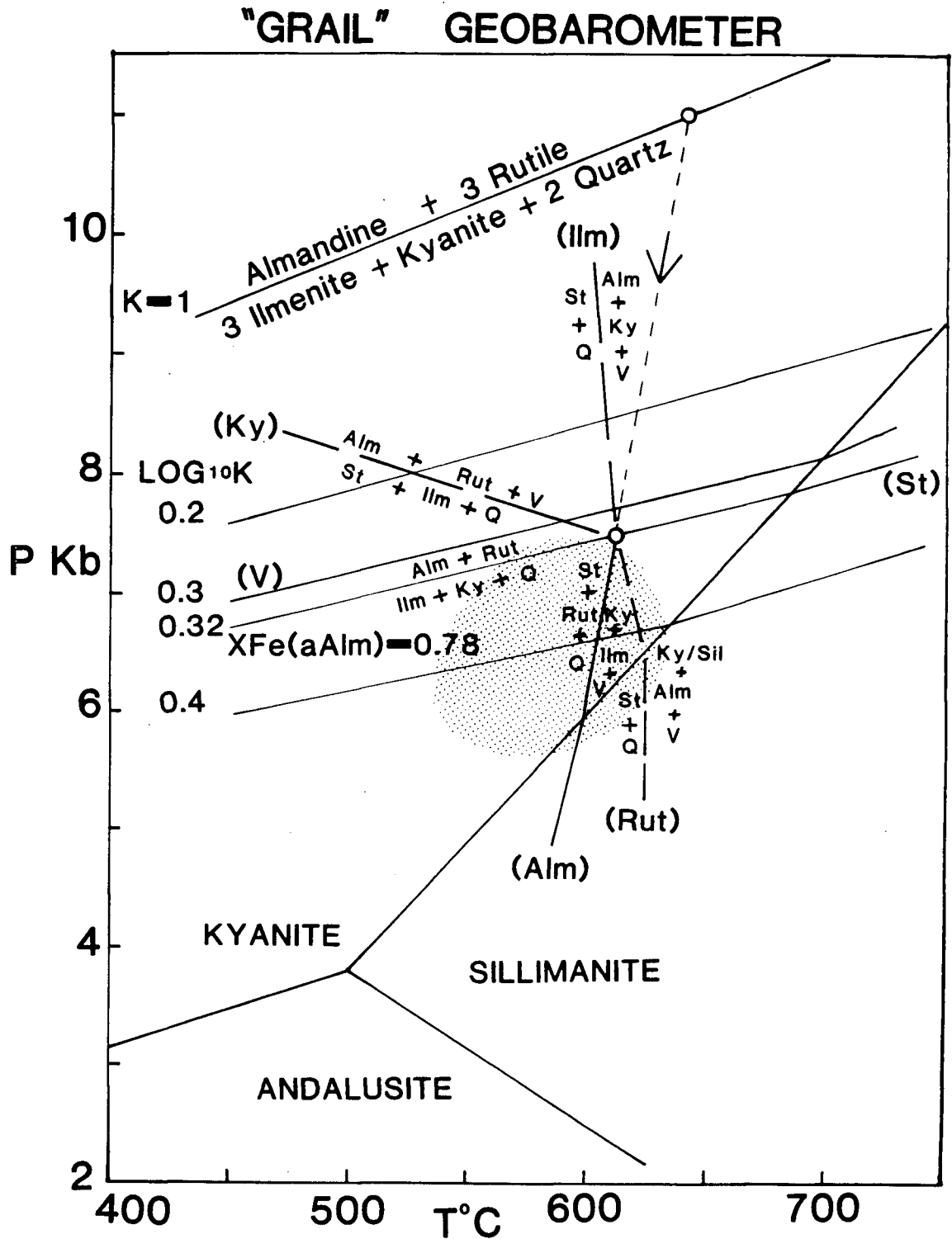
Figure 43. Pressure/temperature diagram of "GRAIL" geobarometer (modified from Bohlen et al. 1983). Shaded area shows approximate P/T conditions indicated by assemblages observed in rocks from Three Ladies Mountain/ Mount Stevenson area.

Figure 44, where a trail of rutile inclusions in staurolite is continuous with a trail of ilmenite grains in the matrix. Elongate grains straddling the rim of the porphyroblast are rutile within the staurolite (or in other places kyanite) and ilmenite where projecting into the matrix. The assemblage ST + RU + QZ appears to be less stable than ST + RU without QZ. Ilmenite is stable with garnet, quartz, kyanite, staurolite, and the other minerals of the pelite matrix.

The remaining three samples containing both ilmenite and rutile are from the apparently higher-pressure kyanite zone (Zone 8). They are the only samples in which rutile occurs both as inclusions in garnet and as individual grains in the matrix without ilmenite rims, but it must be noted that rutile is a very minor constituent of these rocks. Rutile inclusions in kyanite still show replacement by ilmenite where in contact with quartz. Perhaps pressures approximating those for the "GRAIL" reaction have been approached.

In staurolite to staurolite-kyanite zone rocks near Three Ladies Mountain, lack of rutile inclusions in garnet suggests a pressure below that of the "GRAIL" reaction. In the same rocks, textures involving rutile, quartz, and staurolite suggest temperatures compatible with the reaction

$$ST + RU + QZ = KY + IL + H_2O, \qquad (3.2)$$
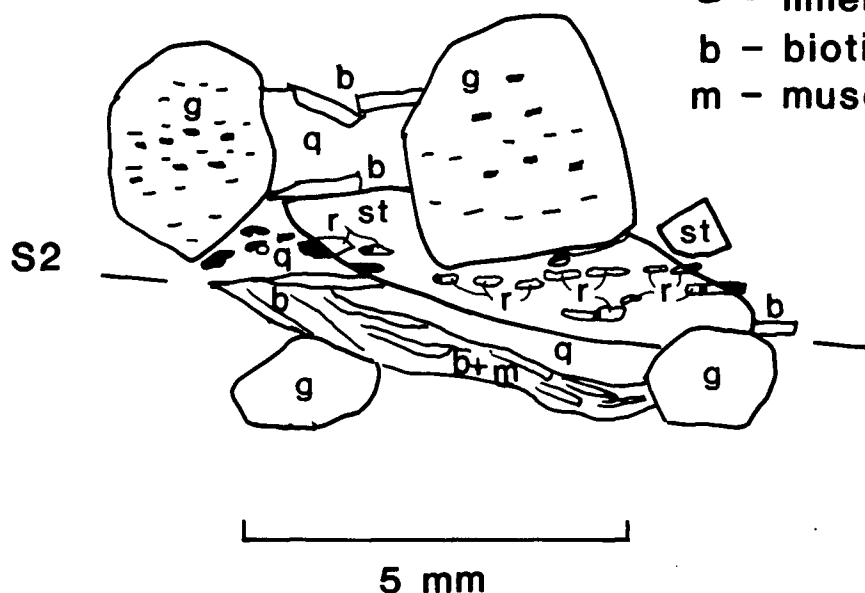
Figure 44. Sketch of photomicrograph (sample 81-344) illustrating how rutile is stable as inclusions in staurolite, but unstable relative to ilmenite where in contact with quartz, as in pelite matrix. Note that garnet, which predates staurolite, contains only ilmenite inclusions, and no rutile. This sample is from the staurolite zone near the kyanite-in isograd, and may be evidence for the reaction
ST + RU + Q = KY + IL + H$_2$O
as shown in Figure 43.

which is stable at temperatures between about 550° and 650°C, and below pressures for the "GRAIL" reaction (3.1) (see Figure 43).

A representative value of 0.78 was chosen (using microprobe data) for XFe in garnet in order to estimate displacement of the "GRAIL" curve to lower pressure (about 7 kb) than that for the same reaction involving pure phases (about 10 kb). Non-garnet phases are assumed to be pure (a = 1). Displacement is estimated using curves from Bohlen et al. (1983). Because of assumptions and generalizations made here, and because accurate P/T conditions for those reactions involving staurolite are incompletely known, the "GRAIL" curve and associated invariant point cannot be exactly located in P/T space. P/T conditions in the Three Ladies Mountain area can be indirectly estimated from the "GRAIL" geobarometer and associated reactions as below about 7 kb and between about 550° and 650°C. These conditions are reasonably consistent with those estimated from other reactions (see Figure 25) for staurolite-kyanite zone rocks near Three Ladies Mountain, considering the uncertainty associated with staurolite.

4.7 GEOBAROMETRY: GROSSULAR-ANORTHITE-ALUMINOSILICATE-QUARTZ

Estimates of pressure can be made using a geobarometer suggested by Ghent (1976) based on the reaction

$$3 \text{ AN} = \text{GR} + 2 \text{ KY/SI} + \text{QZ} \qquad (4.1)$$

Other authors including Newton and Haselton (1981) and Lang and Rice (1985) have refined the method. Newton and Haselton (1981) present activity models for grossular and plagioclase, methods of calculation, and discussion of the thermodynamics of the geobarometer. Following Newton and Haselton (1981), equation (4.1) is rewritten with grossular as $CaAl_2/_3SiO_4$, such that

$$3 \text{ AN} = 3 \text{ GR} + 2 \text{ KY} + \text{QZ} \qquad (4.1a)$$

$$3 \text{ AN} = 3 \text{ GR} + 2 \text{ SI} + \text{QZ} \qquad (4.1b)$$

Their formulation is given as follows:

$$\Delta G^{\circ}_r + RT \ln(a_{gr}/a_{an})^3 + P\Delta\overline{V}_r \simeq 0 \qquad (4.2)$$

(Newton and Haselton 1981, p. 132).

ΔG°_r (at 1 bar) can be approximated by $-P^\circ \Delta V^\circ_r$, where P° is the pressure of the end-member equilibrium at T and ΔV° is the end-member volume change. The end-member reaction can be represented in P/T space by the line

$$P = -7111.9 + 22.77 \, T \quad \text{(for kyanite)} \tag{4.3}$$

(Lang and Rice 1985).

To modify equation (4.3) for sillimanite, the following method was used. A similar linear approximation for the reaction SI = KY was obtained (from Rice, pers. comm., modified from Ghent 1976):

$$P = -6367.2 + 20.23 \, T^\circ C \text{ or}$$
$$P = -11893 + 20.23 \, T \, (K) \tag{4.4}$$

Pressure terms from reactions (4.3) and (4.4) are multiplied by ΔV_r° to give energy terms, ΔG_r°. ΔV of reaction is -6.57 J/bar for (4.1a), -5.40 J/bar for (4.1b), and -0.581 J/bar for SI = KY. P is in bars, and ΔG° is in joules. Subtracting $2*\Delta G_r^\circ$ for SI = KY from ΔG_r° (4.1a) gives ΔG_r° (4.1b).

$$3 \text{ AN} = 3 \text{ GR} + 2 \text{ KY} + \text{QZ} \qquad (4.1a)$$

$$- (2 \text{ SI} = 2 \text{ KY})$$

$$3 \text{ AN} = \text{GR} + 2 \text{ SI} + \text{QZ} \qquad (4.1b)$$

ΔG_r° for reaction (4.1b) is then divided by ΔV for reaction (4.1b) to give the expression shown in (4.5). Thus, for sillimanite,

$$P = -6093.6 + 23.35 \text{ T (for sillimanite)} \qquad (4.5)$$

P is in bars; T in Kelvins.

ΔV is the partial molar volume change at 1 bar. Partial molar volume of garnet depending on composition can be read directly from the graph given in Newton and Haselton (1981, p. 138). Differential compressibilities are neglected. Volume of anorthite was used for $\bar{V}$ of anorthite component in plagioclase.

Activity models used for grossular in garnet and anorthite in plagioclase are those given by Lang and Rice (1985), which are modified from Newton and Haselton (1981).

$$a_{gr} = X_{Ca}^{Gt} \cdot \gamma_{gr} \qquad \text{(where Gr = CaAl}_2/_3\text{SiO}_4\text{)}$$

$$a_{gr} = X_{Ca}^{Gt} \cdot \exp\{\frac{W_{CaMg}[\,(X_{Mg}^{Gt})^2 \; + \; X_{Mg}^{Gt} \cdot X_{Fe}^{Gt}\,]}{RT}\} \qquad (4.6)$$

where W_{CaMg} = 13807 − 6.3 T (J,K)

$$a_{an} = \frac{X_{an}(1 + X_{an})^2}{4} \cdot \exp[\frac{(1 - X_{an})^2}{T}(1032 + 4726X_{an})] \quad (4.7)$$

Putting this all together and isolating P on one side of the equation, pressure may be calculated using the following formula:

$$P = \frac{-\Delta G_r^{\circ} - RT \ln(a_{gr}/a_{an})^3}{\Delta \bar{V}_r} \qquad (4.8)$$

Seven of the eight microprobe samples from the Three Ladies Mountain area contain the required assemblage garnet-plagioclase-aluminosilicate-quartz. Plagioclase rim composition ranges from An_{22} to An_{38}, and is consistent within each sample, but does not show any consistent pattern of distribution across the area; but systematic changes with P and T would only be expected in maximum-phase assemblages. The aluminosilicate is kyanite only in two samples (81-279 and 81-325), and sillimanite only in two samples (80-19 and 80-31). The remaining three samples (80-33, 80-119, and 81-278) contain both kyanite and sillimanite, as they are taken from the staurolite-kyanite-sillimanite zone, representing the KY = SI isograd.

Pressure estimates for these samples have been calculated using the geobarometer outlined above and the temperatures at 6 kb given by garnet-biotite geothermometry using the method of Newton and Haselton (1981) (see section on garnet-biotite geothermometry, Table II). Pressure estimates using the grossular-anorthite geobarometer range from 4.6 kb to 6.6 kb (Table III), but do not vary systematically across metamorphic isograds in the area. No matter how the group of samples is subdivided on reasonable geologic grounds, the pressure estimates cannot be narrowed down any further or forced to show any significant gradient. The two closest samples in the field, 81-278 and 81-279, found within a few hundred meters of one another, give a pressure estimate difference of nearly 2 kb between them.

TABLE III. GROSSULAR-ANORTHITE-ALUMINOSILICATE GEOBAROMETRY

Sample	81-325	80-19	81-279	81-278	80-33	80-119	80-31
MET. ZONE	KY	ST-SI	KY-ST	ST-KY-SI	ST-KY-SI	ST-KY-SI	SI
XAn	0.374	0.381	0.228	0.307	0.263	0.277	0.217
XFeGt	0.758	0.784	0.806	0.770	0.801	0.811	0.806
XMgGt	0.108	0.089	0.087	0.089	0.085	0.090	0.094
XCaGt	0.085	0.076	0.075	0.079	0.061	0.063	0.058
XMnGt	0.049	0.051	0.032	0.064	0.031	0.036	0.041
V.gr [1]	12.67	12.61	12.60	12.63	12.51	12.52	12.50
ΔV KY	-6.43	-	-6.50	-6.47	-6.59	-6.58	-
ΔV SI	-	-5.32	-	-5.30	-5.42	-5.41	-5.43
ΔV r KY	-6.57	-	-6.57	-6.57	-6.57	-6.57	-
ΔV r SI	-	-5.40	-	-5.40	-5.40	-5.40	-5.40
T (°C) [2] at 6kb	545	522	541	491	520	546	536
P (bar) KY	5559		6610	4695	4906	5391	
SI		4687		4946	5071	5552	6144

[1] V in J/bar.
[2] T2, method of Newton and Haselton (1981).

Using only one sample per metamorphic zone may not be sufficient to produce significant results, and the simplified activity models may make the results sensitive to mineral composition.

In conclusion, garnet-plagioclase pressures for all samples considered average 5.5 ± 0.7 kb. Temperatures calculated for these rocks using the method of Newton and Haselton (1981) for P = 6 kb average around 530°C. These P/T conditions are approximately consistent with the KY = SI isograd, but not with the P/T conditions calculated from staurolite breakdown reactions.

4.8 CONCLUSION

Pelitic rocks of late Proterozoic Snowshoe Group were
metamorphosed to greenschist to amphibolite facies
conditions during the mid-Jurassic Columbian Orogeny, and
can be divided into zones corresponding to classic divisions
of the Barrovian series. The distribution of metamorphic
zones as defined by mineral assemblages and textures in
amphibolite facies pelitic schist in the Three Ladies
Mountain/Mount Stevenson area implies an increase in
metamorphic grade over a distance of 10 km from garnet zone
in the northwest to sillimanite zone in the southeast.

Textural zoning and static overgrowths of porphyroblasts
are due to metamorphic crystallization outlasting
deformation (high temperatures outlasting active strain) and
to discontinuous reactions involving solid-solution minerals
as expected during conditions of increasing T and P. There
is no unequivocal evidence to support more than one episode
of prograde metamorphism involving recrystallization of
garnet, staurolite, or kyanite. Discontinuous reactions
involving garnet and staurolite breakdown interpreted from
microscopic textures, along with garnet zoning profile
trends, suggest a metamorphic temperature increase from west
to east, with a pressure increase from north to south. The
intersection of the staurolite breakdown reaction with
KY = SI defining the bathograd between bathozones 4 and 5
(Carmichael 1978) should correspond to the intersection of
the staurolite-out isograd with the sillimanite-in isograd

in the field, thus establishing a pressure-temperature point
somewhere near Long Creek south of Welcome Mountain (see
Plate III). Unfortunately, estimates of this point of
intersection in P/T space vary from Carmichael (1978), who
places it empirically at about 4.75 kb and 540°C; to
Archibald et al. (1983), who place it at about 5.5 kb and
580°C; to calculations in this study which only approximate
the appropriate reaction and place the intersection at about
7-7.3 kb and 670-690°C. The latter is clearly too high to
be reasonable.

Maximum pressure estimated using the GRAIL geobarometer
(Bohlen et al. 1983) is about 7 kb; compatibility of
kyanite, ilmenite, staurolite, and quartz also suggests
temperatures between 550° and 650°C. These are higher than
garnet-biotite temperatures but lower than temperatures
estimated from other staurolite breakdown reactions.
Estimates of metamorphic conditions based on reactions
involving staurolite tend to give higher temperatures than
other methods. Further experimental and thermodynamic work
on staurolite is required for resolution of this problem.

Geothermometry and geobarometry results show no
significant temperature or pressure gradient across the map
area corresponding to the variation in metamorphic grade as
indicated by mapped isograds. Unfortunately, no samples
from the garnet zone were suitable for garnet-biotite
geothermometry. Garnet-biotite geothermometry using the
correction-method of Newton and Haselton (1981) gives

average peak metamorphic temperatures of around 525 ± 18°C at 5 kb and 528 ± 18°C at 6 kb for the whole area, including the kyanite-sillimanite transition zone. Using these temperatures, pressures calculated according to the grossular-anorthite-aluminosilicate-quartz geobarometer average 5.5 ± 0.7 kb with no systematic variation in distribution across the study area. These temperatures and pressures are reasonable for the staurolite-kyanite zone rocks which cover most of the Three Ladies Mountain/Mount Stevenson area. However, the lack of P or T gradients demonstrated by these geothermometric and geobarometric methods does not reflect the gradients in conditions which are represented by progressive changes in mineral assemblages, even though these changes correspond well with the typical Barrovian series of metamorphic zones in pelites.

The resolution of these methods as used here seems to be no better than 50°C for garnet-biotite temperatures and about 1-2 kb for garnet-plagioclase pressures. Temperature and pressure gradients required for metamorphic changes from staurolite zone to first sillimanite zone may be smaller than these values. Although the mapped changes in metamorphic assemblages are real, they may not indicate large changes in P and T. For instance, presence of staurolite may be more strongly controlled by bulk composition of the host pelite than by measurable gradients in temperature and pressure within the large stability field

for staurolite, although if the isograd reactions were truly univariant, this effect would be eliminated.

The large area covered by a comprehensive staurolite-kyanite zone (8 km wide between garnet zone and sillimanite zone, and at least 25 km long in a northeast direction) indicates that the dip of significant metamorphic isograds such as KY = SI must be relatively shallow to the northwest, crosscutting the slightly more steep and northerly regional dip of the metamorphosed strata (see Figure 45).

There is no unusually steep metamorphic gradient in this area (nor any inverted isograds), although there is significant post-metamorphic displacement along the Little River Fault.

Given peak metamorphic conditions of about 5-6 kb and 500-600°C, metamorphism occurred at a depth of about 15-20 km with a geothermal gradient of about 30°C/km. This is a normal geothermal gradient so no special temperature and pressure conditions need to be invoked to explain the regional metamorphism. However, metamorphism could not have been simply by burial. If the apparent bathograd shown in Figure 45 is rotated to horizontal, the isotherms appear to outline a thermal dome under Three Ladies Mountain.

Structural conditions necessary for regional metamorphism are (1) subsidence to 20 km with the required thickness of overlying rock, (2) accompanying compressive deformation, and (3) subsequent uplift to present position.
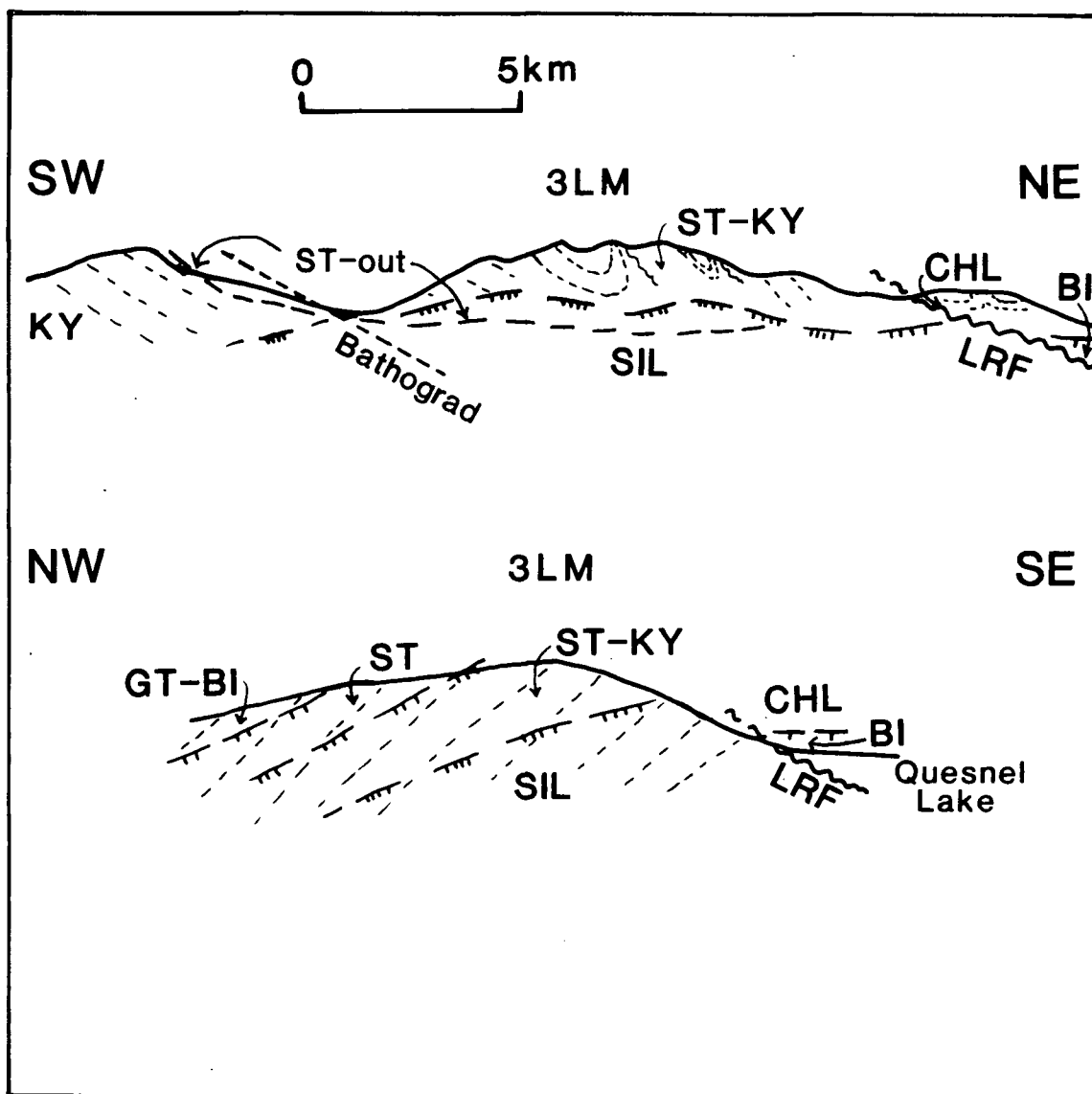
Figure 45. Schematic cross sections of Three Ladies Mountain (3LM) area showing relationship between metamorphic isograds (symbols as on Plate III), foliation (dashed lines), and Little River Fault (LRF).

If the Snowshoe Group rocks, which are presently at least 6 km thick, are late Proterozoic Windermere-equivalent strata, then they were deposited in one of the thickest sections of the Cordilleran miogeosyncline, which formed during nearly continuous subsidence of the North American continental margin from about 1500 Ma to about 200 Ma. The entire Paleozoic miogeosynclinal section could have been deposited above the Snowshoe Group prior to metamorphism, amounting in the thicker sections to well over 10 km of overlying sediment. Additional thickness could have been caused by pile-up of accreted terranes during collision with North America in the mid-Jurassic (Monger et al. 1982). This event was also responsible for the intense deformation which accompanied regional metamorphism. Uplift and thrusting during the Cretaceous removed much of the overlying rock either tectonically or by erosion (see Figure 46).

Plagioclase-quartz-muscovite pegmatite formed anatectically in deep-seated metamorphic rocks during regional metamorphism and intruded kyanite and sillimanite zone rocks in the Three Ladies Mountain/Mount Stevenson area. Renewed heating in the Cretaceous reset the muscovite age in the pegmatite, giving a cooling date of 86 Ma (see section on geochronology). Third phase folding, which affected the pegmatite, was accompanied in pelites by muscovite recrystallization. This "thermal event" is not considered to be a separate episode of prograde regional
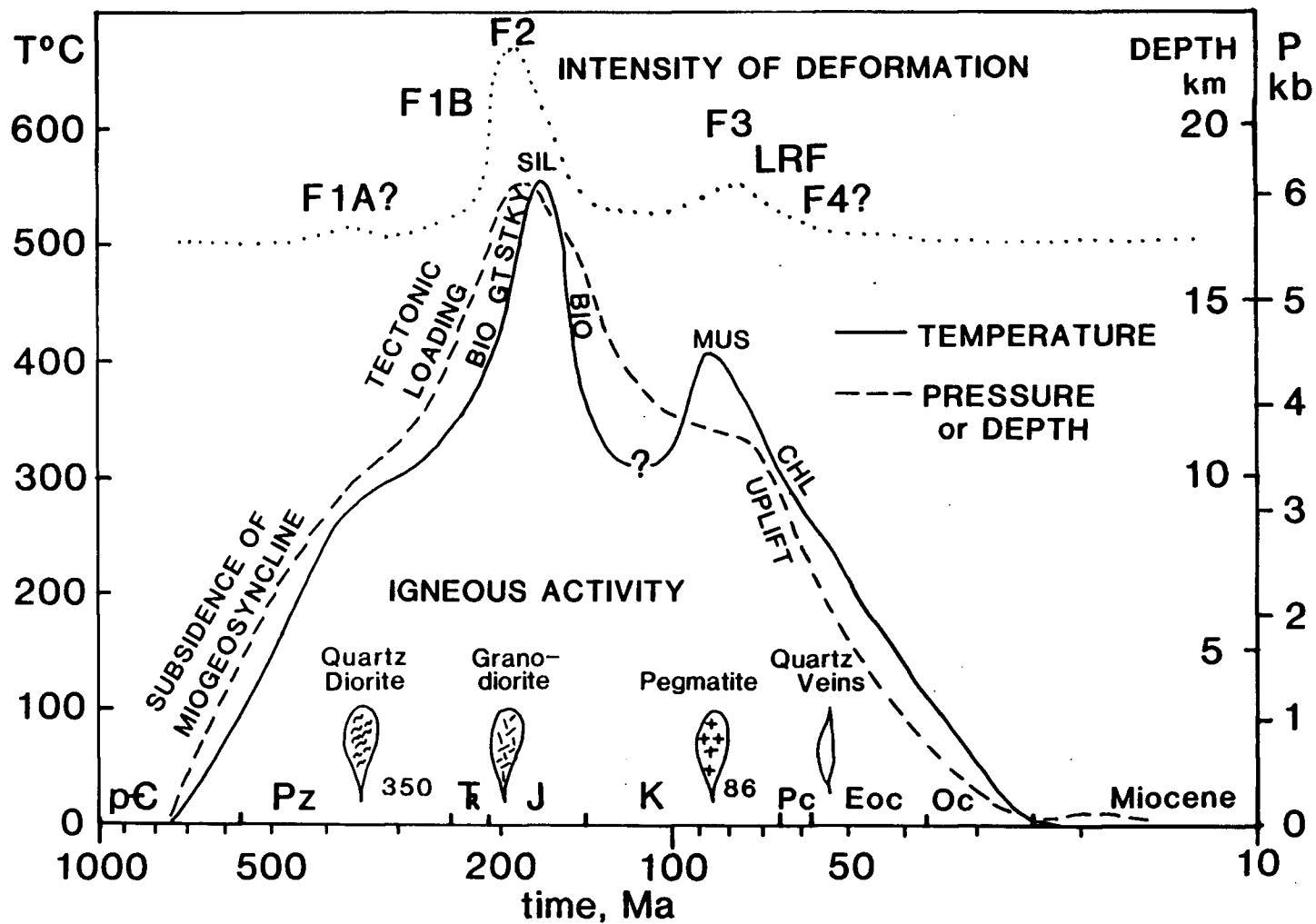
Figure 46. Summary diagram showing variation of
temperature, pressure (or depth), and "intensity of
deformation" through time, plotted on logarithmic scale.

metamorphism in this area, but rather an intermediate thermal high during a general uplift and cooling trend which was characterized metamorphically primarily by retrograde chlorite.

5. IGNEOUS ACTIVITY

Igneous activity occurred at several intervals in the history of the Snowshoe Group in the Three Ladies Mountain/Mount Stevenson area. See the section on geochronology for a discussion of timing of igneous episodes.

5.1 QUARTZ DIORITIC GNEISS

Quartz dioritic sills, containing biotite, hornblende, and epidote, are common in the lower micaceous quartzite and pelite of the Snowshoe Group. They constitute about a 20% of the lower sequence, thus accounting for some of the great thickness of this unit. The sills vary in width; one that has been mapped for several kilometers averages about 50 m thick. Amphibolite lenses tend to be concentrated at or near the contacts with the adjacent quartzite and pelite. They are small, irregular, and contain minor sulfides, and are different from the amphibolites near Three Ladies Mountain, in that they are not associated with carbonates. The quartz dioritic gneisses display well-developed foliation subparallel to that in the adjacent metasedimentary rocks; they appear to be folded by east-verging phase F1B folds, so their foliation may have been formed parallel to axial planes of F1A isoclines. In a few places the gneisses crosscut limbs of earlier, nearly isoclinal, intrafolial folds in the metasedimentary rocks. The foliation in the gneiss is parallel to the axial plane

of the intrafolial folds and also to the general foliation
in the micaceous quartzite. It could be that this kind of
feature is caused by later shearing along the axial plane
foliation of folds involving both quartz dioritic gneisses
and the rocks they intrude, and that it represents
small-scale tectonic slides rather than a truly crosscutting
relationship. The distinction between fold phases F1A and
F1B is difficult and it may in some cases be meaningless.
Mineral lineations in the quartz dioritic gneiss are
generally parallel to those in the surrounding rocks; some
trending WSW and W are parallel to fold axes of phase F1B,
but most trend within the spread of values for F2 axes. The
quartz dioritic layers superficially resemble metamorphosed
greywackes, and in places are difficult to distinguish from
intercalated micaceous quartzites. However, crosscutting
relationships and relatively homogeneous composition that is
more mafic than that of the common psammite in the area, as
well as idiomorphic hornblende and igneous accessory
minerals such as zircon and allanite, are convincing
evidence for an igneous origin. Because these sills are
involved in pre-F2 folding and appear to be restricted to
the lower sequence of the Snowshoe Group, they are included
in the lithologic column (see Figure 2). Isotopic dates on
igneous zircons from the quartz dioritic gneiss give a
possible minimum age for deposition of the Snowshoe Group of
approximately 335 Ma (see section on geochronology).

5.2 GRANODIORITIC GNEISS

Granodioritic and quartz monzonitic sills, more leucocratic than the quartz dioritic group, are also found in the Snowshoe Group. The largest bodies occur on the slope toward Quesnel Lake, as indicated by abundance of angular granitic float boulders, but cannot be mapped in detail due to heavy vegetation. These granitic gneisses were mapped by Campbell (1963, 1978) as "Kg", or Cretaceous granite.

Between Three Ladies Mountain and Welcome Mountain, granodioritic gneiss layers are parallel to compositional layering and general foliation, and folded by F2 folds. Foliation and mineral lineations in the granodioritic sills are parallel to F2 trends. Apophyses of these bodies crosscut the schist as dikes connecting two sills on the ridge north of Welcome Mountain. Although the granodioritic gneiss seems to be related to nearby dikes and irregular bodies of pegmatite, structural relations demonstrate that the granodioritic gneiss must be an earlier igneous phase. Whereas the granodioritic gneiss sills must have been intruded prior to the end of F2 deformation, the pegmatite dikes are mainly post-kinematic. Intruded sediments are not baked or contact-metamorphosed. Locally, the granodioritic gneiss contains large grains of magnetite up to 1 cm across.

5.3 PEGMATITE

Large areas of pegmatite are exposed on the west side of the North Arm of Quesnel Lake, southeast of Mount Stevenson, and near Welcome Mountain. The larger bodies, located mainly in the lower sequence of the Snowshoe Group, are irregular masses of coarse-grained, leucocratic pegmatite consisting of quartz, plagioclase, and muscovite with minor garnet, but no K-feldspar. Grain size varies from 0.5 to 5 cm. Locally, mesoscopic graphic texture may be observed. The pegmatites are compositionally homogeneous, with no unusual minerals, not even tourmaline. These are regarded as forming from melting of metamorphic rocks at depth. Higher in the section where the pegmatite bodies are smaller they tend to occur in the form of dikes parallel to the F2 axial plane. This is shown by the close correspondence on a stereographic projection of the poles of F2 axial planes and the poles of pegmatite dike contacts (Figure 18 B). Some pegmatites have intruded along other surfaces as well. The largest pegmatite dike in the study area is about 150 m thick and extends from the northwest flank of Mount Stevenson for at least 10 km to the ESE where it joins a larger pegmatite body and its contacts become obscured in the forest. The larger bodies of pegmatite contain up to 30 % xenoliths of schist and quartzite, most of which retain structural attitudes consistent with those of the surrounding metasedimentary rocks. There is some rotation of schistosity especially near the contacts with the larger

dikes. Crude foliation in the larger bodies and folds in the pegmatite dikes are believed to be related to F3 deformation.

Pegmatites like these may have formed from partial melting of paragneisses during metamorphism at upper sillimanite zone conditions. It is also possible that they are late-stage differentiates of the same magma that produced the granodioritic gneisses, but more K-spar would be expected. The pegmatites contain little or no K-feldspar.

A Rb-Sr date of 86 Ma on a muscovite separate has been obtained and is thought to represent cooling through 400° to 500°C. This is interpreted as indicating slow cooling from mid-Jurassic metamorphism or reheating during the late Cretaceous.

5.4 QUARTZ VEINS

Quartz veins averaging about one meter thick are present but not common. Those observed are roughly planar and crosscut earlier structures. Whereas some occur along joint surfaces probably related to the Little River Fault, others are parallel or at a low angle to compositional or metamorphic layering. Some quartz veins parallel to foliation are the result of early segregation of quartz in the rocks during formation of foliation; these are common features in metamorphic rocks of this grade.

Many quartz veins in the Mount Stevenson area are nearly vertical and northeast-trending, parallel to F4 axial planes. This is an example of how quartz veins in areas of simple fold systems with steeply dipping axial surfaces tend to occur parallel to the axial planes. Rusty alteration zones along their borders, some associated with local faults, contain sparse molybdenite, pyrite, and chalcopyrite.

5.5 ECONOMIC GEOLOGY

The Snowshoe Group in the Three Ladies Mountain/Mount Stevenson area is mostly barren of economic mineral deposits. Teck Corporation examined a small molybdenite prospect at Mount Stevenson, but has abandoned it. Many sulfide-bearing amphibolites have been staked in small areas, but no work appears to have been done on these prospects. Several samples of pyritic quartzite and similar rocks collected during mapping near Three Ladies Mountain were assayed for gold at the Universtiy of British Columbia; gold values were below limits of detection (A.J. Sinclair, pers. comm.). Where the Snowshoe Group is in greenschist facies, as in the Wells and Barkerville area to the northwest, quartz veins trending north and northeast have yielded rich gold mines in the past. Other mineral showings are minor and can be found on maps showing mining districts.

5.6 VOLCANIC ROCKS

Olivine basalt flows of limited extent were discovered on the floor of a cirque at 1800 m elevation, 3 km east of Mt. Stevenson. They are small flows no more than 3 m thick, nearly horizontal, and lying in two adjacent cirques along with glacial deposits. The basalt exhibits crude columnar jointing, is vesicular and diktytaxitic, and is uniform grey in colour, with pale green olivine phenocrysts (2 mm) in an aphanitic groundmass. At contacts with glacial clay, pillow structures with cooled, glassy margins have developed, with baked clay embedded in the cracks. Basalt boulders are glacially striated.

The evidence suggests that the lava was erupted into wet glacial clay, or into a tarn, or beneath an alpine glacier occupying the cirque at the time of eruption. The cirques where the lava flows were found are east-facing and form part of the headwaters of Devoe Creek, which lies in a deep U-shaped valley. More olivine basalt flows and basaltic volcaniclastic rocks located at the mouth of Devoe Creek lie in a horizontal pile about 250 m thick above lake level, restricted to a small area. The top of this section of volcanic rocks is level with glacial terraces in outwash next to it and elsewhere along the lake shore. These lavas probably had a local source vent near lower Devoe Creek, and pooled up against a large glacier occupying the North Arm of Quesnel Lake at that time. The previously unmapped lavas higher up in the cirques probably had their own source

vents. Similar lavas are located on the west side of the junction of the North Arm and main arm of Quesnel Lake, and along Grain Creek. South of Grain Creek near Tasse Lake, a small conical hill with a central depression looks like a small volcano covered with trees. It has been mapped as a Recent or Interglacial cinder cone (Campbell 1978). These olivine basalts are probably related to the Anahim volcanic belt that extends all the way across B.C. into Wells Gray Park (Hickson and Souther 1984, Fiesinger and Nicholls 1977).

6. GEOCHRONOLOGY

6.1 GEOCHRONOLOGY ABSTRACT

In the Three Ladies Mountain area, Quesnel Highland, British Columbia, the Snowshoe Group consists of siliceous pelite, micaceous quartzite, impure carbonate, and minor amphibolitic rocks, which have been metamorphosed to upper amphibolite facies and multiply deformed. A Rb-Sr model depositional age of approximately 750 Ma, assuming an initial $^{87}Sr/^{86}Sr$ ratio of 0.708 for the Snowshoe Group clastic metasedimentary rocks, supports correlations with late Proterozoic strata. Early to mid-Paleozoic plutonism is indicated by a Rb-Sr whole-rock isochron date of 530 ± 94 Ma with initial $^{87}Sr/^{86}Sr$ ratio of 0.706 for quartz dioritic gneiss intrusive into the Snowshoe Group early in its deformational history (pre- or synkinematic to F1 folding), and by U-Pb dates on zircon from the same quartz dioritic gneiss, which indicate a minimum age of 335 Ma and a maximum age of about 450 Ma. No Rb-Sr isochron could be determined for younger, syndeformational (pre-F2 folding), Sr-rich granodioritic gneiss. Late to post-metamorphic (post-F2 folding) pegmatite cooled through 400-500°C at 86 ± 3 Ma, consistent with Jurassic metamorphism inferred from regional geology.

179

6.2 INTRODUCTION

This isotopic dating study is part of a PhD thesis on the structural and metamorphic history of the Snowshoe Group in the Three Ladies Mountain/Mount Stevenson area. The Snowshoe Group (Campbell et al. 1973) comprises quartz-rich pelitic metasedimentary rocks, impure marbles, minor amphibolites, and associated orthogneisses of inferred late Proterozoic to Paleozoic age. It occurs in a fault-bounded western part of the Omineca Belt. To the west is the eugeosynclinal Intermontane Belt (Quesnellia) and to the east are North American sediments such as the Kaza Group.

The study area is included in the Barkerville terrane (Struik 1984). Monger and Berg (1984) suggest equivalence of the Barkerville and Kootenay terranes. Polyphase deformation in the Barkerville terrane was accompanied by regional metamorphism of the Barrovian type. Rocks of the Snowshoe Group range in metamorphic grade from lower greenschist facies northwest of Wells, B.C., to sillimanite zone of amphibolite facies in Quesnel Highland and Wells Gray Park, where they are a northwest part of the Shuswap metamorphic complex.

The stratigraphic position of the Snowshoe Group has long been unclear; no fossils have been reported. The Snowshoe Group was believed by early workers to overlie the Cariboo Group, and is shown as "Lower Cambrian or later" on maps by R.B. Campbell (1961, 1963). Later work by Campbell et al. (1973) suggested that the Snowshoe Group was "a

western facies of the Kaza Group" (p. 32), and thus of late Proterozoic Windermere age. Getsinger (1982) suggested that the Snowshoe Group resembles parts of the late Proterozoic Horsethief Creek Group, rather than the Kaza Group. Struik proposed that one of the uppermost units of the Snowshoe Group (northwest of Wells, B.C.), is late Paleozoic in age, based on an uncertain lithologic correlation with a nearby unit consisting of marble, slate, and crinoidal limestone which yielded Mississippian conodonts (Struik 1982). Further uncertainty would be involved in making a lithologic correlation across 100 km (even along strike) of unfossiliferous rocks which themselves cannot be traced with complete confidence directly into the Three Ladies Mountain--Mount Stevenson area.

Previous dating in the Quesnel Highland has been limited to studies of the Quesnel Lake Gneiss, a heterogeneous suite of granitic intrusions and augen gneiss associated with the Snowshoe Group near Quesnel Lake. It is exposed about 5 km south of Grain Creek, and was not included in the mapped study area. Blenkinsop (1972) reported a whole-rock Rb-Sr date of 752 ±76 Ma on Quesnel Lake Gneiss collected by C.J.N. Fletcher from the East Arm of Quesnel Lake. K-Ar dates on the East Arm gneiss, collected by Okulitch, are 153 ± 8 Ma on hornblende (metamorphic age) and 108 ± 4 Ma on biotite (reset by Cretaceous plutonism) (Stevens et al. 1982). Okulitch et al. (in preparation) report a U-Pb date of 350 Ma on zircons from the East Arm gneiss,

with inherited Precambrian lead. Okulitch (written communication, 1981) also suggested a preliminary U-Pb date of about 350 Ma on zircons from Quesnel Lake Gneiss which I collected in 1981 at the junction of the North Arm of Quesnel Lake (see Appendix IIIB, samples JSG-80-QLGNW and JSG-81-166). K-Ar and Rb-Sr dates on post-metamorphic plutons in Wells Gray Park are 143 ± 14 Ma and 163 ± 7 Ma, respectively (Wanless et al. 1965; Pigage 1977).

6.3 GEOLOGIC SETTING OF DATED SAMPLES

In the study area, west of the North Arm of Quesnel Lake, the Snowshoe Group is primarily in staurolite-kyanite zone and sillimanite zone. The clastic metasedimentary rocks include grey micaceous quartzites and quartz-rich, garnet-bearing two-mica schists with staurolite, kyanite, and/or sillimanite. Impure carbonates have recrystallized as calc-silicate marbles and minor amphibolite. These rocks experienced at least two phases of penetrative deformation (F1 and F2) during prograde metamorphism, with nearly coaxial folds plunging northwest. Metamorphic temperatures reached a maximum after F2 folding. Retrograde metamorphism accompanied brittle deformation (F3) characterized by kink folds and crenulations with variable axial planar attitudes and northwest or southeast plunging axes. Post-metamorphic, low-angle normal faulting (Little River Fault) was followed by gentle warping (F4), with fold axes plunging shallowly to the northeast.

Mapping in the Three Ladies Mountain--Mount Stevenson area indicates several episodes of igneous intrusion during the structural and metamorphic history of the Snowshoe Group. Four groups of rock types have been selected for dating from samples collected during 1979-1982 field seasons. Relative ages, from oldest to youngest, are: metasediments, quartz dioritic gneiss, granodioritic gneiss, and pegmatite. This order is based on the following field observations. Quartz dioritic gneiss sheets intrusive into

layered paragneisses are involved in east-verging F1 folds. In a few places, the orthogneiss appears to crosscut an earlier foliation in the paragneiss, implying intrusion syndeformational to F1 folding. Younger, granodioritic dikes and sills are folded only by F2 structures, and are foliated and lineated along F2 trends only. The granodioritic gneisses and F2 structures are crosscut by pegmatite dikes, many of which have been intruded parallel to axial planes of F2 folds. Rocks metamorphosed during and after F2 folding contain pegmatitic segregations in some places, and are clearly crosscut by pegmatite dikes elsewhere, implying a late to post-metamorphic relative age for the pegmatitic intrusions.

6.4 RESULTS AND INTERPRETATION

Analytical methods in use at UBC are summarized in Appendix IIIA. Sample locations are shown in Figure 47, and rock descriptions in Appendix IIIB. Analytical results are presented in Table IV (Rb-Sr) and Table V (U-Pb), Rb-Sr isochrons in Figure 48, and concordia plot in Figure 49.

The calculated regression for the Snowshoe Group metasediment isochron (Fig. 2) gives a date of 418 ± 54 Ma and an initial $^{87}Sr/^{86}Sr$ ratio of 0.726 (method of York 1967). The scatter of points exceeds that of experimental error alone, and therefore the interpretation of the date is heavily dependent on the model used to calculate it (Cameron et al. 1981). Rb-Sr whole rock analyses of clastic metasedimentary rocks give isochrons that may range from age of protolith to age of metamorphism (Spanglet et al. 1978; Chaudhuri 1976). In general, isochrons from unmetamorphosed pelites approximate time of deposition or diagenesis, while those from psammites approach the age of provenance. Metamorphism causes rotation of initial isochrons toward the metamorphic age, in some cases nearly completely, as a result of redistribution of radiogenic strontium, especially during deformation. The calculated initial $^{87}Sr/^{86}Sr$ ratio for such metasedimentary rocks is usually high, suggesting rotation of the isochron during metamorphism. The resulting date may not necessarily be assumed to represent the age of metamorphism, and may be meaningless (Field and Raheim 1969). However, an estimate of the age of deposition can be
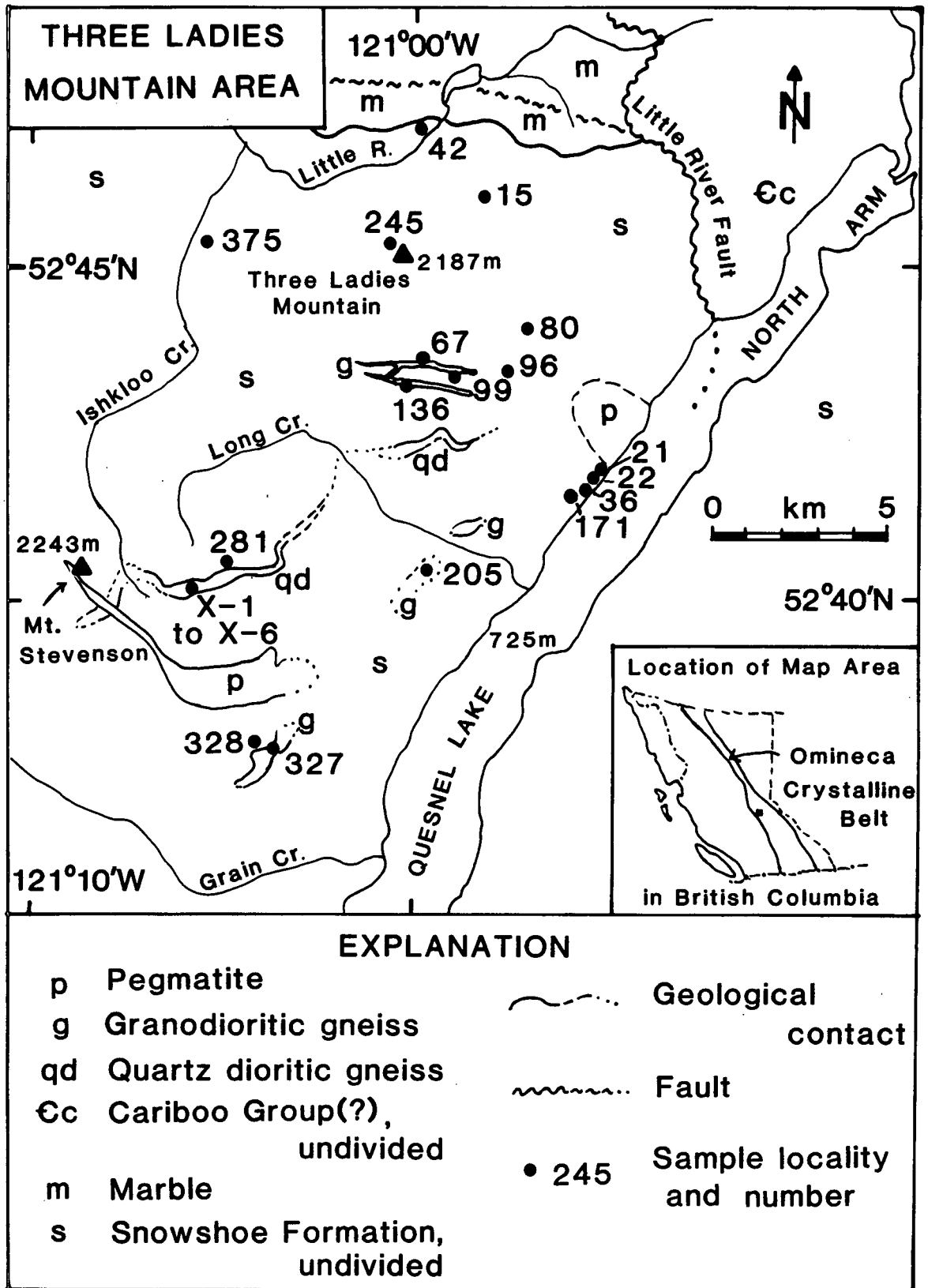
Figure 47. Sample locality map for dated samples.

Table IV. Rubidium-strontium analytical data

Sample	Description	Sr (ppm)	Rb (ppm)	Rb 87 / Sr 86	Sr 87 / Sr 86
	Metasedimentary Rocks				
80-42	Gar-bio-ms schist	122	134	3.19	0.7356
79-15	Gar-bio schist	85	228	7.81	0.7728
80-67	Gar-staur schist	237	133	1.63	0.7393
80-80	Micaceous quartzite	193	90	1.36	0.7349
80-96	Gar-bio-ms schist	83	161	5.68	0.7580
82-375	Ms-bio-gar schist	114	137	3.50	0.7471
81-245	Amphibolite	408	74	0.53	0.7075
80-21	Biotite gneiss	240	115	1.39	0.7350
80-22	Muscovite schist	85	282	9.66	0.7470
81-171	Biotite gneiss	283	118	1.21	0.7224
81-281	Gar-bio-chl schist	74	134	5.28	0.7562
81-328	Kyanite schist	96	172	5.25	0.7687
	Orthogneiss				
81-X1	Quartz dioritic gneiss	495	52	0.30	0.7093
81-X2	Quartz dioritic gneiss	355	138	1.13	0.7139
81-X3	Quartz dioritic gneiss	1082	67	0.18	0.7070
81-X4	Quartz dioritic gneiss	1037	80	0.22	0.7066
81-X5	Quartz dioritic gneiss	508	118	0.67	0.7108
81-X6	Quartz dioritic gneiss	612	94	0.45	0.7099
80-99	Granodioritic gneiss	1879	60	0.09	0.7081
80-136A	Granodioritic gneiss	1463	11	0.02	0.7084
81-205	Granodioritic gneiss	862	52	0.18	0.7051
81-327	Granodioritic gneiss	137	183	3.88	0.7484
	Pegmatite				
80-36-WR	Pegmatite - whole rock	752	35	0.13	0.7150
80-36-MUS	Muscovite from pegmatite	115	298	7.50	0.7239
80-36-PL	Plagioclase from pegmatite	768	8.0	0.03	0.7146

Table V. U-Pb zircon data from quartz dioritic gneiss intrusive into Snowshoe Formation

Sample Number		JSG-81-X (A)	JSG-81-X (B)
Size Fraction (μm), handpicked		74-149	44-74
Weight (mg)		9.8	6.3
U (ppm)		357.8	581.2
Pb (ppm)		21.6	34.7
Abundances:[1]	^{206}Pb	100	100
	^{207}Pb	5.596	5.462
	^{208}Pb	16.30	17.41
	^{204}Pb	0.0067	0.0007
Observed ^{206}Pb/^{204}Pb		3823	12989
Mole % Blank Pb		0.5	0.4
Radiogenic Pb/(Radiogenic + Common Pb)[2]		0.996	0.999
Atomic ratios:	^{206}Pb/^{238}U	0.05760	0.05646
	^{207}Pb/^{235}U	0.4366	0.4244
	^{207}Pb/^{206}Pb	0.05498	0.05452
Dates (Ma):[3] (± 2σ)	^{206}Pb/^{238}U	361.0 ± 3.1	354.1 ± 3.1
	^{207}Pb/^{235}U	367.9 ± 3.3	359.2 ± 3.2
	^{207}Pb/^{206}Pb	411.3 ± 3.2	392.4 ± 2.6

[1] Corrected for blank Pb. Total blank = 0.5 ng.

[2] Isotopic composition of common lead is that of 345 Ma old Pb on the growth curve of Stacey and Kramers (1975).

[3] Decay constants: ^{238}U, $0.155125 \times 10^{-9} a^{-1}$; ^{235}U, $0.98485 \times 10^{-9} a^{-1}$; ^{238}U/^{235}U = 137.88.
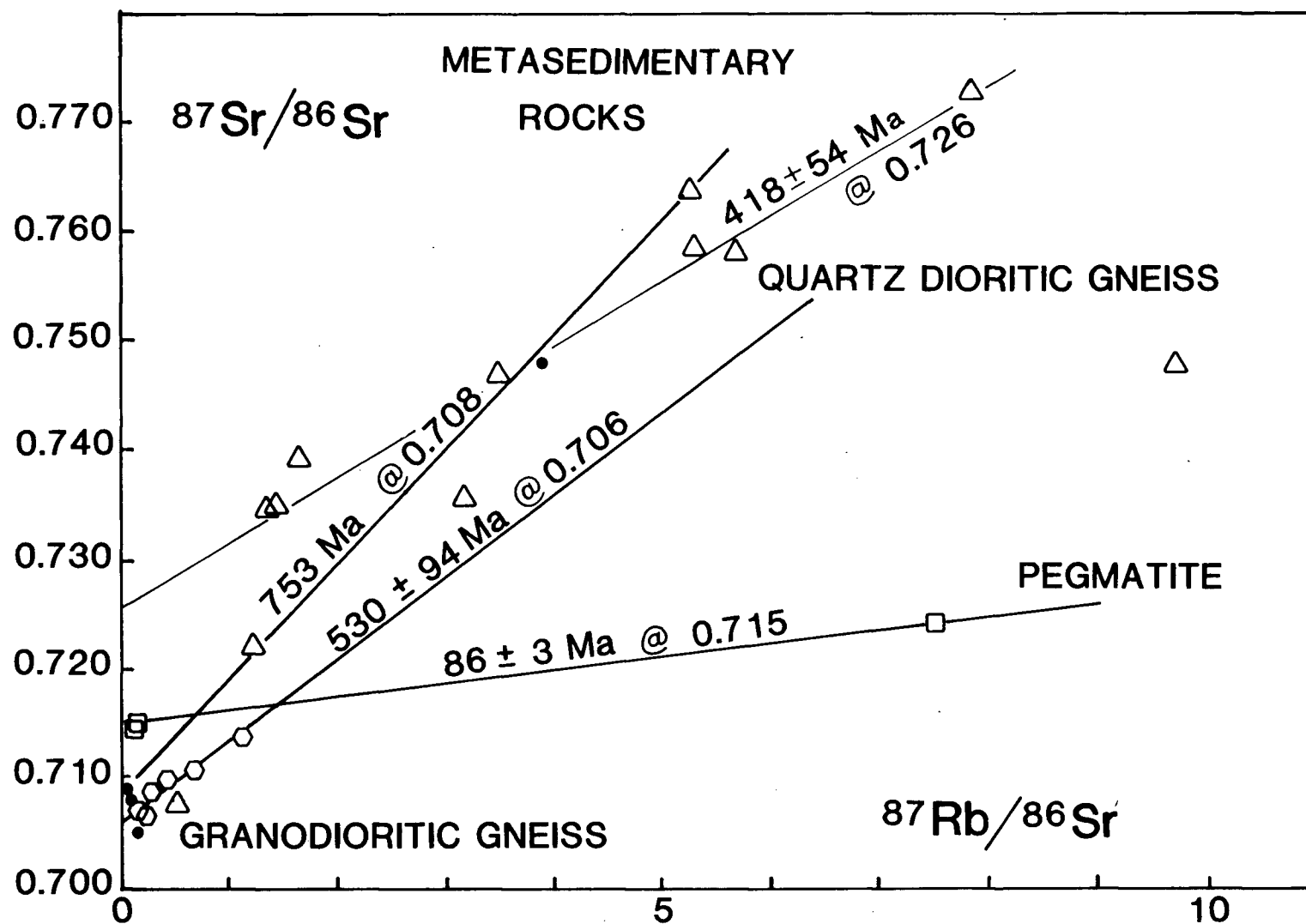
Figure 48. Rb-Sr isochrons for metasedimentary rocks
(triangles), quartz dioritic gneiss (hexagons),
granodioritic gneiss (solid circles), and pegmatite (squares).
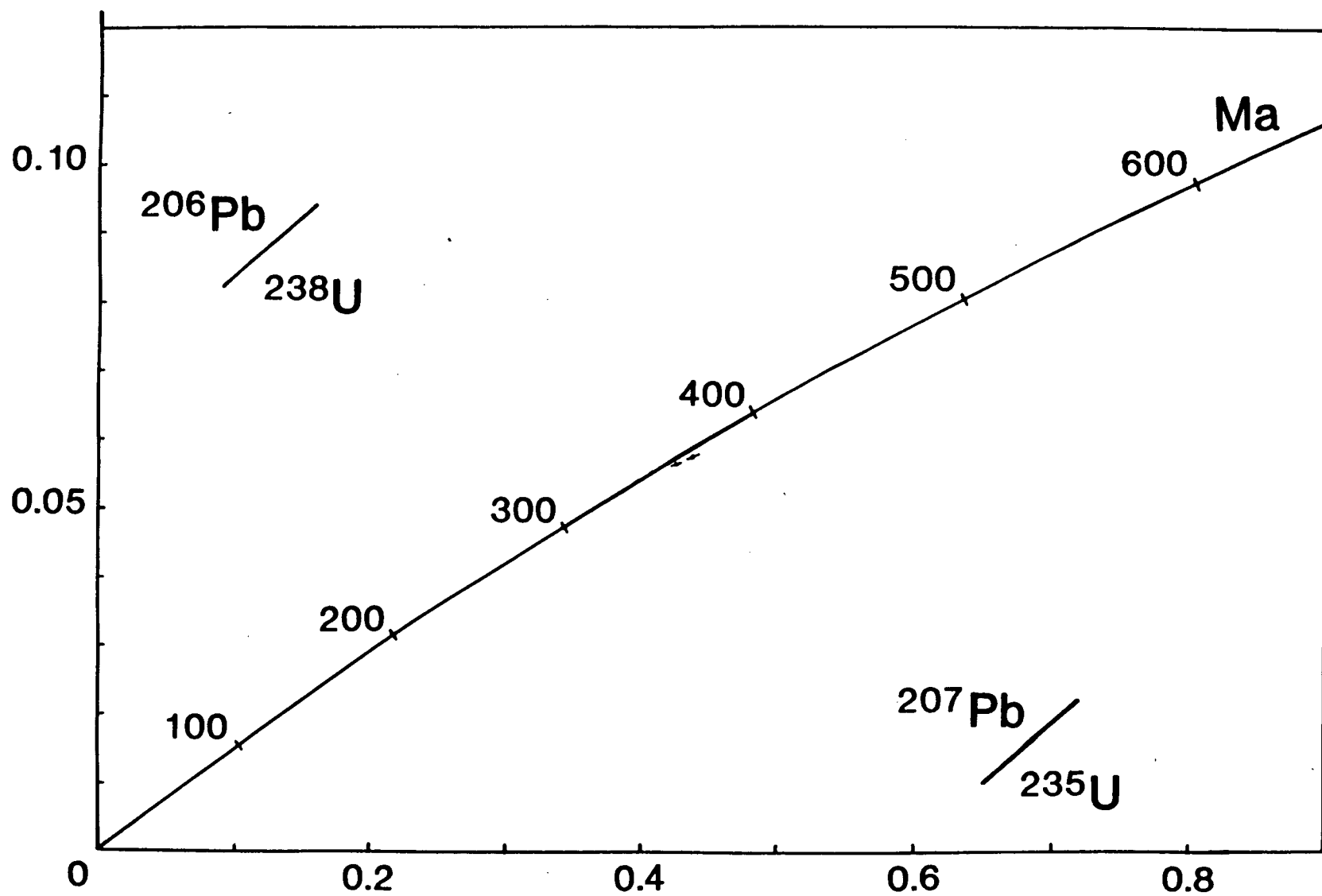
Figure 49. U-Pb zircon concordia for quartz dioritic gneiss (sample 81-X).

made using an an assumed initial $^{87}Sr/^{86}Sr$ ratio and the centre of gravity of the sample distribution, around which the isochron is presumed to have rotated by metamorphism (Peterman 1966; Spanglet et al. 1978; Cameron et al. 1981). A reasonable initial $^{87}Sr/^{86}Sr$ ratio for sediments deposited in early Paleozoic or late Proterozoic seawater is 0.708 (Faure and Powell 1972, p. 78). Using this ratio, and a centre of gravity based on an arithmetic average of the data points, a date of 753 Ma was calculated (a meaningful error cannot be calculated). This late Proterozoic date supports previous correlations of Snowshoe Group with part of the Windermere Supergroup.

Six whole-rock samples of quartz dioritic gneiss from one collecting were site were analysed for Rb-Sr and combined to produce a zircon concentrate for U-Pb dating. Rb-Sr whole rock isochrons in meta-igneous rocks tend to preserve age of crystallization (Faure and Powell 1972). The quartz dioritic gneiss isochron gives a date of 530 ± 94 Ma with an initial $^{87}Sr/^{86}Sr$ ratio of 0.706. This implies a Cambrian or older age for the Snowshoe Group into which the gneiss intrudes, but the uncertainty is large.

Zircons from the quartz dioritic gneiss are typically colourless to pale pink, subhedral prisms with rounded edges and terminations. Handpicked zircons consist of clear, uncracked, whole crystals of two size fractions: 74-140 μm (100-200 mesh) and 44-74 μm (200-325 mesh). On a $^{206}Pb/^{238}U$ vs. $^{207}Pb/^{235}U$ concordia graph, these points lie just below

the concordia curve near 360 Ma (Figure 49; Table V).
The analytical errors are small enough that the points are
clearly discordant. Two possible interpretations are
suggested:

a) If a straight chord is plotted through the two
points, it intersects the concordia curve around 335 Ma.
This "reverse discordance" could indicate that the gneiss
has a minimum age of Mississippian, and inherited a small
amount of older lead from the country rocks. Mesozoic
metamorphism causing lead loss could bring the lower
intercept below the true value for initial crystallization
of the gneiss.

b) These points could be part of a discordant series of
points from a gneiss which was older (perhaps Ordovician,
around 450 Ma) and lost lead during Mesozoic metamorphism
(around 175 Ma).
With only two nearly overlapping points, either
interpretation is possible. In either case, an early to
mid-Paleozoic minimum age of intrusion is indicated.

Early Paleozoic intrusions have only recently been
recognized in localities scattered through the Cordillera,
and are probably more common than generally realized.
Cambrian-Ordovician plutonism in east-central Idaho was
reported by K.V. Evans (1981). Mortensen (1983) defined
four plutonic suites intrusive into a sequence of
metasedimentary rocks in the Yukon-Tanana terrane that are
lithologically similar to metasedimentary rocks of the

Snowshoe Group in Quesnel Highland. Dates on the intrusions are 359 ± 6 Ma, 349 ±5 Ma, and 342 ± 12 Ma, with a suggested maximum age of 400 Ma. The Quesnel Lake Gneiss and similar orthogneisses in the Omineca Belt have been dated by A.V. Okulitch at about 350 Ma (Okulitch et al. 1975; Wanless and Okulitch 1976; Okulitch, written communication, 1981; Okulitch et al., in preparation).

It is unclear as yet whether the Quesnel Lake Gneiss belongs to the same intrusive suite as the quartz dioritic gneiss dated here. Although some of the quartz dioritic gneiss occurs along Quesnel Lake near the Quesnel Lake Gneiss, no contact is exposed. These two gneisses are distinctly different petrologically and structurally. The Quesnel Lake Gneiss is a large body (over 30 km long and 2-4 km wide) of coarse-grained, leucocratic, gneissose granite with potassium feldspar megacrysts. It is generally concordant with layering in the Snowshoe Formation as well as parallel to the border of the Intermontane Belt; it is unclear whether the contact with the Snowshoe Group is intrusive or tectonic (Blenkinsop 1972; Rees 1981). In contrast, the quartz dioritic gneiss dated here is more mafic (30%), finer-grained, and lacks potassium feldspar, either as megacrysts or in groundmass. It is intimately interlayered with and intrusive into metamorphic rocks of the Snowshoe Group and was clearly folded and metamorphosed along with the metasedimentary rocks. This quartz dioritic gneiss occurs in sills no wider than a few hundred meters

within the Snowshoe Group from Mount Stevenson to Quesnel Lake. Although the quartz dioritic gneiss dated here and the Quesnel Lake Gneiss may be similar in age, it is suggested that they belong to two different intrusive suites..

Four whole-rock samples of granodioritic gneiss were analysed for Rb-Sr. Two of them (80-99, 80-136A) are from closely related sills connected by dikes which crosscut F1 structures in the surrounding schist, but which are folded, foliated, and lineated by F2 folding and metamorphism. These syndeformational intrusions should approximate the age of F2 deformation and metamorphism. Both samples contain extremely high concentrations of strontium (over 1000 ppm; see Table IV) and have initial ratios of about 0.708, regardless of their exact age. In order to establish an age for this granodioritic gneiss, samples with a wider range of Rb/Sr ratio or zircons for U-Pb dating are required. Sample 81-327 plots within the Snowshoe paragneiss field; this suggests either an old age or synmetamorphic equilibration with the metasedimentary rocks. Sample 81-205 stands isolated with a rather low $^{87}Sr/^{86}Sr$ ratio of 0.705. This sample was collected from an isolated outcrop in an area largely covered with vegetation; because field relations are obscure, no conclusions can be drawn.

One typical specimen of pegmatite was separated into mineral fractions. A plagioclase-muscovite-whole rock isochron gives a date of 86.4 ± 3.3 Ma approximating

post-metamorphic cooling through about 400-500°C (Jager et al. 1967; Harrison et al. 1978). The cooling date is consistent with dates from similar post-metamorphic pegmatites elsewhere in the Omineca Belt (Parrish 1979). Time of metamorphism has been dated by other workers as mid-Jurassic (Wanless et al. 1965; Wheeler 1970; Pigage 1977). Mid-Cretaceous cooling ages imply either a very gradual cooling from a middle Jurassic metamorphism (about 100-200°C in 70 Ma, or about 2°C/million years), or renewed heating during the mid-Cretaceous.

6.5 CONCLUSIONS

The time of deposition of the Snowshoe Group is approximately 750 Ma (late Proterozoic) assuming an initial $^{87}Sr/^{86}Sr$ ratio of 0.708. Quartz dioritic gneiss intruded early in the deformational history of the Snowshoe Group gives a Rb-Sr date of 530 ± 94 Ma with an initial $^{87}Sr/^{86}Sr$ ratio of 0.706. U-Pb dating of zircons from the same gneiss suggests Paleozoic intrusion with a minimum age of 335 Ma and a maximum age around 450 Ma. Such gneisses in the Snowshoe Group and other parts of the Cordillera indicate widespread early to mid-Paleozoic deformation and metamorphism, now almost completely overprinted by Jurassic orogeny. Younger, syndeformational granodioritic gneiss with high strontium concentrations and initial $^{87}Sr/^{86}Sr$ ratio of 0.708 was not successfully dated. Coarse muscovite, from pegmatite intruded after F2 folding and metamorphism, was dated by Rb-Sr as 86 ±3 Ma, consistent with Jurassic metamorphism and subsequent gradual cooling through 400-500°C.

7. <u>SUMMARY</u>

The geologic history of the Three Ladies Mountain/Mount Stevenson area is summarized briefly, starting with the earliest events that can reasonably be interpreted from the rocks, continuing up to the present time.

LATE PROTEROZOIC TO EARLY PALEOZOIC

- Deposition of sediments on continental margin of western North America (Kaza, Snowshoe, Cariboo Groups)

- Lithification of sandstone, mudstone, shale, limestone, marl; bedding

- Subsidence, heating, diagenesis

- Beginning of prograde metamorphism, quartz segregations and mica recrystallization (chlorite, muscovite)

- Possible deformation, formation of foliation

EARLY TO MID-PALEOZOIC

- Intrusion of quartz dioritic sills and amphibolite protolith into lower sequence (possibly axial planar to isoclines although also folded)
  Quartz dioritic gneisses display WSW and W to NW lineations (L1)

- Asymmetrical tight to isoclinal folding (F1B), east-verging; folds foliation and quartz diorite, WNW to NW plunge (L1); some axial planes SW-dipping, some parallel to foliation; preserved mainly in competent quartzite layers; F2 axial plane cleavage (S2) is superimposed across many F1 folds in pelitic hinge zones

- Dominant foliation (S1B) is formed parallel to axial planes of F1B folds

PALEOZOIC TO MESOZOIC

- Prograde metamorphism continues into amphibolite facies; early garnet growth

- Granitic sills and dikes intruded locally (granodiorite, quartz monzonite); they look like finer-grained precursors of pegmatite intrusions which come later and with which they are associated in the field; they show F2 structures (S2, L2)

MID-JURASSIC

- F2 folding: west-verging, asymmetrical, tight to normal, inclined plunging folds, with NW plunge and NE-dipping axial planes (very consistent); axial plane cleavage with complete transposition in pelitic layers is common especially in large fold hinges; refolds F1A and F1B folds; lineations (L2) nearly coaxial with F1 lineations (L1); F2 axial planar foliation (S2) is developed most strongly in pelitic schist in F2 hinge zones

- Peak of prograde metamorphism; growth of porphyroblasts; synkinematic garnets, postkinematic kyanite and staurolite; sillimanite

JURASSIC TO CRETACEOUS

- Intrusion of pegmatite dikes in F2 axial planes

LATE CRETACEOUS

- Uplift and cooling

LATE CRETACEOUS TO EARLY TERTIARY

- F3 kink-folding and crenulation folding, with varying
  attitudes including NW-trending, SW-dipping axial
  planes (S3); best developed in pelite; seen superimposed
  on S2 and on F1B folds; some development of crude
  foliation in pegmatite; chlorite growth on axial planes
- Major faulting, formation of Little River Fault system;
  slickensides and drag indicate upper plate moved down
  toward ESE
  Fault surfaces vary from F2 A-C joints to 170/20E
  Metamorphic displacement at Quesnel Lake is sillimanite
  zone adjacent to chlorite-biotite zone
- Retrograde metamorphism:
  Late muscovite replaces kinked and folded biotite;
  chloritization of micas especially on F3 axial planes;
  chloritization of biotite and garnet and staurolite;
  local sericitization of kyanite and staurolite
- F4 folding: broad, open warps or flexures with gentle NE
  plunge; some crenulation in pelite; quartz veins are
  axial planar; reverses plunges of F2 folds
- Late quartz veins injected along joints, faults, and
  F4 axial planes, and parallel to foliation
  Minor mineralization, including molybdenite, pyrite, and
  chalcopyrite

MIOCENE (?)

- Uplift and erosion; formation of widespread erosion
  surface

- Minor high-angle faulting, N, NE trends, EW trends, displacement on N and NE trends down to west

PLEISTOCENE (?)

- Glaciation; erosion by alpine and valley glaciers
- Extrusion of olivine basalt and volcaniclastics above Devoe Creek, at Quesnel Lake, and Tasse Lake cinder cone (subglacial and synglacial)
- Glaciers melt; deposition of till, outwash and moraines

RECENT

- Erosion

8. CONCLUSION

Structural and metamorphic history of the Three Ladies Mountain/Mount Stevenson area may be related to larger tectonic events. Refer to Figure 50 for schematic cartoons showing reconstructions of possible tectonic settings through time. Figure 50A depicts the development of the Cordilleran miogeocline up to the early Mesozoic. Snowshoe Group sedimentary rocks were deposited in a continental slope to shelf environment, perhaps on transitional crust outboard of cratonic basement, probably in the late Proterozoic to Paleozoic, some time between about 753 Ma and 418 Ma, according to Rb-Sr dates given in this study (see Figure 47). Late Proterozoic to Cambrian Cariboo Group shallow marine clastics and carbonates are shown closer to the shore of North America, but partly time-equivalent and partly overlapping the Snowshoe Group rocks. Sediments overlying the Snowshoe Group may have been as thick as 10-15 km by the early Mesozoic, so some metamorphic recrystallization may have begun during the Paleozoic.

Mafic sills (now quartz dioritic gneisses and minor amphibolitic bodies) were intruded into the Snowshoe Group in the mid-Paleozoic; minor deformation may have accompanied intrusion. These quartz dioritic gneisses yield a tentative Rb-Sr date of 530 ± 94 Ma and somewhat discordant U-Pb zircon dates of around 335 Ma to 450 Ma (see Figures 47 and 48). A west-dipping subduction zone may have existed off the edge of the continent. Island arc rocks, parts of
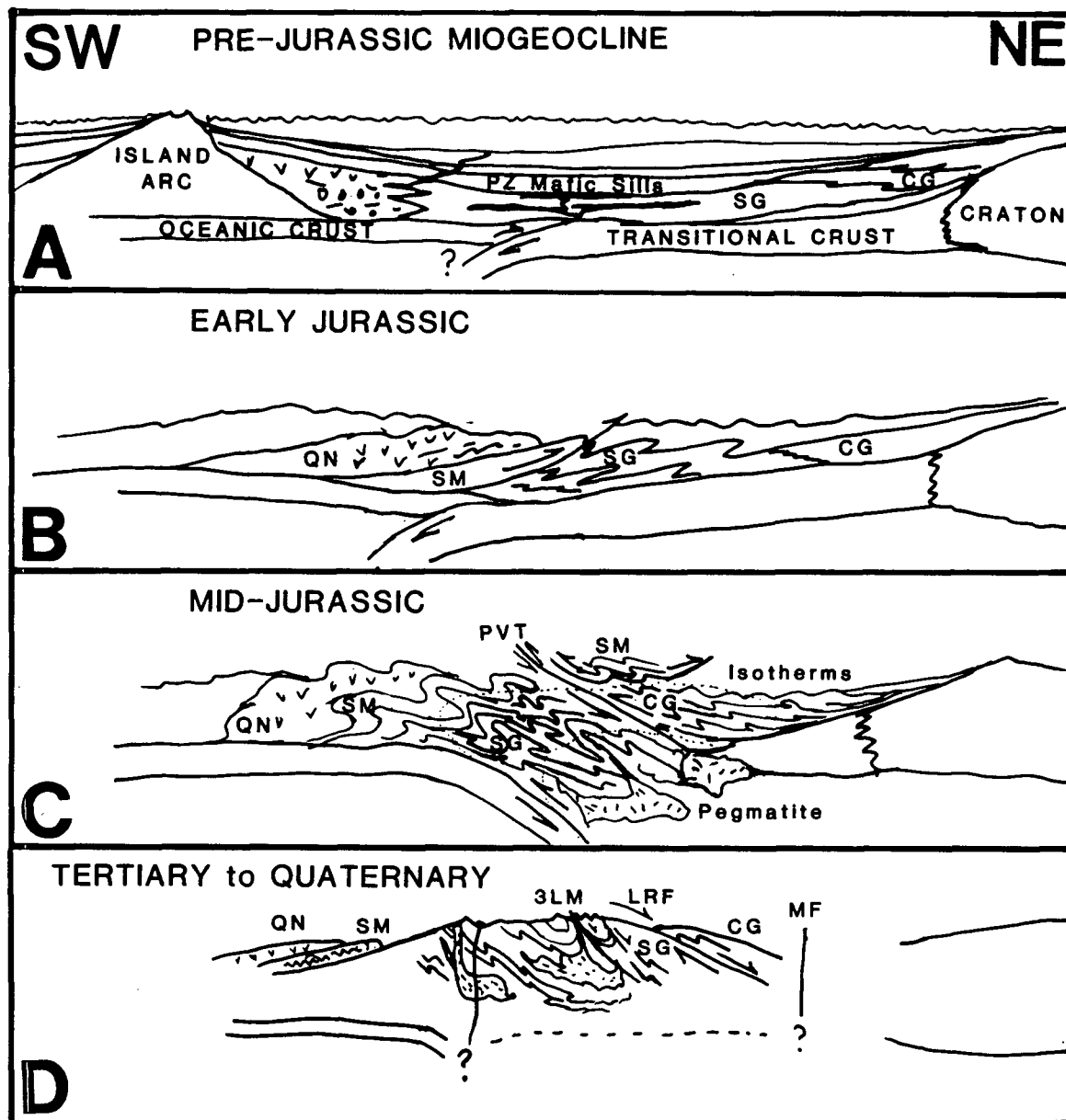
Figure 50. Schematic tectonic history of the Omineca Belt in the vicinity of the Three Ladies Mountain/Mount Stevenson area. Not to scale.
SG = Snowshoe Group, CG = Cariboo Group, SM = Slide Mountain Terrane, QN = Quesnellia, PVT = Pleasant Valley Thrust, LRF = Little River Fault, 3LM = Three Ladies Mountain, MT = Matthew River Fault.

Quesnellia and Slide Mountain terranes, accumulated in arc and ocean environments to the west.

By the early Jurassic, plate convergence bringing in island arcs from the west had begun to affect the miogeocline, which had been relatively stable for over a billion years (1 Ga). Figure 50B shows continued west-dipping subduction as rocks of the Slide Mountain terrane and Quesnellia were obducted to the east over continental margin sediments of the Barkerville and Cariboo terranes. Folding was mainly easterly-directed; large nappes may have developed in some areas at this time. Northeasterly-overturned F1B folds, some of which involve quartz dioritic sills in the Three Ladies Mountain/Mount Stevenson area, may be related to this event.

As Slide Mountain terrane and Quesnellia piled up, the crust was tectonically thickened, causing further subsidence of the miogeoclinal rocks to depths of 20-25 km. Thickening of the crust may have been accompanied by a reversal of subduction in the mid-Jurassic, as it was around this time that island arc and oceanic rocks from the west, and perhaps some of the deeper parts of the miogeocline, began underthrusting the continental margin from southwest to northeast (see Figure 50C). This may have been the cause of the second, and strongest, phase of deformation recorded in the rocks of the Three Ladies Mountain/Mount Stevenson area. A marked asymmetry, indicating shearing in a northeast over southwest direction, characterizes second phase structures

throughout the Omineca Belt. F2 folds in the Three Ladies Mountain/Mount Stevenson area are dominantly southwesterly-verging. Their similar to flattened flexural slip style and microscopic fabrics indicate formation in warm, ductile conditions, accompanied by maximum metamorphic recrystallization. Metamorphic assemblages synkinematic to postkinematic to F2 folding indicate conditions of pressure at 5.5 ± 0.7 kb and temperature around 525 ± 20°C, corresponding to a depth of around 18-20 km with a normal geothermal gradient of about 30°/km (see Figure 46).

Parts of the Cariboo Group may have been thrust over the Snowshoe Group to the west along the east-dipping Pleasant Valley Thrust, which is a pre- to synmetamorphic reverse fault, according to Struik (1982). Although some telescoping of these units has clearly occurred during deformation, the Pleasant Valley Thrust may not be a major terrane boundary. The Barkerville terrane is considered here to be parautochthonous rather than suspect.

There is no evidence in the Three Ladies Mountain/Mount Stevenson area for the existence or necessity of having isolated blocks of continental crust move in from west of the miogeoclinal basin in order to explain crustal thickening and southwesterly-directed folding, although this may have been the case for the Monashee Complex, which is cored by much older rocks (Read and Brown 1983). Northeastward underthrusting during progressive convergence of oceanic terranes with North America has also been

proposed by Murphy (in preparation) to explain westerly-verging F2 structures in the Premier Range, in North American rocks of the Kaza Group. This general view is consistent with structures observed in the Three Ladies Mountain/Mount Stevenson area, but a more specific kinematic model such as that proposed by Murphy (in preparation) is beyond the scope of this study.

Tectonically loaded continental crust consisting of deformed and metamorphosed geosynclinal rocks to the west of the North American craton would have been anomalously thick following the mid-Jurassic, resulting in relatively rapid uplift. Partial melting of lower crustal rocks formed pegmatites and other plutonic bodies which intruded deformed rocks higher in the crust. Continued, but less severe, convergence from the west during uplift caused tightening and/or overturning of F2 folds by F3 structures. Third phase deformation occurred in a more brittle regime in the Three Ladies Mountain/Mount Stevenson area than did F2 folds, as indicated by sparsely-distributed F3 kink-folding and minor recrystallization of retrograde minerals, such as chlorite, which indicate lower metamorphic temperatures. Postmetamorphic pegmatite was intruded along F2 axial planar surfaces in kyanite and sillimanite zone rocks of the Snowshoe Group prior to F3 deformation. One Rb-Sr mineral separate date was obtained for such a pegmatite, indicating cooling through 400°C at 86±3 Ma. This has been interpreted as representing a late Cretaceous heating event rather than

merely extremely slow cooling after mid-Jurassic metamorphism. High heat flow in the Cretaceous and thickened crust contributed to uplift and erosion of deep-seated metamorphic rocks in the Omineca Belt in early Tertiary time.

Tectonic denudation, represented by low-angle normal faults such as the Little River Fault in the Three Ladies Mountain area, contributed to more uplift and erosion (see Figure 50D). The Little River Fault is approximately contemporaneous with many decollement zones associated with metamorphic core complexes, having moved at some time between the late Cretaceous and mid-Tertiary. Structures in the Snowshoe Group schists and gneisses suggest that it is a low-angle, extensional fault associated with uplift of the high grade rocks forming the core of the Three Ladies Mountain/Mount Stevenson block, and that the low-grade rocks of the hanging wall (Cariboo Group) slid down toward the east-southeast, at least near the present trace of the Little River Fault east of Three Ladies Mountain.

Later broad warping (F4 folding) along a northeast trend, and high-angle block-faulting along north, northeast, and northwest trends, occurred with minor disruption of earlier structures.

There is no evidence in the Three Ladies Mountain/Mount Stevenson area for strike-slip faulting.

Minor basaltic volcanic rocks are associated with Pleistocene glacial deposits and geomorphologic features

suggesting approximately synglacial eruption. These olivine
basalts may have a mantle source, but there is no evidence
of the structural control of their present distribution.

REFERENCES

Archibald, D.A., Glover, J.K., Price, R.A., Farrar, E., and
Carmichael,D.M. 1983. Geochronology and tectonic
implications of magmatism and metamorphism, southern
Kootenay Arc and neighbouring regions, southeastern British
Columbia. Part I: Jurassic to mid-Cretaceous. Canadian
Journal of Earth Sciences, 20, pp. 1891-1913.

Blenkinsop, J. 1972. Computer-assisted mass spectrometry
and its application to rubidium-strontium geochronology.
PhD thesis, University of British Columbia.

Bohlen, S.R., Wall, V.J., and Boettcher, A.L. 1983.
Experimental investigations and geological applications of
equilibria in the system FeO-TiO2-Al2O3-SiO2-H2O.
American Mineralogist, 68, pp. 1049-1058.

Brown, R.L. 1981. Metamorphic complex of S.E. Canadian
Cordillera and relationship to foreland thrusting.
IN Thrust and nappe tectonics. The Geological Society
of London, pp. 463-473.

Brown, R.L., and Read, P.B. 1983. Shuswap terrane of
British Columbia: a Mesozoic "core complex". Geology,
11, pp. 164-168.

Cameron, M., Collerson, K.D., Compston, W., and Morton, R.
1981. The statistical analysis and interpretation of
imperfectly-fitted Rb-Sr isochrons from polymetamorphic
terrains. Geochimica et Cosmochimica Acta, 45,
pp. 1087-1097.

Campbell, K.V. 1971. Metamorphic petrology and structural
geology of the Crooked Lake area, Cariboo Mountains,
British Columbia. PhD. thesis, University of Washington,
Seattle, Washington, 192 p.

Campbell, K.V., and Campbell, R.B. 1970. Quesnel Lake
map-area, British Columbia. IN Report of activities,
part A. Geological Survery of Canada, Paper 70-1,
pp. 32-35.

Campbell, R.B. 1961. Quesnel Lake, west half, British
Columbia. Geological Survey of Canada, Map 3-1961.

Campbell, R.B. 1963. Quesnel Lake, east half, British
Columbia. Geological Survey of Canada, Map 1-1963.

Campbell, R.B. 1978. Quesnel Lake (93A) map-area, British
Columbia. Geological Survey of Canada, Open File map 574.

Campbell, R.B., Mountjoy, E.W., and Young, F.G. 1973. Geology of McBride map-area, British Columbia (93H). Geological Survey of Canada, Paper 72-35, 104 p.

Carmichael, D.M. 1978. Metamorphic bathozones and bathograds: a measure of the depth of postmetamorphic uplift and erosion on the regional scale. American Journal of Science, 278, pp. 769-797.

Chaudhuri, S. 1976. The significance of rubidium-strontium age of sedimentary rock. Contributions to Mineralogy and Petrology, 59, pp. 161-170.

Coney, P.J. 1980. Cordilleran metamorphic core complexes: an overview. Geological Society of America, Memoir 153, pp. 7-31.

Crittenden, M.D., Jr., Coney, P.J., and Davis, G.H. 1980. Cordilleran metamorphic core complexes. Geological Society of America, Memoir 153, 490 p.

Dechesne, R.G., Simony, P.S., and Ghent, E.D. 1984. Structural evolution and metamorphism of the southern Cariboo Mountans near Blue River, British Columbia. IN Current Research, Part A, Geological Survey of Canada, Paper 84-1A, p. 91-94, 1984.

Engi, J.E. 1984. Structure and metamorphism north of Quesnel Lake and east of Niagara Creek, Cariboo Mountains, British Columbia. MSc thesis, University of British Columbia, Vancouver, B.C., 137 p.

Evans, K.V. 1981. Evidence from U-Th-Pb zircon ages for Cambrian-Ordovician plutonism in east-central Idaho. Geological Society of America Abstracts with Programs, 13, p. 195.

Faure, G., and Powell, J.L. 1972. Strontium isotope geology. Springer-Verlag, New York, 188 p.

Ferry, J.M., and Spear, F.S. 1978. Experimental calibration of the partitioning of Fe and Mg between biotite and garnet. Contributions to Mineralogy and Petrology, pp. 113-117.

Field, D., and Raheim, A. 1979. A geologically meaningless Rb-Sr total rock isochron: Nature, 282, pp. 497-499.

Fiesinger, D.W., and Nicholls, J. 1977. Petrography and petrology of Quaternary volcanic rocks, Quesnel Lake region, east-central British Columbia. Geological Association of Canada, Special Paper 16, pp. 25-38.

Fletcher, C.J.N. 1972. Structure and metamorphism of Penfold Creek area, near Quesnel Lake, central British Columbia. PhD thesis, University of British Columbia, Vancouver, B.C., 123 p.

Fletcher, C.J.N., and Greenwood, H.J. 1979. Metamorphism and structure of Penfold Creek area, near Quesnel Lake, British Columbia. Journal of Petrology, 20, pp. 743-794.

Ganguly, J., and Saxena, S.K. 1984. Mixing properties of aluminosilicate garnets: constraints from natural and experimental data, and applications to geothermo-barometry. American Mineralogist, 69, pp. 88-97.

Getsinger, J.S. 1982. Metamorphism and structure of Three Ladies Mountain area, Cariboo Mountains, British Columbia. IN Current research, part A. Geological Survey of Canada, Paper 82-1A, pp. 317-320.

Getsinger, J.S. 1983a. Relative timing of folding, metamorphism, and low-angle faulting in high-grade crystalline rocks, Quesnel Highland, British Columbia, southern Canadian Cordillera. Geological Society of America,

Getsinger, J.S. 1983b. Metamorphic history of the Three Ladies Mountain/Mount Stevenson area, Quesnel Highland, B.C. Geological Association of Canada, Program with Abstracts, 8, p. A26.

Harrison, T.M., Armstrong, R.L., and Clarke, G.K.C. 1978. Thermal models and cooling histories from fission-track, K-Ar, Rb-Sr, and U-Pb mineral dates, northern Coast Plutonic Complex, British Columbia, IN Short papers of the Fourth International Conference, Geochronology, Cosmochronology, Isotope Geology 1978. Edited by R.E. Zartman. United States Geological Survey Open File Report 78-701, pp. 167-170.

Hickson, C.J., and Souther, J.G. 1984. Late Cenozoic volcanic rocks of the Clearwater--Wells Gray area, British Columbia. Canadian Journal of Earth Sciences, 21, pp. 267-277.

Holland, S.S. 1954. Yanks Peak--Roundtop Mountain area, Cariboo District, British Columbia. B.C. Department of Mines, Bulletin 34.

Jager, E., Niggli, E., and Wenk, E. 1967. Rb-Sr Altersbestimmungen an Glimmern der Zentralalpen. Beitrage zur Geologischen Karte der Schweiz, Neue Folge, 134, Leiferung.

Klepacki, D.W. 1980. Structure and metamorphism of Maeford Lake area, Cariboo Mountains, B.C. Map from unpublished M.Sc. thesis manuscript, University of British Columbia.

Klepacki, D.W. 1981. The Little River Fault--a low angle boundary fault of the northern Shuswap Complex, Quesnel Lake, British Columbia. Geological Association of Canada, Program with Abstracts, 6, p. A-32.

Krogh, T.E. 1973. A low contamination method for hydrothermal decomposition of zircon and extraction of U and Pb for isotopic age determinations. Geochimica et Cosmochimica Acta, 37, pp. 485-494.

Lang, H.M., and Rice, J.M. 1985. Geothermometry, geobarometry and T-X (Fe-Mg) relations in metapelites, Snow Peak, Northern Idaho.
Journal of Petrology, in press.

McIntyre, G.A., Brooks, C., Compston, W., and Turek, A. 1966. The statistical assessment of Rb-Sr isochrons. Journal of Geophysical Research, 71, pp. 5459-5468.

Monger, J.W.H., and Berg, H.C. 1984. Lithotectonic terrane map of western Canada and southeastern Alaska (1:2,500,000). United States Geological Survey Open File Report 84-523.

Monger, J.W.H., Price, R.A., and Tempelman-Kluit, D.J. 1982. Tectonic accretion and the origin of the two major metamorphic and plutonic welts in the Canadian Cordillera. Geology, 10, p. 70-75.

Mortensen, J.K. 1983. U-Pb and Rb-Sr evidence for the age and timing of tectonism of the Yukon-Tanana terrane in southeastern Yukon Territory. Geological Association of Canada, Program with Abstracts, 8, p. A49.

Murphy, D.C. 1984. Suprastructure-infrastructure transition, southern Cariboo Mountains, British Columbia: geometry, kinematics, and tectonic implications.
(In preparation)
(Will probably appear in Journal of Structural Geology.)

Murphy, D.C., and Journeay, J.M. 1982. Structural style in the Premier Range, Cariboo Mountains, southern British Columbia: preliminary results. IN Current research, part A., Geological Survey of Canada, Paper 82-1A, pp. 289-292.

Murphy, D.C., and Rees, C.J. 1983. Structural transition and stratigraphy in the Cariboo Mountains, British Columbia. IN Current research, part A. Geological Survey of Canada, Paper 83-1A, pp. 245-252.

Newton, R.C., and Haselton, H.T. 1981. Thermodynamics of the garnet-plagioclase-Al2SiO5-quartz geobarometer. IN Thermodynamics of minerals and melts. Vol. 1. EDITED BY R.C. Newton, A. Navrotsky, and B.J. Wood. Springer-Verlag, New York, New York, pp. 131-147.

Okulitch, A.V. 1984. The role of the Shuswap Metamorphic Complex in Cordilleran tectonism: a review. Canadian Journal of Earth Sciences, 21, pp. 1171-1193.

Okulitch, A.V., Read, P.B., Wanless, R.K., and Loveridge, W.D. (In preparation.) Paleozoic plutonism in southeastern British Columbia. Geological Survey of Canada, Paper.

Okulitch, A.V., Wanless, R.K., and Loveridge, W.D. 1975. Devonian plutonism in south-central British Columbia. Canadian Journal of Earth Sciences, 12, pp. 1760-1769.

Parrish, R.P. 1979. Geochronology and tectonics of the northern Wolverine Complex, British Columbia. Canadian Journal of Earth Sciences, 16, pp. 1428-1438.

Pell, J. 1982. New correlations of Hadrynian strata, southern Canadian Cordillera. Geological Association of Canada, Program with Abstracts, 7. p. 73.

Pell, J., and Simony, P.S. 1981. Stratigraphy, structure and metamorphism in the southern Cariboo Mountains, British Columbia. IN Current research, part A. Geological Survey of Canada, Paper 81-1A, pp. 227-230.

Pell, J., and Simony, P.S. 1982. Hadrynian Horsethief Creek Group correlations in the southern Cariboo Mountains, British Columbia. IN Current research, part A. Geological Survey of Canada, Paper 82-1A, pp. 305-308.

Pigage, L.C. 1977. Rb-Sr dates for granodiorite intrusions on the northeast margin of the Shuswap Metamorphic Complex, Cariboo Mountains, British Columbia. Canadian Journal of Earth Sciences, 14, pp. 1690-1695.

Pigage, L.C. 1978. Metamorphism and deformation on the northeast margin of the Shuswap Metamorphic Complex, Azure Lake, British Columbia. PhD. thesis, University of British Columbia, Vancouver, B.C., 289 p.

Pigage, L.C., and Greenwood, H.J. 1982. Internally consistent estimates of pressure and temperature: the staurolite problem. American Journal of Science, 282, pp. 943-969.

Poulton, T.P., and Simony, P.S. 1980. Stratigraphy, sedimentology, and regional correlation of the Horsethief Creek Group (Hadrynian, Late Precambrian) in the northern Purcell and Selkirk Mountains, British Columbia. Canadian Journal of Earth Sciences, 17, pp. 1708-1724.

Raeside, R.P., and Simony, P.S. 1983. Stratigraphy and deformational history of the Scrip Nappe, Monashee Mountains, British Columbia. Canadian Journal of Earth Sciences, pp. 639-650.

Rees, C.J. 1981. Western margin of the Omineca Belt at Quesnel Lake, British Columbia. IN Current research, part A. Geological Survey of Canada, Paper 81-1A, pp. 223-226.

Rees, C.J., and Ferri, F. 1983. A kinematic study of mylonitic rocks in the Omineca-Intermontane Belt tectonic boundary in east-central British Columbia. IN Current research, part B. Geological Survey of Canada, Paper 83-1B, pp. 121-125.

Spanglet, M., Brueckner, H.K., Senechal, R.G. 1978. Old Rb-Sr whole-rock isochron apparent ages from Lower Cambrian psammites and metapsammites, southeastern New York. Geological Society of America Bulletin, 89, pp. 783-790.

Stacey, J.S., and Kramers, J.D. 1975. Approximation of terrestrial lead isotope evolution by a two-stage model. Earth and Planetary Science Letters, 26, pp. 207-221.

Stevens, R.D., Delabio, R.N., and Lachance, G.R. 1982. Age determinations and geological studies, K-Ar Isotopic Ages, Report 15. Geological Survey of Canada, Paper 81-2.

Struik, L.C. 1979. Stratigraphy and structure of the Barkerville--Cariboo River area, central British Columbia. IN Current research, part B. Geological Survey of Canada, Paper 79-1B, pp. 33-38.

Struik, L.C. 1981a. Snowshoe Formation, central British Columbia. IN Current research, part A. Geological Survey of Canada, Paper 81-1A, pp. 213-216.

Struik, L.C. 1981b. Bedrock geology of Cariboo Lake, Spectacle Lakes, Swift River, and Wells map areas, Cariboo District, British Columbia. Geological Survey of Canada, Open File Map 858.

Struik, L.C. 1982. Snowshoe Formation (1982), central British Columbia. IN Current research, part B. Geological Survey of Canada, Paper 82-1B, pp. 117-124.

Struik, L.C. 1983. Bedrock geology of Spanish Lake and adjoining areas, British Columbia. Geological Survey of Canada, Open File Map 920.

Struik, L.C. 1984a. Stratigraphy of Quesnel Terrane near Dragon Lake, Quesnel map area, central British Columbia. IN Current Research, Part A, Geological Survey of Canada, Paper 84-1A, p. 113-116.

Struik, L.C. 1984b. Geology of Quesnel Lake and part of Mitchell Lake. Geological Survey of Canada, Open File Map 962.

Sutherland Brown, A. 1957. Geology of the Antler Creek area, Cariboo district, B.C. British Columbia Department of Mines, Bulletin 38.

Sutherland Brown, A. 1963. Geology of the Cariboo River area, B.C. British Columbia Department of Mines, Bulletin 47.

Tipper, H.W., Woodsworth, G.J., and Gabrielse, H. 1981. Tectonic assemblage map of the Canadian Cordillera and adjacent parts of the United States of America. Geological Survey of Canada, Map 1505A.

Wanless, R.K., and Okulitch, A.V. 1976. Geochronologic studies of the Shuswap Metamorphic Complex, southern British Columbia. Geological Association of Canada, Program with Abstracts, 1, p. 47.

Wanless, R.K., Stevens, R.D., Lachance, G.R., and Rimsaite, R.Y.H. 1965. Age determinations and geological studies. Geological Survey of Canada, Paper 64-17, part 1. pp. 15-16.

Wheeler, J.O. 1970. Structure of the southern Canadian Cordillera. Geological Association of Canada, Special Paper 6, 166p.

York, D. 1967. The best isochron. Earth and Planetary Science Letters, 2, pp. 479-482.

APPENDIX I: METAMORPHIC MINERALS

ABBREVIATIONS AND MINERAL NAMES

```
AB = ALBITE
AM = ALMANDINE
AN = ANORTHITE
AP = APATITE
BI = BIOTITE
CA = CALCITE
CH = CHLORITE
CD = CHLORITOID
DI = DIOPSIDE
DO = DOLOMITE
EP = EPIDOTE
GT = GARNET
GP = GRAPHITE
GR = GROSSULAR
HE = HEMATITE
HB = HORNBLENDE
IL = ILMENITE
KS = K-FELDSPAR
KY = KYANITE
LI = LIMONITE
MG = MAGNETITE
MC = MICROCLINE
MS = MUSCOVITE
OL = OLIVINE
OP = OPAQUES (MG, IL, GP, PY)
OR = ORTHOCLASE
PL = PLAGIOCLASE
PY = PYRITE
PR = PYROPE
QZ = QUARTZ
RU = RUTILE
SC = SCAPOLITE
SI = SILLIMANITE
SS = SPESSARTINE
SP = SPHENE
ST = STAUROLITE
TO = TOURMALINE
TR = TREMOLITE
ZR = ZIRCON
ZO = ZOISITE
```

DESCRIPTIONS OF MINERALS

SECTION I. PELITES

Note: S_i and S_e refer to internal and external S-surfaces relative to porphyroblasts in thin section, respectively.

QUARTZ

Quartz is ubiquitous in pelites (5-50%). U(+). Grain size varies even within same rock. Xenoblastic. Boundaries may be granoblastic to granoblastic polygonal; mosaic; sutured; dentate. Combinations common in many rocks. Commonly occurs in quartz segregation layers subparallel to foliation and interstitial to other minerals, and as inclusions in other minerals. Undulatory extinction is common, as well as ribbon quartz, and some mortar texture. Fine-grained quartz defines internal S-surfaces in garnets, particularly in the cores where S_i is straight.

PLAGIOCLASE

(+) Relief; cleavage (010) and (100); 2V high (-) to high (+). Occurs in small amounts in most pelites. Twins: albite, pericline Zoning may be normal, patchy, reverse Composition mostly An25 to An35, may be as high as An55, low as An22; commonly calcic oligoclase to sodic andesine. An content is slightly higher in sillimanite zone. Deformation twins in some rocks; rusty along cracks and grain boundaries. Usually associated with quartz in matrix of pelite, but in some places plagioclase forms porphyroblasts or glomeroblasts. Rotational trails of inclusions indicate porphyroblast growth at same time as staurolite (80-69a, 80-135). Commonly altered to sericite or other fine-grained minerals (saussuritization does not appear to be common in pelites). Not much newly recrystallized feldspar; much looks overgrown by mica foliation.

K-FELDSPAR

Occurs in only a few pelites, <5% in those. (-) Relief; untwinned to hazy twins; possibly perthitic in places. Poikiloblastic both inside and outside garnet (82-380). Occurs also in 81-322, 325 (kyanite zone) and 80-19 (Sil. zone). K-spar occurs in orthogneisses of granodioritic to quartz monzonitic composition, but is rare in pegmatite (plagioclase is dominant).

CHLORITE

Pale green to dark green pseudo-uniaxial(-) or (+)? Mica-like habit and form. Anomalous blue to brown birefringence. Occurs as foliation-forming mineral with muscovite in low-grade zones, chlorite zone and biotite zone; may occur stably in some higher-grade rocks, but it is difficult to tell. Most commonly chlorite is a retrograde mineral over most of the area, in some localities more than others. It replaces garnet rims and may replace the garnet completely; forms from breakdown of biotite; forms in axial planes of F3 kinks and crenulations after muscovite; may be kinked by F3 or F4 folds as well; may also replace staurolite.

MUSCOVITE

Nearly ubiquitous in pelites from chlorite zone to sillimanite zone; formed at various stages throughout rock history. Colorless, though may appear greenish in hand specimen. $(-)2V$ 40-45; $\delta = 0.038$ (2° blue). Mica habit and appearance. Formed during the following stages of crystallization history:

1. Original foliation, in chlorite zone and higher zones.
2. Associated with biotite in crystallization foliation (S1,S2). or chlorite in lower zones.
3. Postkinematic and post-biotite porphyroblast growth in zone 2, and locally elsewhere; as large, crosscutting grains either involved in late kinks or mimetic on polygonal arcs of late crenulation cleavage (non-penetrative). Replaces biotite in some rocks.
4. As replacement of unstable aluminosilicate minerals and staurolite as pseudomorphs of kyanite, staurolite, and garnet; muscovite here is fine-grained, sericitic; may also replace feldspar in form of sericite.

Muscovite is stable over entire field area to Quesnel Lake. Second sillimanite zone is never reached; k-spar is rare. Some muscovite postdates retrograde chlorite.

SERICITE

Fine-grained, random white mica replacing unstable minerals such as kyanite, staurolite, rarely garnet, and plagioclase.

BIOTITE

Olive to green, a = brownish yellow; mica form and habit. Defines dominant foliation in magnetite-bearing schists. Birefringence is too high for chlorite. Some is bent, some might be mimetic. Reaction: GT to BI to CH (79-1, 79-27)

Brown and reddish-brown; mica form and habit; pseudo-uniaxial(-). Commonly involved in crystallization foliation, but may be mimetic around polygonal arcs and also occurs as late, postkinematic porphyroblasts. Can be bent or kinked, or undeformed; found in pressure shadows; crosscutting earlier foliation. Replaces garnet in some rocks; is in equilibrium with new garnets in kyanite and sillimanite zones; may be interstitial to kyanite. Biotite is commonly retrograded to chlorite, and in some places has gone to form rutilated chlorite (79-22). Biotite contains zircon inclusions outlined by pleochroic haloes; they are more obvious in the lighter colored chlorite. Postkinematic biotite porphyroblasts in zone (2) are kinked and crosscut by even later muscovite. Biotite is seen only as inclusions in garnet in kyanite zone or sillimanite zone, not in staurolite-kyanite or staurolite zone.

GARNET

Idioblastic to subidioblastic, some skeletal, some atoll garnets. Isotropic, pale pink (not color-zoned), high relief. Composition: 2/3 almandine, the rest subequal parts of pyrope, spessartine, and grossular (see probe data). Zoning patterns in composition are seen in probe data. Textural zone patterns reveal much about the history. Size of garnets ranges from 0.1 mm to 15 mm; bimodal in that most garnets below sillimanite grade are 2-15 mm; sillimanite and kyanite zone garnets are <2 mm. The largest garnets (10-15 mm) are in the ST-KY zone. Garnets are commonly poikiloblastic except in the highest grades. Typically they contain internal S surfaces defined by trails of quartz, and/or opaques; other inclusions tend not to be aligned on definite layers as not abundant enough. Internal S may be straight or curved, in a few places folded, many cases rotational (snowball). Patterns of inclusions show textural zoning. In general, toward higher grades garnets get bigger and more complexly zoned, then appear to be breaking down, become embayed and atoll, and finally they become small relicts which then provide nucleation sites for new garnets coming in with the the aluminosilicate after breakdown of staurolite. Garnets are stable across the entire field area, but in different forms. The area has been divided into 10 metamorphic zones based on mineral assemblages combined with distinctive textures of porphyroblasts, particularly garnet, staurolite, and kyanite.

CHLORITOID

Pleochroic formula: a = pale green, β = pale slate blue, γ = colorless; $a = \beta > \gamma$; δ = grey; (+)2V med.-high; r>v. Occurs as a few grains included in a large garnet (79-13 only), between inner core and outer zone, within rotational zone of garnet, implying that folding was taking place during chloritoid growth. Rock is now in ST-KY zone. Chloritoid in this rock is distinctly different from chlorite inclusions in same garnet; chlorite is pale green to dark green, and has much lower 2V. Some chlorite inclusions in garnet (and in 81-315 perhaps also staurolite) may be replacements of earlier chloritoid grains.

STAUROLITE

Low δ; r>>v; (+)2V 70-80; parallel extinction. Pleochroic
formula: a = pale yellow, β = yellow, γ = golden yellow;
$\gamma>\beta>a$. Idioblastic to subidioblastic porphyroblasts up to
3 cm long by 1 cm wide. Rarely twinned. Mode is 2-5% of
rock except in one unit where it is 10-25% (80-69, 80-135).
Inclusions are: ilmenite, rutile, quartz, tourmaline,
graphite, garnet, kyanite, biotite, zircon. Some $S_i = S_e$,
some straight, some curved (helicitic) or rotational S_i.
Retrograde reactions: ST to CH + MS + QZ. Ilm inclusions
left over. Some staurolites are completely pseudomorphed by
fine-grained chlorite and sericite. Rocks with abundant
staurolite also have plagioclase porphyroblasts. Staurolite
may be included in big garnets as small xenoblastic grains
(perhaps after chloritoid (in 81-315)) or near the rim of a
garnet. Staurolite may include idioblastic garnets as in
80-69 and 80-135. Staurolite includes some kyanite, but
kyanite surrounds end of staurolite, so must be about same
age. Poikiloblastic staurolite may contain smaller
staurolite and kyanite, also rutile (79-28). Rutile
inclusions in staurolite become ilmenite at rim of
staurolite where rutile is in contact with quartz (best
example is 81-344). Synkinematic, rotational staurolite is
seen in 80-45; later embayed. Some staurolites show two
distinct growth periods:
1. Abundant inclusions, vaguely foliated;
2. Post-kinematic, clear (80-95).
Staurolite including folded Si, or helicitic (80-69,
81-234). Staurolites in sillimanite zone are embayed,
breaking down. Staurolite is clearly being replaced by
fibrolite in transition zone (ST-KY-SIL zone).

KYANITE

Low δ, colorless, high relief, length slow; parallel
extinction and good cleavage seen looking at (010), (001).
Extinction angle = 30° on (100); (−)2V = 82. Cleavage
{100}, poor {001} visible on (010). Up to 2 cm long in
schist; in isolated ky-qz-ms segregations kyanite is up to
2 cm by 10 cm. Commonly tabular, pale blue to grey in hand
specimen. Kyanite may form up to 10% of rock. Inclusions:
Ilmenite, muscovite, rutile, quartz, tourmaline, biotite.
Alters to :sericite (± chlorite); chlorite, biotite may be
interstitial to cracked kyanite. Kyanite is somewhat
aligned on foliation and lineation, but not entirely
oriented. Kyanite tends to be syn- to postkinematic with
respect to F2 folding; but some is bent, kinked, and has
undulose extinction. Some contains rotational inclusions,
is synkinematic (79-22). Generally S_i is parallel to S_e .
Kyanite gets more embayed closer to transition to
sillimanite zone. In Kyanite-only zone near Mt. Stevenson,
kyanites are very tiny and aligned on foliation, and may be
confused with sillimanite, although they do not occur in the
same rock, and kyanite properties are distinctive in thin
section. These small kyanites appear to come in with the
reaction ST + MS + QZ = KY + BI + GT, along with small
garnets and new biotite. Older, larger kyanites are gone,
except as large segregations; older, larger garnets are
gone, except as embayed relicts. Rutile inclusions trapped
in kyanite are OK as long as they do not come in contact
with quartz. If they do, they go to ilmenite; outside the
kyanite, or where rutile comes in contact with quartz,
rutile goes to ilmenite; this is the same relationship as
seen in staurolite with rutile inclusions. Kyanite is
contemporaneous with staurolite for the most part, although
in some rocks crystallization of staurolite both pre- and
postdates kyanite growth.

SILLIMANITE

Length-slow, acicular prisms in fibrous masses (fibrolite).
Biref. is first order; no crystals are big enough to
determine regular optical properties. Sillimanite is
associated with biotite; replaces staurolite; also
associated with small garnets. Clumps of sillimanite may be
in cores of folds (80-30). Knots of sillimanite are visible
on outcrop on Quesnel Lake(80-31). Sillimanite does not
replace kyanite directly. Kyanite in the transition zone is
embayed and replaced by sericite, quartz, and biotite.
Sillimanite appears to be replacing staurolite:
ST + MS + QZ = BI + GT + SIL + H_2O .

OPAQUES

Opaque dust--commonly interpreted as GRAPHITE. May be
identified in hand specimen in some rocks (81-234). Defines
trails of inclusions in porphyroblasts, but is not common in
matrix, except in some schists, especially those within 1 km
of contact with Bralco Limestone. Fault rocks have a very
high percentage of graphite.

Blocky, probably cubic: may be MAGNETITE, PYRITE.
MAGNETITE may be determined with magnet in some specimens;
some schists are magnetic enough to swerve the Brunton 90°
or so, but have no effect outside of about a meter from the
rock surface. Magnetite-bearing schists are most common
near the amphibolite unit, and contain green rather than
red-brown biotite; they are interlayered with other schists
so do not appear to be at a different metamorphic grade.
Some elongate opaques are also iron oxides as shown by
probe, but may be retrograded ilmenites.

PYRITE may be recognized in hand specimen, and is
indistinguishable from magnetite, etc. in transmitted light.
It occurs in some schists and many micaceous quartzites,
particularly those interlayered with amphibolite unit, and
carbonates.

ILMENITE

Opaque, elongate, platy, forms along schistosity or random.
Nearly stoichiometric composition confirmed by probe data,
although some opaques turned out to be pure iron oxide.
Lath-shaped to skeletal; defines S_i in some porphyroblasts
such as garnet, staurolite, kyanite; in some rocks it is
characteristically included in mainly certain zones of the
porphyroblast, or preferentially so. Some garnets have more
quartz inclusions in the core, then more ilmenite in the
rotational and outer zones as well. In places ilmenite is
surrounded by sphene or rutile. In ST-KY zone, ilmenite is
stable as inclusions in garnet and in matrix, or in
ST or KY. Rutile inclusions in the same KY or ST react to
form ilmenite where in contact with quartz. Ilmenite is
common in all pelites, 1-2%.

RUTILE

Very high relief and high absorption, reddish brown, more orange than sphene, and less euhedral, and less red than hematite. Occurs as little ovoid blobs rarely in matrix of pelite, more commonly trapped inside kyanite or staurolite where not in contact with quartz. In ST-KY zone, rutile inclusions with an abrupt change from one end of the mineral grain to the other, or else the rutile is surrounded by ilmenite. Rutile is not commonly associated with garnet, except in the kyanite or sillimanite zones (81-283, 81-298, 81-310, 80-119). Most of the study area is below the reaction
ALM + RUT = ILM + ALS + QZ.

TOURMALINE

Trigonal shape; U(-); idioblastic, small. $\omega > \epsilon$; ω = blue-green to olive; ϵ = colorless to pale green. Zoned, concentric to c-axis, not lengthwise, most commonly blue-green to brown-green, but also more complex zoning, as in 80-33: (1) bluish-green to brown, (2) olive green, (3) pale yellowish olive, (4) olive green. In many pelites, end-sections of tourmaline are very common in thin sections cut perpendicular to lineation (= fold axis) implying that tourmaline growth is synkinematic. Inclusions seen in tourmaline: QZ, ZR (80-33), opaques (80-148), May crosscut biotite. In 81-279, tourmaline inclusions inside kyanite show one zone, with inclusions S_i (to) = S_i (ky) = S_e ; tourmaline outside kyanite has two zones. Possibly outer zone of tourmaline grew at same time as kyanite. Tourmaline occurs in lowest grade phyllites also, and is zoned there. Tourmaline with the most zones is in ST-KY-SI zone. No tourmaline noted in Kyanite zone or Sillimanite zone. Large tourmalines (up to 1 cm) occur in massive veins with chlorite near contact of amphibolite unit and pelite on east side of middlepeak of Three Ladies Mountain, where the rocks look as though they have undergone partial melting or hydrothermal alteration. Most tourmalines in pelites are too small to see in hand specimen, <0.1 mm.

ACCESSORY MINERALS

APATITE

U(+), grey δ, small prisms, length fast, med.-high relief.
Minor constituent of most pelites.

HEMATITE

Bright red absorption. Late vein-filler; in tiny fractures
and grains, esp. in retrograde schists (ex. 80-123).
Probably from oxidation of magnetite or ilmenite.

SPHENE

High relief, sphene shape, brownish δ and absorption. Rare
in pelites (81-340, 82-382, 81-295, 80-123, 81-333, 79-36,
79-38, 81-204), and a very minor constituent of these.

ZIRCON

Tetragonal shape; U(+); very high relief and δ. Common as
inclusions in biotite, surrounded by pleochroic haloes.
Also included in chlorite which has replaced biotite; haloes
very obvious in paler chlorite. May be up to 1% of rock but
commonly much less in pelites.

SECTION II.   CALC-SILICATES

Calc-silicate rocks vary in composition from nearly pure marbles to amphibolites. Assemblages were not as useful as those in pelites for distinguishing metamorphic zones. All green amphiboles are hornblende rather than actinolite as determined by very dark green color, association, and optical properties. The metamorphic grade is at least amphibolite facies. There is no albite. Minerals suggestive of higher metamorphic grades in calcsilicate rocks are diopside, zoisite, scapolite, and k-feldspar, but are not restricted to one metamorphic zone, except for zoisite. Calc-silicates from Quesnel Lake in the sillimanite zone are distinctive, containing calcite, plagioclase, quartz, k-feldspar, diopside, epidote (zoned pistacite, high (-)2V, yellow), zoisite (β-zoisite, near pseudo-uniaxial(+)), opaques, ± garnet, sphene, apatite, or scapolite. Sphene and scapolite do not occur in the same rock. Textures indicate many reaction relationships involving diopside and garnet, plagioclase and epidote, two phases of K-feldspar, and feldspar-zoisite intergrowths. The only occurrence of scapolite that is not in the sillimanite zone is in a vein in calcareous schist near sample 79-28, in definite staurolite-kyanite zone. Diopside and K-feldspar-bearing calc-silicates also occur in the Staurolite-Kyanite zone, but not below it; many samples in this zone containing K-feldspar were collected adjacent to granodioritic gneisses. As most of the calc-silicate and amphibolitic units occur within the staurolite-kyanite zone, most of the samples are of the same metamorphic grade, although their compositions vary widely.

I

APPENDIX II: MICROPROBE ANALYSES

The electron microprobe at the Department of Geological Sciences, University of British Columbia, was used for mineral analyses.

Accelerating potential = 15 KV

Specimen current on Al = 40 namps

Aperture size = 200 μ

Count time = 10 s or 20 s.

Analyses of minerals are shown on the following tables. There are three tables with garnet analyses, two tables with biotite analyses, one table with plagioclase analyses, and one table with staurolite analyses.

Standards used for electron microprobe analyses are from
the reference standards collection (number in parentheses)
at the Department of Geological Sciences, University of
British Columbia. All minerals were analyzed using the same
standards, except as noted.

Element	Standard	Number	Origin
F	F-Phlogopite	(24)	(synthetic)
Na	Albite	(20)	(Oregon)
Mg	Forsterite	(22)	(synthetic)
Al	Andalusite	(26)	(Brazil)
Si	Wollastonite	(21)	(New York)
K	Orthoclase	(96)	(New York)
Ca	Wollastonite	(21)	(New York)
Ba	Benitoite	(35)	(California)
Ti	Rutile	(13)	(synthetic)
Mn	Pyroxmangite	(245)	(Japan)
Fe	Fayalite	(250)	(synthetic)

Some garnets were also analyzed using:

Mg	Pyrope garnet	(235)	(New Zealand)
Al	Pyrope garnet	(235)	(New Zealand)
Si	Pyrope garnet	(235)	(New Zealand)

GARNET ANALYSES

Sample	80-19 RIM	80-19 CORE	80-31 RIM	80-31 CORE	80-33 RIM	80-33 CORE
Analyses	9	7	10	7	20	11

WEIGHT % (σ)

MgO	2.22 (0.17)	3.33 (0.30)	2.36 (0.12)	2.66 (0.04)	2.10 (0.15)	2.34 (0.21)
Al_2O_3	21.15 (0.62)	21.16 (0.45)	20.74 (0.37)	20.76 (0.36)	21.65 (0.26)	21.89 (0.44)
SiO_2	37.21 (0.30)	37.61 (0.60)	36.97 (0.41)	36.89 (0.54)	36.98 (0.47)	37.02 (0.59)
CaO	2.64 (0.20)	3.04 (0.18)	2.03 (0.12)	1.62 (0.03)	2.11 (0.14)	1.60 (0.15)
TiO_2	0.02 (0.01)	0.12 (0.32)	0.01 (0.01)	0.00 (0.00)	0.05 (0.13)	0.01 (0.01)
MnO	2.27 (0.12)	1.36 (0.31)	1.82 (0.25)	3.34 (0.41)	2.31 (0.13)	3.48 (0.43)
FeO	35.04 (0.28)	34.21 (0.31)	35.93 (0.73)	34.45 (1.20)	35.32 (0.50)	34.35 (0.42)
Total	100.55 (0.54)	100.83 (0.64)	99.86 (0.84)	99.72 (1.44)	100.52 (0.95)	100.69 (1.01)

FORMULA (σ)

MgO	0.267 (0.018)	0.395 (0.035)	0.286 (0.015)	0.322 (0.006)	0.251 (0.016)	0.280 (0.023)
Al_2O_3	2.003 (0.048)	1.985 (0.037)	1.983 (0.033)	1.986 (0.034)	2.052 (0.028)	2.069 (0.026)
SiO_2	2.992 (0.031)	2.993 (0.035)	2.999 (0.029)	2.994 (0.036)	2.974 (0.017)	2.969 (0.015)
CaO	0.227 (0.017)	0.276 (0.047)	0.176 (0.011)	0.141 (0.003)	0.182 (0.012)	0.138 (0.014)
TiO_2	0.001 (0.001)	0.007 (0.019)	0.001 (0.001)	0.000 (0.000)	0.003 (0.008)	0.001 (0.001)
MnO	0.155 (0.008)	0.077 (0.030)	0.125 (0.016)	0.229 (0.029)	0.158 (0.009)	0.237 (0.029)
FeO	2.356 (0.027)	2.277 (0.027)	2.438 (0.045)	2.338 (0.058)	2.376 (0.025)	2.304 (0.042)
Total	8.001	8.010	8.007 (0.019)	8.009 (0.027)	7.996 (0.013)	7.996 (0.016)

GARNET ANALYSES

Sample	80-119 RIM	80-119 INC1	80-119 INC2	81-278 RIM	81-279 RIM
Analyses	20	4	3	15	12

WEIGHT % (σ)

	80-119 RIM	80-119 INC1	80-119 INC2	81-278 RIM	81-279 RIM
MgO	2.26 (0.17)	3.08 (0.15)	2.98 (0.03)	2.23 (0.11)	2.18 (0.14)
Al_2O_3	21.16 (0.17)	21.48 (0.37)	21.43 (0.17)	21.02 (0.14)	20.88 (0.42)
SiO_2	37.03 (0.46)	37.41 (0.57)	36.76 (0.44)	36.95 (0.40)	36.98 (0.67)
CaO	2.19 (0.40)	2.33 (0.12)	1.74 (0.13)	2.72 (0.56)	2.61 (0.43)
TiO_2	0.04 (0.03)	0.05 (0.04)	0.01 (0.01)	0.03 (0.02)	0.05 (0.04)
MnO	1.58 (0.26)	1.48 (0.13)	1.44 (0.02)	2.84 (0.21)	1.42 (0.11)
FeO	36.15 (0.51)	34.85 (0.29)	35.66 (0.54)	34.53 (0.55)	36.10 (0.59)
Total	100.41 (0.74)	100.68 (0.61)	100.02 (0.94)	100.32 (0.38)	100.22 (1.55)

FORMULA (σ)

	80-119 RIM	80-119 INC1	80-119 INC2	81-278 RIM	81-279 RIM
MgO	0.272 (0.020)	0.367 (0.020)	0.358 (0.004)	0.269 (0.013)	0.263 (0.018)
Al_2O_3	2.011 (0.038)	2.021 (0.030)	2.038 (0.017)	2.000 (0.016)	1.990 (0.025)
SiO_2	2.986 (0.030)	2.986 (0.025)	2.965 (0.010)	2.983 (0.020)	2.990 (0.022)
CaO	0.189 (0.035)	0.199 (0.010)	0.150 (0.013)	0.236 (0.048)	0.226 (0.035)
TiO_2	0.002 (0.002)	0.003 (0.003)	0.001 (0.001)	0.002 (0.002)	0.003 (0.003)
MnO	0.105 (0.017)	0.100 (0.009)	0.098 (0.001)	0.194 (0.014)	0.097 (0.009)
FeO	2.438 (0.027)	2.327 (0.031)	2.406 (0.020)	2.332 (0.042)	2.442 (0.028)
Total	8.005 (0.013)	8.001 (0.019)	8.016 (0.004)	8.015 (0.015)	8.011 (0.013)

GARNET ANALYSES

Sample	81-325 RIM	81-325 CORE	82-389 RIM	82-389 CORE
Analyses	25	13	13	4

WEIGHT % (σ)

MgO	2.72 (0.18)	3.09 (0.08)	2.55 (0.50)	2.10 (0.42)
Al_2O_3	20.85 (0.45)	20.87 (0.38)	21.24 (0.59)	20.74 (0.37)
SiO_2	36.85 (0.47)	37.00 (0.40)	37.36 (0.56)	37.77 (0.55)
CaO	2.98 (0.14)	2.90 (0.10)	6.21 (0.86)	6.78 (0.64)
TiO_2	0.01 (0.02)	0.04 (0.09)	0.06 (0.05)	0.09 (0.04)
MnO	2.16 (0.26)	1.70 (0.10)	1.55 (0.48)	3.32 (0.39)
FeO	34.02 (0.38)	34.37 (0.39)	31.32 (0.68)	30.28 (0.39)
Total	99.59 (0.88)	99.97 (0.62)	100.29 (0.87)	101.08 (0.45)

FORMULA (σ)

MgO	0.328 (0.021)	0.372 (0.010)	0.304 (0.059)	0.249 (0.048)
Al_2O_3	1.990 (0.033)	1.983 (0.028)	1.998 (0.055)	1.944 (0.046)
SiO_2	2.985 (0.020)	2.982 (0.014)	2.982 (0.033)	3.003 (0.029)
CaO	0.259 (0.012)	0.250 (0.009)	0.531 (0.074)	0.577 (0.054)
TiO_2	0.001 (0.001)	0.002 (0.005)	0.004 (0.003)	0.006 (0.003)
MnO	0.148 (0.017)	0.116 (0.006)	0.105 (0.033)	0.224 (0.028)
FeO	2.305 (0.032)	2.317 (0.035)	2.090 (0.038)	2.014 (0.027)
Total	8.017 (0.011)	8.022 (0.013)	8.013 (0.013)	8.016 (0.012)

BIOTITE ANALYSES

Sample	80-19	80-19 B	80-31	80-33	81-278	81-279
Analyses	9 (dif. gr.)	16 (same gr.)	6	14	10	8

WEIGHT % (σ)

F	0.37 (0.15)	0.29 (0.14)	0.24 (0.08)	0.39 (0.13)	0.35 (0.13)	0.31 (0.16)
Na$_2$O	0.21 (0.03)	0.22 (0.04)	0.38 (0.05)	0.31 (0.06)	0.29 (0.07)	0.23 (0.03)
MgO	9.35 (0.47)	9.65 (0.19)	8.66 (0.25)	9.00 (0.38)	10.11 (0.35)	8.81 (0.85)
Al$_2$O$_3$	18.31 (0.61)	18.25 (0.60)	19.26 (0.18)	19.09 (0.82)	19.30 (0.53)	19.59 (0.47)
SiO$_2$	35.61 (0.81)	36.08 (0.75)	35.56 (0.87)	35.42 (0.83)	35.42 (0.67)	35.54 (0.71)
K$_2$O	8.93 (0.36)	8.49 (1.15)	8.24 (0.07)	8.74 (0.30)	8.42 (0.01)	8.06 (0.33)
CaO	0.00 (0.01)	0.01 (0.01)	0.01 (0.01)	0.00 (0.01)	0.01 (0.01)	0.03 (0.07)
BaO	0.36 (0.08)	0.32 (0.07)	0.20 (0.07)	0.11 (0.05)	0.07 (0.04)	0.16 (0.04)
TiO$_2$	1.98 (0.31)	1.76 (0.09)	2.81 (0.23)	2.22 (0.34)	1.70 (0.19)	1.70 (0.33)
MnO	0.03 (0.03)	0.03 (0.02)	0.03 (0.02)	0.04 (0.01)	0.04 (0.02)	0.04 (0.05)
FeO	19.48 (1.04)	19.23 (0.60)	18.77 (0.31)	20.42 (1.16)	18.45 (0.56)	20.62 (1.40)
Total	94.63 (1.12)	94.43 (1.42)	94.16 (0.69)	95.74 (0.98)	94.16 (1.07)	95.09 (0.53)

FORMULA

Oxygens	22.000	22.000	22.000	22.000	22.000	22.000
Si	5.484	5.535	5.442	5.397	5.409	5.424
Al IV	2.516	2.465	2.558	2.603	2.591	2.576
Sum IV	8.000	8.000	8.000	8.000	8.000	8.000
Al VI	0.807	0.835	0.915	0.825	0.894	0.947
Ti	0.230	0.203	0.324	0.254	0.199	0.196
Fe^{2+}	2.508	2.466	2.403	2.604	2.365	2.634
Mn	0.004	0.004	0.004	0.006	0.005	0.006
Mg	2.147	2.203	1.977	2.044	2.313	2.003
Sum	5.696	5.711	5.623	5.733	5.776	5.786
Ca	0.000	0.002	0.001	0.001	0.002	0.005
Na	0.063	0.092	0.113	0.091	0.088	0.069
K	1.754	1.659	1.609	1.699	1.646	1.570
Ba	0.021	0.018	0.012	0.006	0.005	0.010
Sum	1.838	1.771	1.735	1.797	1.741	1.654
OH	3.937	3.908	3.883	3.810	3.835	3.850
F	0.063	0.092	0.117	0.190	0.165	0.150

BIOTITE ANALYSES

Sample	80-119	80-119 INC1	80-119 INC2	81-325	82-389
Analyses	17	3	3	15	7

WEIGHT % (σ)

F	0.28 (0.10)	0.47 (0.15)	0.30 (0.11)	0.37 (0.14)	0.50 (0.17)
Na$_2$O	0.30 (0.05)	0.44 (0.03)	0.37 (0.03)	0.40 (0.04)	0.25 (0.10)
MgO	8.72 (0.47)	11.24 (0.13)	11.05 (0.23)	10.09 (0.15)	11.77 (0.52)
Al$_2$O$_3$	19.27 (0.90)	18.17 (0.28)	19.75 (0.15)	18.68 (0.36)	18.05 (0.18)
SiO$_2$	35.20 (0.43)	36.24 (0.94)	35.59 (0.10)	36.15 (0.32)	36.58 (0.23)
K$_2$O	8.44 (0.19)	8.33 (0.05)	7.86 (0.43)	8.45 (0.20)	8.84 (0.40)
CaO	0.03 (0.04)	0.00 (0.01)	0.00 (0.01)	0.02 (0.04)	0.01 (0.01)
BaO	0.12 (0.04)	0.09 (0.03)	0.09 (0.04)	0.13 (0.05)	0.07 (0.04)
TiO$_2$	2.38 (0.42)	2.23 (0.03)	1.86 (0.13)	2.06 (0.19)	1.41 (0.08)
MnO	0.04 (0.02)	0.03 (0.02)	0.02 (0.02)	0.06 (0.06)	0.03 (0.02)
FeO	20.42 (0.95)	16.52 (0.18)	17.24 (0.56)	17.93 (0.50)	16.75 (0.42)
Total	95.20 (0.57)	93.76 (0.46)	94.13 (1.05)	94.34 (0.55)	94.26 (0.24)

FORMULA

Oxygens	22.000	22.000	22.000	22.000	22.000
Si	5.382	5.523	5.392	5.509	5.563
Al IV	2.618	2.477	2.608	2.491	2.437
Sum IV	8.000	8.000	8.000	8.000	8.000
Al VI	0.854	0.788	0.919	0.864	0.797
Ti	0.273	0.256	0.212	0.236	0.161
Fe^{2+}	2.612	2.106	2.184	2.286	2.130
Mn	0.005	0.003	0.002	0.007	0.004
Mg	1.988	2.555	2.496	2.291	2.669
Sum	5.732	5.708	5.813	5.684	5.761
Ca	0.004	0.001	0.001	0.003	0.002
Na	0.089	0.130	0.109	0.119	0.073
K	1.646	1.619	1.519	1.643	1.741
Ba	0.007	0.005	0.005	0.008	0.005
Sum	1.746	1.755	1.634	1.773	1.821
OH	3.864	3.771	3.857	3.822	4.000
F	0.136	0.229	0.143	0.178	

PLAGIOCLASE ANALYSES

Sample	80-19	80-31	80-33	80-119	81-278	81-279	81-325
Analyses	9	4	4	1	3	4	8
WEIGHT % (σ)							
F	0.04 (0.07)	0.03 (0.04)	0.04 (0.09)	0.00	0.06 (0.06)	0.02 (0.05)	0.04 (0.06)
Na$_2$O	6.90 (0.21)	9.05 (0.13)	8.74 (0.18)	8.82	7.99 (0.70)	9.15 (0.34)	6.85 (0.20)
MgO	0.00 (0.00)	0.00 (0.01)	0.02 (0.01)	0.00	0.00 (0.01)	0.00 (0.00)	0.02 (0.05)
Al$_2$O$_3$	25.84 (0.51)	23.38 (0.40)	24.11 (0.51)	25.55	25.23 (0.36)	24.53 (0.34)	25.73 (0.26)
SiO$_2$	57.83 (0.71)	62.22 (0.38)	61.13 (0.52)	59.91	59.32 (0.75)	62.54 (0.28)	59.00 (0.99)
K$_2$O	0.08 (0.02)	0.10 (0.01)	0.10 (0.03)	0.07	0.07 (0.02)	0.08 (0.01)	0.07 (0.02)
CaO	7.75 (0.54)	4.57 (0.19)	5.69 (0.40)	6.11	6.43 (0.29)	4.93 (0.39)	7.46 (0.18)
BaO	0.01 (0.02)	0.03 (0.05)	0.00 (0.00)	0.00	0.01 (0.02)	0.01 (0.02)	0.00 (0.01)
TiO$_2$	0.00 (0.00)	0.01 (0.01)	0.01 (0.01)	0.00	0.01 (0.01)	0.01 (0.01)	0.00 (0.01)
MnO	0.00 (0.00)	0.00 (0.00)	0.01 (0.01)	0.00	0.01 (0.02)	0.01 (0.01)	0.01 (0.01)
FeO	0.04 (0.11)	0.03 (0.01)	0.21 (0.13)	0.02	0.13 (0.09)	0.07 (0.04)	0.12 (0.12)
Total	98.49 (0.64)	99.42 (0.49)	100.05 (0.43)	100.48	99.26 (1.18)	101.35 (0.48)	99.30 (0.87)
FORMULA (σ)							
F	0.006 (0.010)	0.008 (0.007)	0.006 (0.012)	0.000	0.008 (0.008)	0.003 (0.006)	0.006 (0.009)
Na$_2$O	0.607 (0.018)	0.782 (0.010)	0.754 (0.020)	0.759	0.696 (0.057)	0.777 (0.031)	0.596 (0.022)
MgO	0.000 (0.000)	0.000 (0.000)	0.001 (0.001)	0.000	0.000 (0.000)	0.001 (0.001)	0.002 (0.003)
Al$_2$O$_3$	1.381 (0.029)	1.228 (0.018)	1.265 (0.019)	1.337	1.336 (0.014)	1.266 (0.013)	1.361 (0.016)
SiO$_2$	2.622 (0.024)	2.772 (0.016)	2.721 (0.011)	2.660	2.665 (0.005)	2.738 (0.012)	2.640 (0.019)
K$_2$O	0.004 (0.001)	0.006 (0.001)	0.006 (0.002)	0.000	0.004 (0.001)	0.004 (0.001)	0.004 (0.001)
CaO	0.376 (0.026)	0.218 (0.009)	0.271 (0.021)	0.291	0.310 (0.017)	0.231 (0.017)	0.359 (0.007)
BaO	0.000 (0.000)	0.001 (0.001)	0.000 (0.000)	0.000	0.000 (0.000)	0.000 (0.000)	0.000 (0.000)
TiO$_2$	0.000 (0.000)	0.000 (0.001)	0.000 (0.000)	0.000	0.000 (0.000)	0.000 (0.000)	0.000 (0.000)
MnO	0.000 (0.000)	0.000 (0.000)	0.000 (0.000)	0.000	0.000 (0.000)	0.000 (0.001)	0.000 (0.000)
FeO	0.002 (0.004)	0.001 (0.000)	0.008 (0.005)	0.001	0.005 (0.003)	0.003 (0.001)	0.004 (0.005)
Total	4.999 (0.011)	5.016 (0.011)	5.032 (0.019)	5.053	5.025 (0.038)	5.023 (0.019)	4.979 (0.027)
XAn	0.381	0.217	0.263	0.277	0.307	0.228	0.374

STAUROLITE ANALYSES

Sample	82-389	81-279	81-278	80-33
Analyses	8	1	1	1

WEIGHT % (σ)

F	0.04 (0.07)	0.00	0.05	0.00
Na_2O	0.01 (0.01)	0.00	0.03	0.03
MgO	·1.76 (0.21)	1.58	1.36	1.39
Al_2O_3	51.85 (0.48)	55.42	52.35	53.84
SiO_2	27.53 (0.38)	27.73	27.34	27.43
K_2O	0.01 (0.01)	0.00	0.02	0.01
CaO	0.01 (0.01)	0.00	0.00	0.00
BaO	0.02 (0.03)	0.00	0.00	0.02
TiO_2	0.64 (0.04)	0.29	0.58	0.50
MnO	0.13 (0.02)	0.07	0.16	0.11
FeO	13.27 (0.20)	14.10	14.34	14.59
Total	95.25 (0.42)	99.21	96.23	97.92

FORMULA

Oxygens	23.00	23.00	23.00	23.00
Si	3.92	3.79	3.87	3.82
Al	8.70	8.94	8.74	8.83
Ti	0.03	0.03	0.06	0.05
Sum	8.73	8.97	8.80	8.88
Fe^{2+}	1.58	1.61	1.70	1.70
Mg	0.38	0.32	0.29	0.29
Mn	0.02	0.01	0.02	0.01
Sum	1.98	1.94	2.01	2.00
Total	14.64	14.70	14.68	14.70
OH	2.00	2.00	1.98	2.00
F	0.00	0.00	0.02	0.00
XFe	0.80	0.83	0.85	0.85

Staurolite Formula: $(Fe,Mg)(2)$ $Al(9)$ $Si(3.75)$ $O(22)$ $OH(2)$

Analytical Techniques.

Rb and Sr concentrations were determined by replicate
analysis of pressed powder pellets using X-ray fluorescence.
U.S. Geological Survey rock standards were used for
calibration; mass absorption coefficients were obtained from
Mo K-α Compton scattering measurements. Rb/Sr ratios have a
precision of 2% (1σ) and concentrations a precision of
5% (1σ). Sr isotopic composition was measured on unspiked
samples prepared using standard ion exchange techniques.
The mass spectrometer, V.G. Isomass 54R, has data
acquisition digitized and automated using a H.P. 85
computer. Experimental data have been normalized to a
$^{86}Sr/^{88}Sr$ ratio of 0.1194 and adjusted so that the NBS
standard $SrCO_3$ (SRM987) gives a $^{87}Sr/^{86}Sr$ ratio of
0.71020 ± 2 and the Eimer and Amend Sr a ratio of
0.70800 ± 2. The precision of a single $^{87}Sr/^{86}Sr$ ratio is
<0.00010 (1σ). Rb-Sr dates are based on a Rb decay constant
of 1.42 x $10^{-11}a^{-1}$. The regressions are calculated
according to the technique of York (1967).
Zircon separate was prepared using standard grinding and
mineral separation procedures for heavy minerals.
Dissolution of zircons and isolation of U and Pb were done
using a procedure based on that of Krogh (1973). The sample
was analysed using single Re filament and silica gel
techniques on an Isomass 54R mass spectrometer in the
Department of Geological Sciences, University of British
Columbia, by P. van der Heyden.

Krogh, T.E. 1973. A low contamination method for
hydrothermal decomposition of zircon and extraction of
U and Pb for isotopic age determinations. Geochimica et
Cosmochimica Acta, 37, pp. 485-494.

APPENDIX IIIB: GEOCHRONOLOGY SAMPLE DESCRIPTIONS

Sample descriptions.

JSG-81-X1 to X6. 52°40.5' N. Lat., 121°05.7' W. Long.
Foliated quartz dioritic gneiss with plagioclase($An_{24.30}$)
(35%), quartz (15%), hornblende (10%), and reddish-brown
biotite (20%) and epidote (15%) from metamorphism of
hornblende, and sphene, minor apatite, allanite, and zircon.
Crystallization foliation is defined by oriented biotite and
hornblende, and incipient segregation of mafic from felsic
layers. Staurolite-kyanite zone.

JSG-81-X1 to X6 were combined for zircon analyses.
Zircons are colorless to light pink, typically subhedral
prismatic with rounded edges and terminations. Length
to width ratio varies from 2 to 6. About 50% of the
coarser (100-200 mesh) grains are broken and
internally cracked. Bulk sample contains 1-2%
non-zircon material. Handpicked fractions consist only
of clear, crack-free, unbroken crystals.

Quesnel Lake Gneiss (for comparison with JSG-81-X):

JSG-80-QLGNW. 52°33.0' N. Lat., 121°04.4' W. Long.
From junction of north and west arms of Quesnel Lake.
Leucocratic, medium-grained, foliated granite with
microcline (40%), quartz (35%), plagioclase (15%), and
chlorite plus muscovite (10%), minor opaques(<2%).
Foliation is defined by mortar texture: fine-grained
mica, quartz, and feldspar between broken grains of
feldspar and quartz with sutured boundaries and
undulose extinction.

JSG-81-166. 52°33.5' N. Lat., 121°01.1' W. Long.
From junction of north and east arms of Quesnel Lake.
Weakly foliated, coarse-grained, pink and green K-feldspar
granite with perthitic microcline megacrysts (20%).
Groundmass is microcline (30%), quartz (30%), epidote and
green biotite (10%), and saussuritized feldspar, chlorite,
sphene, and muscovite (10% together), and minor allanite.
Foliation is cataclastic rather than metamorphic.

JSG-80-36. 52°41.75' N. Lat., 120°55.8' W. Long.
Pegmatite with quartz (40%), plagioclase (50%), and
muscovite (10%); average grain size is >1 cm.
Intruded as late to post-metamorphic dikes.

JSG-80-99. 52°43.3' N. Lat., 120°58.8' W. Long.
Foliated granodioritic gneiss with large (up to 1 cm)
magnetite grains locally. Staurolite-kyanite zone.

JSG-80-136A. 52°43.3' N. Lat., 120°59.8' W. Long.
Foliated granodioritic gneiss with plagioclase (50%),
quartz (30 %), perthitic potassium feldspar (10%),
biotite (10%), and minor opaque oxides.
Staurolite-kyanite zone.

JSG-81-205. 52°40.6' N. Lat., 120°59.2' W. Long.
Weakly foliated granodioritic gneiss. Sillimanite zone.

JSG-81-327. 52°37.85' N. Lat., 121°03.85' W. Long.
Foliated granodioritic augen gneiss, with foliation
subparallel to layering in adjacent paragneiss.
Augen up to 1 cm are feldspar (45%); other minerals are
quartz (30%), biotite (20-25%), and minor oxides.
Kyanite zone.

JSG-80-42. 52°47.2' N. Lat., 120°59.55' W. Long.
Graphitic garnet-kyanite(?)-bearing biotite-muscovite
schist. Garnets up to 1 cm; quartz segregation layers
parallel schistosity. Staurolite-kyanite zone.

JSG-79-15. 52°46.15' N. Lat., 120°58.0' W. Long.
Quartz-rich schist with garnet, biotite, muscovite, and
plagioclase. Staurolite-kyanite zone.

JSG-80-67. 52°43.5' N. Lat., 120°59.3' W. Long.
Well-foliated biotite-muscovite schist with porphyroblasts
of staurolite, garnet, and plagioclase. Staurolite zone.

JSG-80-80. 52°44.2' N. Lat., 120°57.9' W. Long.
Well-lineated micaceous quartzite with quartz, biotite,
and plagioclase. Kyanite to sillimanite zone.

JSG-80-96. 52°43.4' N. Lat., 120°58.1' W. Long.
Folded, lineated quartz-biotite-muscovite schist with garnet
porphyroblasts. Staurolite-kyanite zone.

JSG-82-375. 52°45.7' N. Lat., 121°04.6' W. Long.
Crenulated quartz muscovite schist with biotite and garnet
porphyroblasts. Metamorphosed to at least garnet zone.

JSG-81-245. 52°45.5' N. Lat., 121°00.05' W. Long.
Coarse-grained, hornblende-plagioclase amphibolite with
some quartz and iron oxides. Staurolite-kyanite zone.

JSG-80-21. 52°42.0' N. Lat., 120°55.4' W. Long.
Foliated gneiss with biotite, quartz, plagioclase, and
some muscovite. Sillimanite zone.

JSG-80-22. 52°41.95' N. Lat., 120°55.5' W. Long.
Crenulated muscovite schist with biotite, quartz,
plagioclase. Sillimanite zone.

JSG-81-171. 52°41.7' N. Lat., 120°56.0' W. Long.
Weakly foliated gneiss with medium to coarse-grained
quartz, plagioclase, and biotite. Sillimanite zone.

JSG-81-281. 52°40.05' N. Lat., 121°05.2' W. Long.
Garnet-biotite schist with plagioclase and chlorite.
Staurolite-kyanite zone.

JSG-81-328. 52°37.85' N. Lat., 121°03.9' W. Long.
Coarse quartz-muscovite-biotite schist with garnet and
kyanite (20%). Kyanite zone.